

**Investigating the anti-proliferative  
properties and their mechanism(s) of action  
of marine derived glycosaminoglycans from  
two marine sources.**

Macauley James Green BSc.

MRes Biological Science.

University of Salford

Environment and Life Sciences

2020



University of  
**Salford**  
MANCHESTER

## Contents:

Abstract – 1

Introduction – 3

Cancer Epidemiology – 3

Leukemia – 4

ALL – 6

AML – 6

CLL – 7

CML – 8

Marine Polysaccharides – 8

GAG Biosynthesis – 16

GAG Structures – 16

GAG Interactions – 18

Marine GAG Structures – 20

Glycosaminoglycan Therapeutics and Cosmetics – 21

Hyaluronic Acid – 21

Keratan Sulfate – 23

Chondroitin Sulfate – 24

Heparan Sulfate – 24

Current Cancer Treatments – 25

Radiotherapy – 25
Immunotherapy – 26
Chemotherapy – 27
Leukemia Treatments – 28
Current GAGs in cancer therapeutics – 30
Method Theories – 30
SDS-PAGE – 30
Affinity Chromatography – 33
MTT Assay – 35
Aims – 36
Methods – 37
GAG Extraction – 37
Nuclear Magnetic Resonance – 38
Cell Culturing – 38
Cell Lysis – 39
Protein Quantification – 39
SDS-PAGE – 39
MTT Plating and Reading – 41
Affinity Chromatography – 42
Monosaccharide and Disaccharide Analysis – 43

## Results – 44

### MTT – 44

#### Comparing Prawns against Cockles – 44

#### Alternative Cell Lines – 45

##### U2OS – 45

##### MDBK – 46

##### BEAS-2B – 47

##### MOLT-4 – 48

#### Quantifying Cell Lysate Protein – 49

#### Affinity Chromatography – 50

#### NMR results – 55

#### Disaccharide Analysis – 56

#### Monosaccharide Analysis – 60

## Discussion – 62

### NMR Analysis – 62

### Disaccharide Analysis – 67

### Monosaccharide Analysis – 72

### MTT Results – 73

#### Cockle vs Prawn K562 Comparison – 73

##### U2OS – 75

MDBK – 76

BEAS-2B – 78

MOLT-4 – 80

Inconclusive/Inaccurate Cell Lines – 81

MTT Comparison – 83

Cell Lines – 90

MTT Limiting Factors – 92

Protein Lysis – 93

SDS-PAGE Results – 94

Highly specific binding proteins – 95

SDS-PAGE Calibration – 97

Affinity Chromatography – 102

Future Study – 106

Conclusion – 108

References – 110

## List of Tables

Table 1: Marine GAG mimetics structures\* - 15

Table 2: Proteins that can bind to GAGs (Varki et al, 1999.) – 19

Table 3: Marine GAGs and associated structures\*. – 20

Table 4: SDS-PAGE gel formula – 40	
Table 5: Absorbance readings in triplicate for the K562 lysates. – 49	
Table 6: Heparin Sulfate abbreviations and relative disaccharides. – 57	
Table 7: Chondroitin Sulfate abbreviations and their relative disaccharide. – 57	
Table 8: Heparin Sulfate disaccharide analysis of prawn GAGs. – 58	
Table 9: Chondroitin Sulfate disaccharide analysis of prawn GAGs. – 58	
Table 10: Data represented by monosaccharide analysis chromatogram. – 61	
Table 11: Heparin Sulfate disaccharide analysis of prawn, cockle and mammalian GAGs. – 68	
Table 12: Chondroitin Sulfate disaccharide analysis of prawn, cockle and mammalian GAG extract. – 69	
Table 13: Chondroitin sulfate sulfation type analysis. – 70	
Table 14: Heparin Sulfate sulfation type analysis. – 71	
Table 15: Cockle and prawn monosaccharide analysis comparison. – 72	
Table 16: A master table of all cell lines tested on and their corresponding cell viability alongside various cell line characteristics. – 84	
Table 17: A brief overview of the contents of each affinity fraction and the reasoning behind the contents of the mobile phase. – 103	
List of Figures:	
Figure 1: A flow chart of the pathogenesis of various leukemic syndromes (Cornell University College of Veterinary Medicine, 2013). -	

Figure 2: Bioactive sulphated marine polysaccharides from seaweed classification (Patel, 2012). – 9

Figure 3: Laminarin extraction process (Deleris, Nazih and Bard, 2016). – 9

Figure 4: Medical uses of Chitosan and its' structure (Babu and Ramesh, 2017). – 11

Figure 5: Carrageenan differing structures (Kariduraganavar, Kittur and Kamble, 2014). – 12

Figure 6: The three most common forms of Fucoidan (van Weelden et al, 2019). – 13

Figure 7: Backbone structure of GAGs (Yamada, Sugahara and Ozbek, 2011). – 17

Figure 8: Distribution of GAGs based upon animal kingdom grouping (Yamada, Sugahara and Ozbek, 2011). – 18

Figure 9: A graphic showing how 2-mercaptoethanol and sodium dodecyl sulphate reduce and linearize the protein molecules to be used on an SDS polyacrylamide gel (MBL Life Science, 2017). – 32

Figure 10: The mathematical equation used to calculate required amount of cell solution volume and media needed to acquire desired cell plating density. – 41

Figure 11: The re-arranged equation to achieve a calculation to work out  $V_2$ . – 42

Figure 12: A comparative graph to show the dosage response of two marine derived GAGs on the K562 cell line using the MTT assay. – 44

Figure 13: A graph of U2OS cell line viability when Prawn GAGs were added and results recorded via the MTT assay. – 45

Figure 14: Cell viability of MDBK cells with various concentrations of Prawn GAGs added and results recorded via the MTT assay. – 46

Figure 15: Outlier corrected BEAS-2B MTT cell viability graph. – 48

Figure 16: Cell viability graph of MOLT-4 cells with prawn GAGs added and recorded via the MTT assay. – 48

Figure 17: Bovine Serum Albumin Standard Curve. – 49

Figure 18: K562 cell lysate affinity chromatography absorbance readings. – 50

Figure 19: K562 cell lysate affinity chromatography absorbance readings of the sham column. – 51

Figure 20: SDS-Gel of affinity fractions, stained with Oriole Fluorescent gel stain, 1-11 with the first column on the left being fraction 11 descending to the right down to fraction 1. – 52

Figure 21: An inversed image of the SDS-PAGE gel for fractions 1-11. – 52

Figure 22: Fractions 12-21 (left hand side 21 descending down to fraction 12 on the right) of the affinity chromatography on SDS-Gel stained with Oriole Fluorescent stain. – 53

Figure 23: Inversed image of the SDS-PAGE gel for fractions 12-21. – 54

Figure 24: Proton NMR (solvent suppressed) of prawn derived GAGs. – 55

Figure 25: Proton NMR (solvent suppressed) of Cockle derived GAGs. – 56

Figure 26: GRIL-LCMS of Heparin Sulfate. – 59

Figure 27: GRIL-LCMS of Chondroitin Sulfate. – 60

Figure 28: Chromatogram of monosaccharide analysis. – 61

Figure 29: Unsuppressed spectra of proton NMR of prawn extract. - 62



Figure 30: Alkynyl hydrogen diagram drawn via ChemDraw™. – 64

Figure 31: Alkyl Halide diagram drawn via ChemDraw™. – 65

Figure 32: Primary alkyl group drawn via ChemDraw™. – 66

Figure 33: Secondary alkyl group drawn via ChemDraw™. – 66

Figure 34: Tertiary alkyl structure drawn via ChemDraw™. – 66

Figure 35: MDBK MTT graph as shown in the results section but with the lowest eight concentrations excluded. – 77

Figure 36: BEAS-2B MTT cell viability graph of highest four concentrations. – 79

Figure 37: Cell viability graph of Wehi-3 cells when various concentrations of prawn GAGs were added and recorded via the MTT assay. – 81

Figure 38: Cell viability of SAOS-2 cell line when various concentrations of prawn GAGs are added and results recorded via the MTT assay. – 83

Figure 39: A graph of IC<sub>50</sub> versus the cell characteristics. – 85

Figure 40: IC<sub>50</sub> mean and range of cell lines when grouped based upon the sourcing of the cells. – 87

Figure 41: Comparing the mean and range IC<sub>50</sub>'s of the investigated cell lines when grouped as healthy and cancerous. – 88

Figure 42: IC<sub>50</sub> mean and range of human healthy and cancerous cells when prawn GAGS are added. – 89

Figure 43: Lysed bacterium stained with Coomassie Blue. – 99

Figure 44: SDS-PAGE gel loaded with affinity fractions 1-11 stained with silver lysate. – 99

Figure 45: Over-developed SDS-Page gel with silver stain. – 100

Figure 46: Molecular weight ladder with Oriole stain under the visible protein setting of the gel imager. – 101

Figure 47: Molecular weight ladder with Oriole stain under the fluorescent protein setting of the gel imager. – 101

Figure 48: SDS-PAGE gel stained with Oriole fluorescent stain and superimposed molecular weight marker to roughly estimate the separated proteins in the affinity fractions after the high salt concentration wash (2M NaCl in phosphate buffer). – 102

## List of Abbreviations:

ALL – Acute Lymphoblastic Leukemia

AML – Acute Myeloid Leukemia

APS – Ammonium Persulfate

BSA – Bovine Serum Albumin

CLL – Chronic Lymphocytic Leukemia

CML – Chronic Myeloid Leukemia

CS – Chondroitin Sulfate

DMSO – Dimethyl Sulfoxide

DNA – Deoxyribose Nucleic Acid

ETV6 – Translocation-Ets-leukemia Virus Protein

FBS – Foetal Bovine Serum

GAG(s) – Glycosaminoglycan(s)

HA – Hyaluronic Acid/Hyluronan

HGF – Human Growth Factor

HS – Heparin Sulfate

IC50 – Half-maximal Inhibitory Concentration

IL – Interleukin

KS – Keratin Sulfate

KSPG – Keratin Sulfate Proteoglycan

LCMS – Liquid Chromatography-mass Spectrometry

MAPT – Microtubule-associated Protein Tau

MTT – 3-(4-5-Dimethylthiazol-2-yl)-2,5-diphenyltetrazolium bromidefor

NMR – Nuclear Magnetic Resonance

OA – Osteoarthritis

PAK1 – p-21 Activated Kinase

PAX5 – B-cell-specific Activator Protein

PBS – Phosphate Buffered Saline

Ppm – Parts Per Million

p53 – Transformation-related Protein 53

RNA – Ribose Nucleic Acid

RPM – Revolutions Per Minute

RT – Radiotherapy

SDS-PAGE – Sodium Dodecyl Sulfate – Polyacrylamide Gel Electrophoresis

SRB – Sulforhodamine B

## Abstract:

The purpose of this study was to investigate the chemotherapeutic properties of marine derived glycosaminoglycans (GAGs) and investigate their mechanism(s) of action. The secondary purpose was to investigate differences between the already studied cockle derived GAGs and prawn derived GAGs.

Nuclear magnetic resonance (NMR) spectroscopy was employed to identify differences between the prawn and cockle derived GAGs. External monosaccharide and disaccharide analysis was also performed on the prawn GAGs. The MTT assay was employed to also investigate the chemotherapeutic differences between the two derived GAGs on K562 cancer cells. Furthermore, the MTT assay was employed to investigate the chemotherapeutic properties of the prawn derived GAGs on healthy and cancer cell lines other than K562. The final aspect of this investigation was using affinity chromatography to separate the cellular proteins that bind to the GAGs and to isolate and visualise them using sodium dodecyl sulfate polyacrylamide gel electrophoresis (SDS-PAGE).

The NMR spectroscopy showed the prawn extract to be a less complex extract than the cockle derived GAGs. The prawn GAGs also had an additional hydrogen environment at 2.5-3.0 ppm which could be of interest. The MTT assays showed that on K562 cells, cockle derived GAGs had an IC<sub>50</sub> 2.2 times lower than the prawn derived GAGs but both were both chemotherapeutic. The MTT investigation of the small sample size of cells overall insinuated a trend of GAGs being more cytotoxic towards cancer cells than healthy cells. Finally, on the SDS-PAGE gel, two individual bands of highly specific binding proteins to the GAGs were isolated between 2-10kDa.

To conclude, further investigations on prawn derived GAGs should be undertaken as they show potential to be a successful chemotherapeutic. Also, successful isolation of high specific binding proteins provide a base for an in-depth investigation into the mechanism(s) of action of the marine derived GAG(s).

## Introduction:

Glycosaminoglycans (otherwise known as GAGs) have long been of interest to researchers in a multitude of branches of science, especially drug design and discovery. GAGs are widely prevalent in the natural environment and have multiple mechanisms of action and uses ranging from angiogenesis, molecular recognition and interacting with growth factors amongst others (Lacetera, Galante, Jimenez-Barbero and Martin-Santamaria, 2016). GAGs are unbranched polysaccharides that are added to a protein core via the Golgi apparatus in a cell to form proteoglycans. GAGs consist of repeating disaccharides of a uronic acid and an amino sugar, with the uronic acid being substituted with sulfate groups (Slack, 2014). They are usually linear and sulphated with usual molecular weights between 10-100 kilodaltons (Kitic et al, 2016). Mammalian GAGs have been subject of many studies into their medicinal properties but for the first time in a recent research paper (Aldairi, Ogundipe and Pye, 2018) marine GAGs derived from shellfish were proven to have anti-cancer properties. This study aims to build upon the findings in this research study and build to further investigate the anti-cancer properties of these marine derived GAGs and to investigate why they are effective unlike their mammalian counterparts and if other marine sourced GAGs have similar anti-cancer properties.

## Cancer Epidemiology:

Cancer is a worldwide major cause of illness and death. A study into the epidemiology of cancer found that in 2012, there was an estimated worldwide 8.2 million deaths in relation to cancer with 14.1 million new cases being registered (Torre et al, 2016). Location plays a major role in the prevalence of specific types of cancer. In North and South America, along with north, west and south Europe, in

addition to Oceania, prostate cancer is the most prevalent among men, however in east Europe, it is lung cancer (Torre et al, 2016).

### Leukemia:

Leukemia can be defined as a type of blood cancer that derives from the bone marrow. Leukemia can be sub-divided into four main groups, acute lymphoblastic leukemia (ALL), chronic lymphocytic leukemia (CLL), chronic myeloid leukemia (CML) and acute myeloid leukemia (AML).



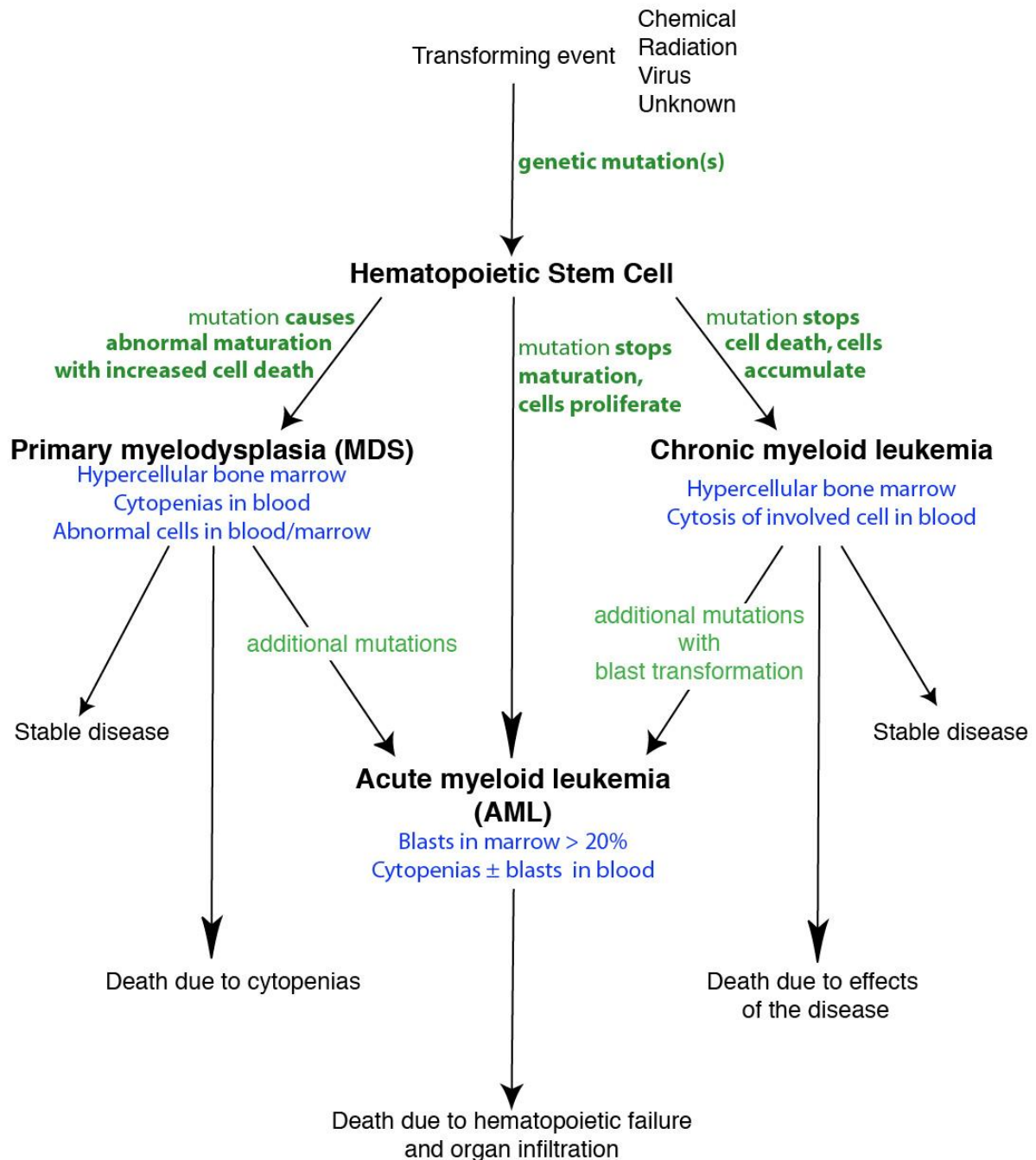


Figure 1: A flow chart of the pathogenesis of various leukemic syndromes (Cornell University College of Veterinary Medicine, 2013).

As shown in the figure above from Cornell University, a transforming event leads to genetic mutation(s) in a haematopoietic stem cell which can cause a variety of cellular developmental pathways to occur leading to the different types of leukemia. The four sub-groups of leukemia will be further discussed in the below sub-sections.

Rare germline mutations to genes such as p53, ETV6 and PAX5 can predispose people to the development of leukemia (Puckett and Chan, 2019).

### ALL:

Acute lymphocytic leukemia accounts for approximately 2 percent of registered lymphoid neoplasms in the United States (Puckett and Chan, 2019). ALL is a malignancy of the T or B lymphocytes which is characterized by uncontrolled proliferation of immature, abnormal lymphocytes and their respective progenitors leading to replacement of bone marrow elements and lymphoid organs resulting in a distinguishable disease pattern characteristic to ALL (Puckett and Chan, 2019). ALL etiology is unknown however polymorphic, somatic variants of IKZF1, CDKN2A and ARD5B genes have been shown to have an association with an increased risk of ALL (Puckett and Chan, 2019).

The common consensus on ALL is that after DNA damage, lymphoid cells experience uncontrolled growth and metastasise around the body and cause sequestration of lymphocytes and platelets in the spleen and liver which leads to splenomegaly and hepatomegaly (Puckett and Chan, 2019).

### AML:

Acute myeloid leukemia is the most common malignant myeloid disorder in adults (20000 cases per year in the United States as of 2016 (Kouchkovsky and Abdul-Hay, 2016)) and is defined as a heterogeneous clonal disorder of haemopoietic progenitor cells (Estey and Dohner, 2006). The majority of deaths with this disease are due to relapse; this is due to clonal evolution at the cytogenic level (Ding et al, 2012).

The mutated genes, usually large chromosomal translocations, in AML predominantly effect haematopoietic proliferation and differentiation which results in

poorly differentiated myeloid cells accumulating (Kouchkovsky and Abdul-Hay, 2016).

The mutations that occur in AML have been discovered and their prevalence calculated. The mutations and relative prevalence are as follows; Nucleophosmin 1 (25-30% of cases), DNA Methyltransferase 3A (18-22% of cases), Fms-Like Tyrosine Kinase 3 (20% of cases), Isocitrate Dehydrogenase (15-20% of cases), Ten-Eleven Translocation 2 (9-23% of cases), Runt-Related Transcription Factor (5-13% of cases), CCAAT Enhancer Binding protein alpha (6-10% of cases), Additional Sex Comb-Like 1 (5-11% of cases), Mixed Lineage Leukemia (11% of cases), Tumour Protein p53 (8-14% of cases), c-KIT (less than 5% of cases) and Splicing factors (20% of cases) (Saultz and Garzon, 2016).

#### CLL:

In Western populations, CLL is the most common adult leukemia and can be characterised by the proliferation of monoclonal B cells (Taneja and Master, 2019). The transformation into leukemia cells is initiated by impairment of apoptosis of clonal B cells (Hallek, 2017).

On a genetic level, it is believed disrupted p53 function and the over-expression of the ZAP-70 gene are two of the common genetic mutations that can cause CLL (Byrd, Stilgenbauer and Flinn, 2004).

CLL can be easily identified due to its' specific immunophenotyping. The typical B lymphocyte markers CD19, CD20 and CD23 will still be all present but in addition, 95% of all patients with leukemia exhibit the CD5 cell surface antigen as well. (Hus and Rolinski, 2015).

### CML:

Chronic myeloid leukemia in adults accounts for approximately 15% of all cases with forty percent of these patients being asymptomatic (Granatowicz et al, 2015). CML can be characterized by a genetic rearrangement known as the Philadelphia chromosome (Jabbour and Kantarijan, 2018). This is where the breakpoint cluster region on chromosome 22q11.2 fuses with the Abelson gene from chromosome 9q34 (Jabbour and Kantarijan, 2018). The resultant product of this fusion is an oncogene known as BCR-ABL1 which causes protein translation of the oncoprotein BCR-ABL1 (Jabbour and Kantarijan, 2018).

### Marine Polysaccharides:

There are a vast number of marine polysaccharides other than GAGs which can be extracted from marine bacteria, plants and animals. The most common and therapeutically used marine polysaccharides are; Ulvan, Galactan, Laminarin, Alginate, Fucoidan, Chitin, Chitosan, and Carrageenan (Mohan et al, 2019). When looking at these with an overarching broad view, they are involved in anticoagulant, anti-stress, antitumour, anti-inflammatory, antimicrobial, anti-stress, immunostimulant and antioxidant activities with also growth promotion effects (Mohan et al, 2019).

A substantial portion of these marine polysaccharides come from seaweeds and are found as follows;

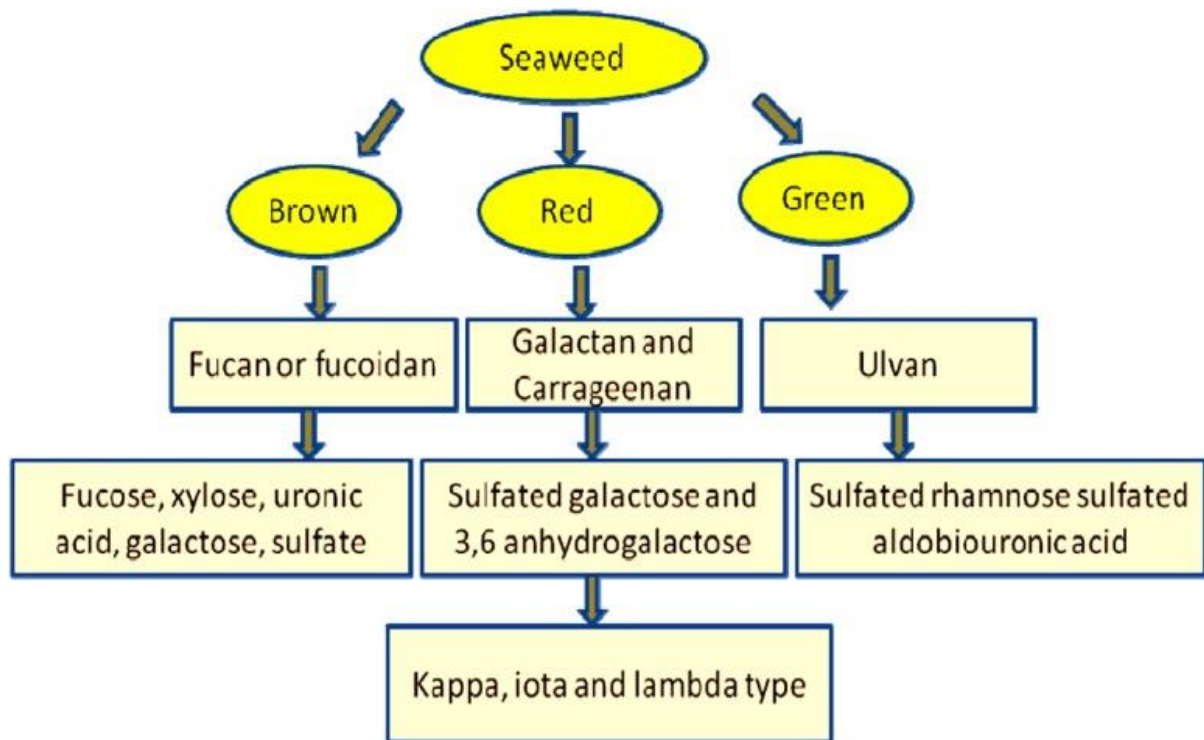


Figure 2: Bioactive sulphated marine polysaccharides from seaweed classification (Patel, 2012).

Laminarin is usually extracted from brown seaweed and is a water-soluble polysaccharide (Ojima, 2013). The below figure outlines the extraction process.

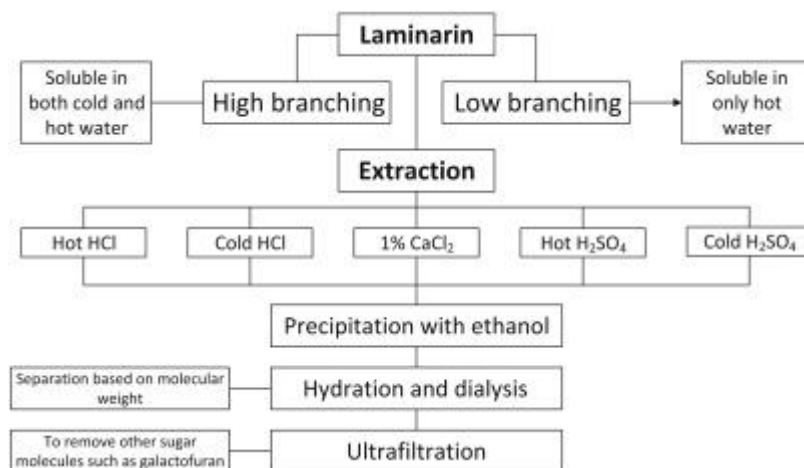


Figure 3: Laminarin extraction process (Deleris, Nazih and Bard, 2016).

Laminarin can be categorised by the present degree of branching. The highly branched oligomers are soluble in cold water with the isomers that are less branched being only soluble in warm water (Spicer et al, 2017). This composes of intrachain  $\beta(1-6)$  branching that is variable depending on the environment and harvest conditions (Spicer et al, 2017). Once extracted, Laminarin has been shown to provide anti-cancer benefits by inhibiting colony formation of SK-MEL-28 and DLD-1 cells of which both are cancerous and inducing apoptosis and inhibiting cancer cell proliferation in T-29 (colon) cells (Deleris, Nazih and Bard, 2016). Laminarin has also been shown to induce dendritic cell maturation in tumour draining lymph nodes and induces interferon gamma, tumour necrosis factor alpha and promotes the proliferation of the murine cell line OT-I and OT-II T-cells in tumours (Song et al, 2017).

Ulván is a soluble fibre sourced from green seaweed and is a cell wall polysaccharide (Kidgell et al, 2019). Ulván provides anti-inflammatory effects as well as antioxidant effects but more importantly it also exhibits anti-cancer properties (Kidgell et al, 2019). A multitude of murine and human cell lines have had apoptosis induced by extracted Ulván *in vitro* however no *in vivo* studies have yet to be carried out (Kidgell et al, 2019).

Ulván is also currently being researched into atherosclerosis treatment and has also been shown to reduce low density lipoprotein and very low-density lipoprotein cholesterol in rats (Patil et al, 2018).

Chitin is the most abundant polymer produced annually after cellulose (Lodhi et al, 2014). Chitosan is derived from the hard shells of crustaceans through degradation of chitin via enzymatic and acidic hydrolyses processes (Park and Kim, 2010) and

has potential to be used in cancer therapeutics (Babu and Ramesh, 2017). Chitosan has many other therapeutic uses as well which usually involve assisting other therapeutics.

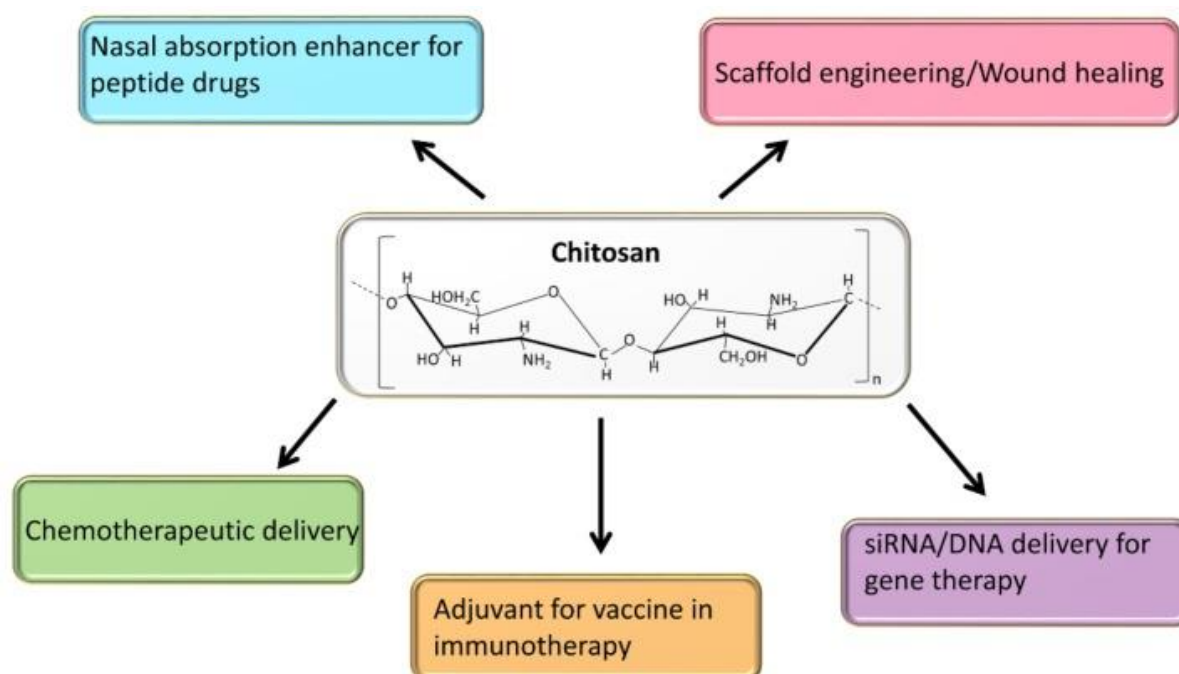


Figure 4: Medical uses of Chitosan and its' structure (Babu and Ramesh, 2017).

Chitosan can be used as an absorption enhancer and in scaffold engineering for drug delivery (Babu and Ramesh, 2017). Regarding cancer, chitosan is an immunoadjuvant for vaccines and can assist in gene and chemotherapeutic delivery (Babu and Ramesh, 2017).

Chitosan itself in nanoparticle form has been shown to exhibit anticancer activity in 293 different cancerous cell types and HeLa cells when mixed with copper in a 2:5 ratio (Adhikari and Yadav, 2018).

When Chitin is degraded into chitooligosaccharide, the solubility greatly increases and it exhibits new therapeutic benefits for diseases such as diabetes, Alzheimer's

and HIV-1 and has an increased absorption profile becoming completely absorbable in the intestinal epithelium (Naveed et al, 2019).

Alginates are present in the cell walls of brown seaweed and alginate like polysaccharides can be produced as an extracellular matrix by bacteria (Nesic and Seslija, 2017). For medicinal purposes, alginate is regularly used to form hydrogels for tissue engineering, wound healing and drug delivery (Lee and Mooney, 2012). From a pharmaceutical aspect, alginate is used as a thickening and stabilising agent, especially in medicines taken via an oral dose (Lee and Mooney, 2012).

Carrageenans are a branch of sulphated galactans that are sourced from red seaweed and are separated into three major types; kappa, iota and lambda (Williams and Phillips, 2003).

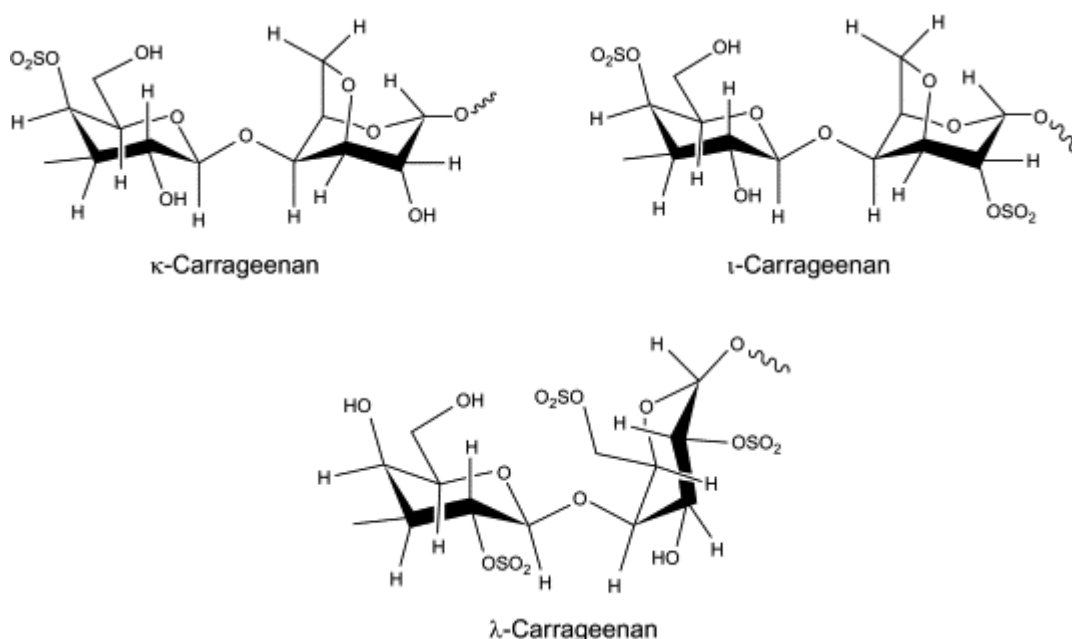


Figure 5: Carrageenan differing structures. (Kariduraganavar, Kittur and Kamble, 2014).

Carrageenans are usually used with meat and dairy products due to them forming gels and their strong binding interactions with proteins but therapeutically they can



also be used in gel form to offer protection against HSV-2 transmission as they bind to the receptors on the herpes virus (Kariduruganavar, Kittur and Kamble, 2014). It can also be administered as a proinflammatory agent via 10% concentration in drinking water for 10 days (Jamwal and Kumar, 2017). This however has only been tested in animal models so far.

Carrageenans are normally used to assist other therapeutics. They have high biocompatibility with a proportion of pharmaceuticals and can improve drug formulations with emphasis on prolonged drug release and can create temperature and pH sensitive drug delivery systems (Khan et al, 2017).

Fucoidan is usually found in brown seaweed, in the cell wall, and some marine animals and has been shown to have strong anticancer properties (van Weelden et al, 2019). Due to the diversity of brown seaweed, fucoidan has a diverse structure depending on its' source (van Weelden et al, 2019). Below is a figure illustrating the three most common forms.

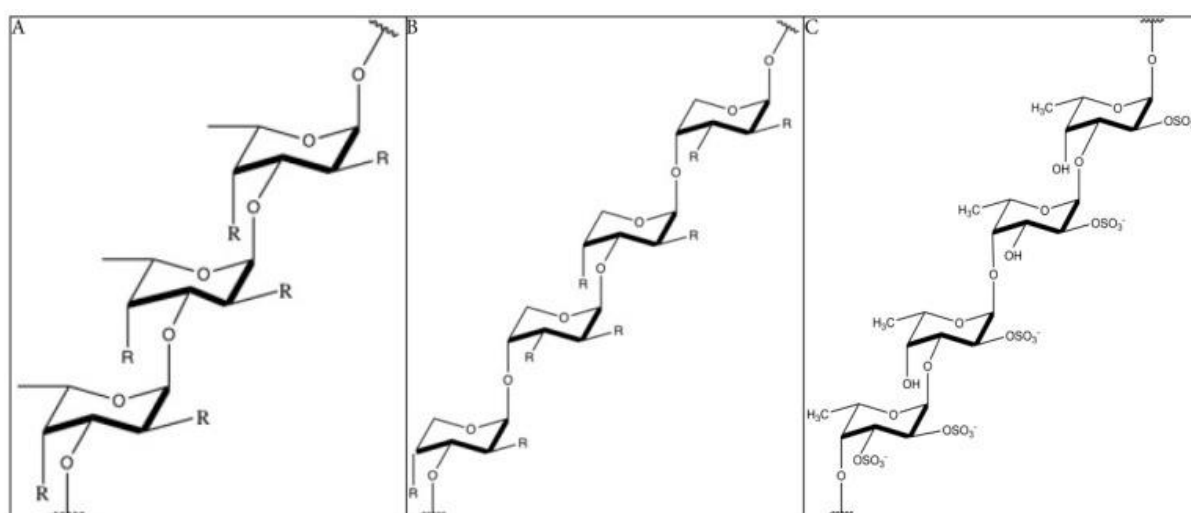
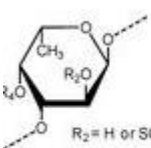
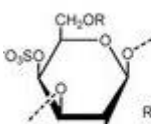
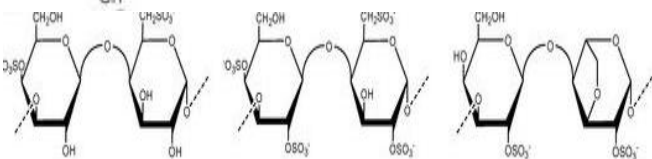
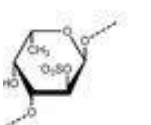
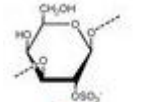
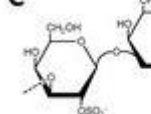
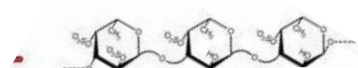
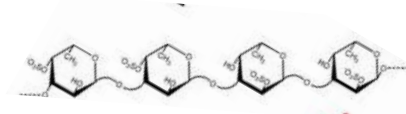
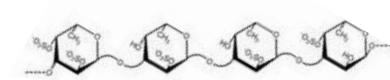


Figure 6: The three most common forms of Fucoidan. The R group can be either a sulfate group or a monosaccharide (van Weelden et al, 2019).

Fucoidan exhibits anticancer properties on a plethora of cell lines *in vitro* spanning multiple cancer types including: breast cancer, b-cell lymphoma, t-cell lymphoma, fibroblastic sarcoma, uterine sarcoma, lung cancer, hepatocellular carcinoma, colorectal cancer, keratinocytes, melanoma, bladder cancer, plasma cell myeloma, leukemia, stomach cancer, pancreatic cancer, ovarian cancer, endometrium carcinoma, prostate cancer and osteosarcoma (van Weelden et al, 2019). However, pharmaceutical studies have shown that as an individual treatment there are better alternatives, but its' interesting use could be as a non-toxic edible product which will therefore be easily administered and be able to deliver the active components (Fitton, Stringer and Karpiniec, 2015).

Most of these marine polysaccharides are found in seaweed. Another class of marine polysaccharides are GAG mimetics where the polysaccharides are not actual GAGs but can simulate the effects of them. These include, sulphated fucans and sulphated galactans. Like actual GAGs, their structure varies depending on where they are sourced from.

Table 1: Marine GAG mimetics structures\*

GAG mimetic	Source	Structure
Sulfated Fucan	<i>Ascophyllum nodosum</i> , <i>Fucus evanescens</i> , <i>Fucus vesiculosus</i> , <i>Ecklonia kurome</i>	 <p><math>R_2 = \text{H or SO}_3^-</math> (<i>Ascophyllum nodosum</i>, <i>Fucus evanescens</i>, <i>Fucus vesiculosus</i>)  <math>R_4 = \text{H or Fuc branch}</math> (<i>Fucus vesiculosus</i>); <math>R_4 = \text{H or SO}_3^-</math> (<i>Ecklonia kurome</i>)</p>
Sulfated Galactan	Green algae	 <p><math>R = \text{H or SO}_3^-</math> (minor)</p>
Sulfated Galactan	Red algae	
Sulfated Fulcan	<i>Strongylocentrotus franciscanus</i>	
Sulfated Galactan	<i>Echinometra lucunter</i>	
Sulfated Galactan	<i>Glyptocidaris crenularis</i>	
Sulfated Fucan-II	<i>Strongylocentrotus purpuratus</i>	
Sulfated Fucan	<i>Strongylocentrotus pallidus</i>	
Sulfated Fucan	<i>Lytechinus variegatus</i>	

\*All diagrams are sourced from Vasconcelos and Pomin, 2017.

As shown in the above table, differing species and genus of both marine algae, seaweed and invertebrates cause differing changes in the GAG mimetic polysaccharides present in the organism. This may lead to differing therapeutic benefits dependent on which organism the polysaccharide is extracted from.

### GAG Biosynthesis:

The biosynthesis of GAGs requires activated sulfate and sugar donors, and a vast array of biosynthetic enzymes (Victor et al 2009). Sulfotransferases have also been shown to play an important role as they generate the binding sites for the proteins to interact with the glycosaminoglycans (Kusche-Gullberg and Kjellen, 2003).

Depending on the contained oligosaccharide, GAGs are synthesised via three biosynthetic pathways (Sasarman et al, 2016). The first biosynthetic pathway is the one hyaluronic acid takes, which contains no linkers and is not attached to a core protein (Sasarman et al, 2016). Keratan sulfate follows the biosynthetic path of containing up to three linkers to residues in core proteins with O-linking to serine or threonine and N-linking to asparagine (Sasarman et al, 2016). The most common biosynthetic pathway is a tetrasaccharide linker O-linked to specific serine residues in the core proteins which is the pathway chondroitin sulfate, heparan sulfate, dermatan sulfate and heparin sulfate take (Sasarman et al, 2016).

### GAG Structures:

Once we separate the GAGs into the four major known classes, the backbone structure can be distinctly identified to help classify them.

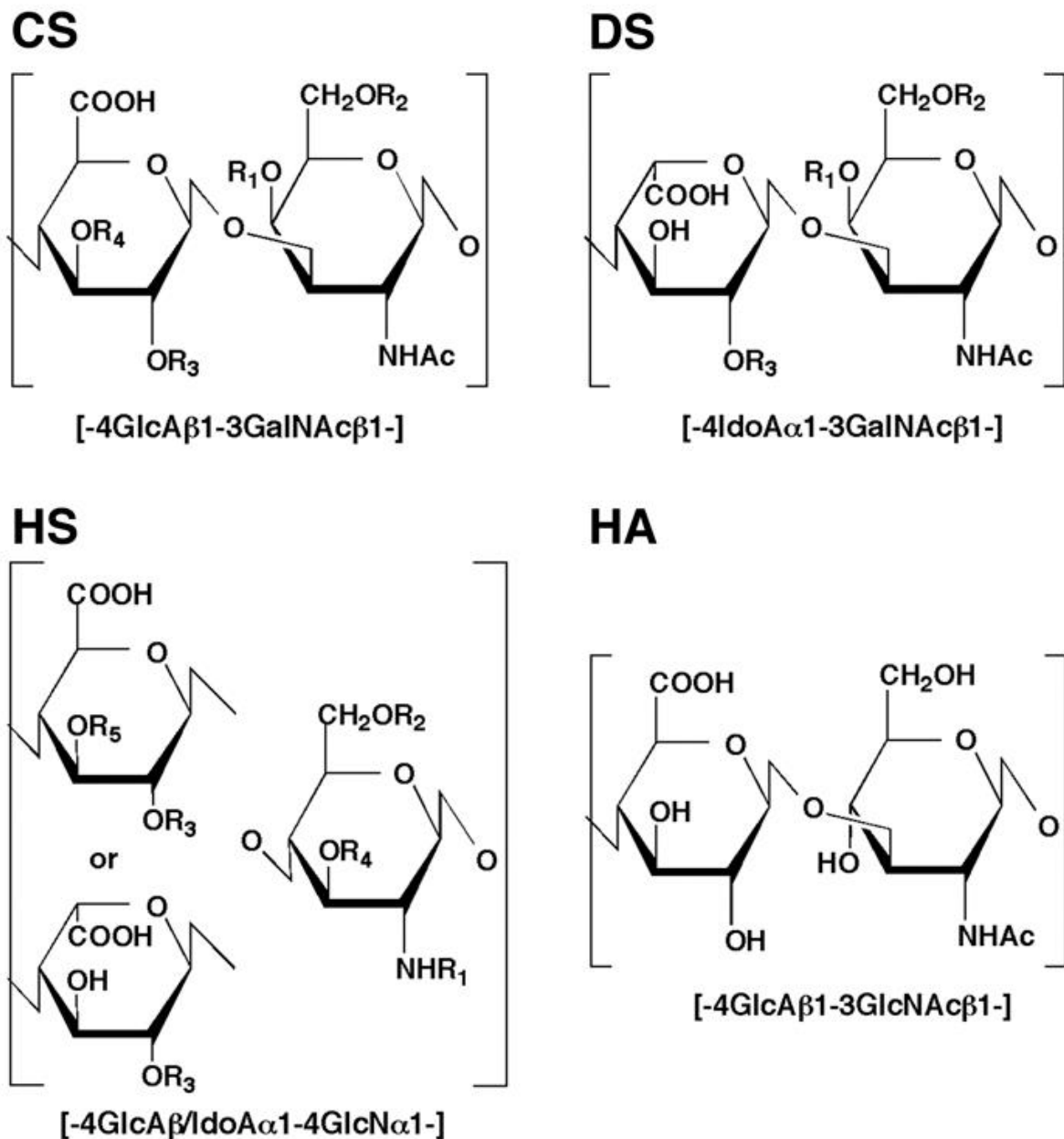


Figure 7: Backbone structure of GAGs (Yamada, Sugahara and Ozbek, 2011).

These four classes of GAG along with keratan sulfate have differing distributions depending on what animal source they have come from. These differing distributions may be one of the reasons that explain why GAGs from different sources using the same extraction method have differing therapeutic benefits.

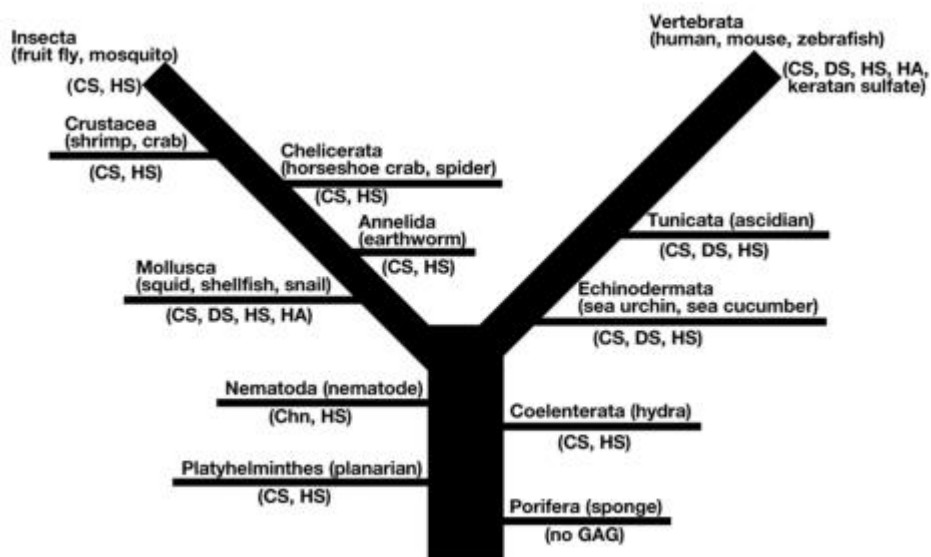


Figure 8: Distribution of GAGs based upon animal kingdom grouping (Yamada, Sugahara and Ozbek, 2011).

As shown by the figure above, Crustacea, which is where the GAGs are derived from for this study, have a different GAG distribution than mammalian Vertebrata GAGs with Vertebrata having additional DS, HA and keratan sulfate which the Crustacea derived GAGs should not possess.

#### GAG interactions:

GAGS can interact with a variety of ligands usually through HS which can cause physiological changes and effects (Varki et al, 1999). These effects range from binding to a signalling receptor to enzyme activity regulation to protein immobilisation (Varki et al, 1999). Below is a table that outlines some of the major proteins that can bind to GAGs.

Table 2: Proteins that can bind to GAGs (Varki et al, 1999.)

<b>Cell/Matrix Interactions</b>	<b>Coagulation/Fibrinolysis</b>	<b>Lipolysis</b>	<b>Inflammation/Growth</b>
Laminin	Antithrombin III	Lipoprotein lipase	FGFs and FGF receptors
Fibronectin	Heparin cofactor II	Hepatic lipase	Scatter factor (HGF)
Thrombospondin	Tissue factor pathway inhibitor	apoE	VEGF
Type I Collagen	Thrombin	LDL	IL-8/MIP-1B
Type III Collagen	Protein c inhibitor		TGF-B
Type V Collagen Vitronectin Tenascin	tPA and PAI-1		L and P selectins Superoxide dismutase

Studies have shown that between proteins and GAGs there will be strong ionic interactions, however it has been shown that ionic interactions only provide 40% of the binding energy with 60% coming from non-ionic interactions. (Gandhi and Mancera, 2008). The main forces involved are van der Waals, hydrophobic interactions with the carbohydrate backbone and hydrogen bonds (Gandhi and Mancera, 2008). With the binding proteins, statistical analysis indicates that Asn, Asp, Glu, Gln, Arg, His and Trp are the most likely amino acids to be involved in GAG binding, especially Trp as this can form an aromatic ring which packs against the hydrophobic face of the GAG (Gandhi and Mancera, 2008). When breaking this down even further to the amino acid residues, arginine binds 2.5 times more strongly than lysine as the guanidino group in arginine forms more stable hydrogen bonds and electrostatic interactions with sulfate groups (Gandhi and Mancera, 2008).

## Marine GAG Structures:

It has been reported that depending on the marine species the GAG is extracted from, the structure and therefore the function of the GAG differs. There is even variability amongst the same species with different genus having differing structures. Below is a table summarising different structures of marine GAGs and highlighting how different species and genus can alter the structure.

Table 3: Marine GAGs and associated structures\*.

GAG Type	Source	Structure
Holothurian Fucosylated Chondroitin Sulfate	<i>Pearsonothuria graffei</i>	
Holothurian Fucosylated Chondroitin Sulfate	<i>Isostichopus badionotus</i>	
Dermatan Sulfate	<i>Ascidia nigra</i>	
Dermatan Sulfate	<i>Stylea plicata</i>	
Heparan Sulfate	<i>Nodipecten nodosus</i>	
Heaprin/heparan sulfate hybrid	<i>Litopenaeus vannamei</i>	

\*All diagrams taken from Vasconcelos and Pomin, 2017.

As shown in the above table, even changes in the genus can affect the structural changes to the same GAG. Both holothurian GAGs come from different genus of sea cucumber and have slight structural differences. When making the change larger,



the *Nodipectin nodosus*, which is a scallop, has a much different structure of heparan sulfate compared to the shrimp (*Litopenaeus vannamei*) which contains a heparin/heparan sulfate hybrid instead. This may indicate variability in therapeutic ability depending on the source of the GAG and is something that is further investigated later in this study.

### Glycosaminoglycan Therapeutics and Cosmetics:

Glycosaminoglycans have long been studied and developed for cosmetic and therapeutic uses and have been said to be 'the most exploited carbohydrates in the pharmaceutical market' (Pomin and Mulloy, 2018). The following subject will delve into a brief overview of the current uses of glycosaminoglycans in a therapeutic and cosmetic setting.

Many glycosaminoglycans that have biological functions are side chains of proteoglycans and can be put into the major classes; hyaluronic acid/hyaluronan (HA), chondroitin sulfates (CS), heparin sulphate (HS) and keratin sulphate (KS) (Volpi, 2006). The following discussion will further explore these major groups independently and their current uses.

### Hyaluronic Acid:

Hyaluronic acid is the key molecule in skin aging due to its' unique role in retaining water (Papakonstantinou, Roth and Karakiulakis, 2012). HA is a non-sulphated GAG with a simple composition (Papakonstantinou et al, 2012). HA is a unique GAG in that it is not covalently attached to a protein core but it can in fact form aggregates with proteoglycans (Papakonstantinou et al, 2012). In biological systems, HA is synthesised by HA synthases, of which three varieties are found in mammals, which

are membrane bound proteins found on the inner surface of the plasma membrane which result in the release of the synthesised HA into the extracellular space (Papakonstantinou et al, 2012).

Hyaluronate is also a molecule that naturally occurs in the synovial fluid and cartilage of mammals (Bowman et al, 2018). The main functions of this molecule differ between the synovial fluid and the cartilage. In the synovial fluid, it acts as a free radical recruiter, regulator of binding of proteins and act as a lubricant (Bowman et al, 2018). In the cartilage, it once again regulates the binding of proteins and acts as a filler of space to help keep the joints open (Bowman et al, 2018).

As shown above, HA plays a major role in two biological systems and processes. Due to this, it has been researched and developed based upon its' biological function to investigate whether or not it can be used as a therapeutic in the case of cartilage diseases and cosmetic in regard to the role in skin aging.

Viscosupplementation (also known as intraarticular hyaluronate injection) is a non-surgical therapy for patients under the suffering of osteoarthritis (OA) (Zhu, Lei and Hu, 2015). Due to HA's role in joint lubrication, an injection of HA can provide a short term benefit of increased lubrication in the joint (Zhu et al, 2015). This is effective due to the pathogenesis of OA. OA causes the depolymerisation of endogenous HA to a lower molecular weight which decreases its' viscoelastic properties (Bowman et al, 2018). By replacing this HA with an injection it provides the patient with a short term supply of higher molecular weight HA until the condition of osteoarthritis causes it to be depolymerised again. However, this treatment has limitations based upon the patient. It is dependent on the levels of hyaluronidases in the patients' synovial fluid

as these cleave HA into smaller pieces making degradation more efficient of HA (Bowman et al, 2018).

HA is also used cosmetically in injections. Due to its' nature as a space filler, it can be used to improve wrinkles and the appearance of scars, and used as a dermal filler. The cosmetic HA is produced by the fermentation of bacterial streptococci and as a result has no species specificity negating the risk of an allergy developing or being triggered (Andre, 2004). As it is biodegradable, no skin testing is also needed (Andre, 2004). The only biochemical modification that needs to be done to the bacterial sourced HA is stabilization to increase the half-life or to increase the ability to fill space (Andre, 2004). A final use of HA injections is dermis and superficial dermis injections to hydrate as opposed to fill the skin (Andre, 2004).

#### Keratan Sulfate:

Keratan sulphate is a naturally occurring proteoglycan (GAG bound to protein core) in mammals that occur in the extra-cellular matrix and on the membrane surface of cells (Olgierd et al, 2019). They are found in the cornea, skeleton and cerebrum and are divided into three major classifications KSI, KSII and KSIII accordingly (Olgierd et al, 2019). It is highly expressed in the bone and cartilage whereas it is not found at all within the mature nervous system with the exception of the cornea (Willerth, 2017).

Morquio syndrome is a medical condition where there is a build-up in tissues, specifically the cornea and cartilage, of keratin sulfate due to the deficiency of either beta-galactosidase or N-acetyl-galactosamine-6-sulfate sulfatase (Kumari, 2018). This leads to defective degradation of keratin sulphate which causes malformations and mental retardation (English and Ettehadgui, 2010).

Therapeutically, keratin sulfate could be targeted as post injury to the central nervous system, it is expressed and participates in glial scarring (Willerth, 2017). Glial scarring is a major therapeutic problem due to its inhibitory nature and blockage of regeneration of neurons via a chemical and physical barrier (Wang et al, 2018). Targeting the synthesis of keratin sulphate may allow for modifications to overcome or lessen these barriers (Willerth, 2017).

Intraperitoneal injection of KS has been shown to reduce cartilage damage and decrease cartilage fragility (Pomin, 2015). Pomin, 2015 also briefly explains how KS plays a role in Burkitt's Lymphoma which is further discussed in the following section on current uses of GAGs in cancer.

#### Chondroitin Sulfate:

A major component of the ECM in nearly all connective tissues is chondroitin sulphate (Henrotin et al, 2010).

*In vitro*, CS has been shown to inhibit synthesis of nitric oxide synthase, microsomal prostaglandin synthase and cyclooxygenase which are all inflammatory intermediates (Henrotin et al, 2010). Due to this inhibition, chondroitin sulfate can be used as a treatment for osteoarthritis. It has also been shown to act upon toll like receptor 4 to inhibit inflammatory cytokines and tumour necrosis factor (Henrotin et al, 2010).

#### Heparan Sulfate:

Heparan sulfate chains covalently attach to a core protein to form heparin sulfate proteoglycans which are glycoproteins found in the extracellular matrix and at the cell surface (Sarrazin, Lamanna and Esko, 2011).

The main and most well-known use of heparin sulfate is the use of heparin as an anti-coagulant which is usually administered subcutaneously or parenterally with ongoing research into oral administration (Paliwal et al, 2012). These are usually unfractionated and/or low molecular weight (Paliwal et al, 2012).

Heparin plays a role in tauopathologies such as Pick's disease, Alzheimer's disease and progressive supranuclear palsy (Naini and Soussi-Yannicostas, 2018). These diseases are caused by hyperphosphorylation and aggregation of microtubule-associated protein tau (MAPT) (Naini and Soussi-Yannicostas, 2018). The discovered tau aggregates are associated with heparin sulfates which are highly sulphated polysaccharides (Naini and Soussi-Yannicostas, 2018). Potential therapeutics regarding this are being investigated, with emphasis on targeting Heparinase and Heparinase 2 (Lorente-Gea et al, 2017).

#### Current Cancer Treatments:

Currently, there is a plethora of cancer treatments that can be used individually or as a combination. These include but are not limited to; radiation, chemotherapy, surgery, immunotherapy and targeted treatments (Huang et al, 2017).

#### Radiotherapy:

Approximately two thirds of cancer patients undergo radiotherapy as part of their cancer treatment plan (Berkey, 2010). The basic principle behind radiation therapy (known as radiotherapy or RT) is the usage of ionizing radiations to treat malignancies (Mehta et al, 2011). The cellular death pathway/mechanism due to radiation therapy is an area of interest still under study by many scientists globally, however, the main consensus is that the radiation causes double stranded breaks in the DNA (deoxyribose nucleic acid) in the cancerous/targeted cells (Mehta et al,

2011). In a clinical situation, the radiation damage is caused indirectly due to radiolysis of the cellular water which forms free radical intermediaries (Mehta et al, 2011). The overall goal of radiation therapy is to maximize the radiation exposure to cancerous cells whilst minimizing the exposure to normal cells (Baskar et al, 2012). Differential cancer cell death is usually achieved due to the differences in the rate of repair between healthy and cancer cells (Baskar et al, 2012). Cancer cells are much less efficient at repairing themselves after cellular damage than their healthy counterparts (Baskar et al, 2012).

Radiotherapy, like the majority of current cancer treatments, has a variety of adverse side effects. The majority of side effects from radiotherapy include; depression and cancer related fatigue, radiation dermatitis, cardiovascular disease, radiation pneumonitis, radiation esophagitis, radiation induced emesis, chronic radiation cystitis, and erectile dysfunction in males and vaginal stenosis in females (Berkey, 2010).

#### Immunotherapy:

Cancer immunotherapy is a precision medicine branch of cancer therapeutics. The main components of cancer immunotherapy are immune checkpoint inhibitors, precision cancer cell killers via tumour antigen recognition (Tumour infiltrating lymphocytes, CAR T cells and TCR T cells) and cancer vaccines derived from tumour cell DNA, RNA or oncolytic viruses or patient derived dendritic cells (Liu and Guo, 2018).

Cancer cells can activate multiple immune checkpoint pathways that have immunosuppressive functions (Darvin et al, 2018). Monoclonal antibodies can target these checkpoints and negate the activation by the cancer cells (Darvin et al, 2018).

So far, PD-1/PD-L1 and CTLA-4 inhibitors have shown positive results in recent studies (Darvin et al, 2018).

Tumour infiltrating lymphocytes are found in tumours, leading to the hypothesis that tumours cause an immune response in the patient which is mediated by tumour antigens which in turn distinguish the cancer cells from the healthy cells and therefore provide an immunological target (Gooden et al, 2011).

TCR-T cells are engineered T cells that can mediate tumour lysis and eradication due to the engineering (Ping, Liu and Zhang, 2018). CAR T cells are engineered for the chimeric antigen receptors (CARs) and are more potent than TCR-T cells but are limited to membrane antigens which only represent 1% of total proteins expressed in the cancer cells (Walseng et al, 2017).

Cancer vaccines promote tumour specific immune responses with emphasis on CD8 positive T cells which show specificity to tumour antigens (Butterfield, 2015).

Provenge, which is personalised dendritic vaccine sipuleucel-T and Prostac-VF which is recombinant viral prostate cancer vaccine PSA-TRICOM have been approved for clinical use (Thomas and Prendergast, 2016). Unlike traditional vaccines which provide immunity to a pathogen, cancer vaccines work to help clear the body of the cancerous cells (Thomas and Prendergast, 2016).

### Chemotherapy:

Chemotherapy is the usage of cytostatic drugs either orally or intravenously which stop the uncontrollable division of cancer cells (IQWIG, 2016). There are four different types of chemotherapy;

Adjuvant chemotherapy targets leftover undetectable cancer cells after surgery,

Curative chemotherapy has the aim of a complete cure from the cancer,

Palliative chemotherapy is the alleviation of cancer effects when the disease is incurable,

Neoadjuvant chemotherapy is the reduction of an inoperable cancer to allow it to be operated upon (IQWiG, 2016).

Chemotherapy however is well renowned for its' adverse side effects. The most common side effects of chemotherapy are as follows; chest pain, constipation, diarrhoea, dyspnoea, fatigue, mucositis, pain, rashes, vomiting and hair loss (Pearce et al, 2017).

#### Leukemia Treatments:

Leukemia treatments can vary depending on what sub-group of leukemia the patient is suffering with.

For CML, if the disease is in the chronic phase, there are four tyrosine kinase inhibitors that are a highly effective treatment. These are imatinib, bosutinib, dasatinib and nilotinib (Eden and Coviello, 2019). Generically speaking, tyrosine kinase inhibitors work via the mechanism of competitive ATP inhibition at the catalytic binding site of tyrosine kinase (Hartmann et al, 2009). However, depending on the inhibitor, they exhibit a range of pharmacokinetics and adverse effects (Hartmann et al, 2009).

However, like most anti-chemotherapeutic drugs on the market, tyrosine kinase inhibitors do not come without adverse side effects. These side effects include but are not limited to; thrombopenia, anaemia, neutropenia, diarrhoea, vomiting,



oedema, nausea and hypothyroidism amongst the most common ones (Hartmann et al, 2009).

ALL, like CML, can be treated with tyrosine kinase inhibitors if it is a recurrent malignancy (Hartmann et al, 2009).

For CML, to prevent recurrence, central nervous system prophylaxis can be undertaken (Penalver et al, 2017). This is delivered via the intrathecal route targeting specifically the leptomeningeal compartment (Penalver et al, 2017). Alternatively, IT methotrexate prophylaxis can take place between chemotherapy cycles in 12mg doses for a total of 4-8 doses (Penalver et al, 2017).

For some instances of AML and ALL, allogenic haematopoietic stem cell transplant can be a treatment option (Talati and Sweet, 2018). Initially, this treatment was used for patients with late-stage leukemia when all other treatments had failed, however recent breakthroughs in medicinal knowledge and research have made this treatment a potential therapeutic for a variety of haematopoietic malignancies (Gyurkocza, Rezvani and Storb, 2010). This treatment is the transplantation of donor haematopoietic stem cells to reconstitute haematopoiesis (Gyurkocza, Rezvani and Storb, 2010).

Alternative research has also targeted leukemic stem cells directly. RNA interference or small molecule inhibition of p-21 activated kinase (PAK1) has been shown to have very positive effects on the inhibition of leukemia both *in vitro* and *in vivo* (Pandolfi et al, 2015). This is due to the identification of PAK1 being a downstream effector molecule for the HLX gene which is a functional gene in AML pathogenesis (Pandolfi et al, 2015).

### Current GAGs in cancer therapeutics:

In Burkitt's lymphoma, keratin sulfate proteoglycans (KSPG's) have been found to play a part in radiation therapy resistance (Pomin, 2015). It has been found that levels of GlcNAc 6-O sulfation reduce radiation induced apoptosis of the cancerous cells (Pomin, 2015). Potentially a combination therapy could be investigated and developed based upon this by combining a keratin sulfate suppressor/degrader in Burkitt's lymphoma, thereby increasing susceptibility to radiation therapy, with radiotherapy.

Yamada and Sugahara in 2008 explained how CS chains may be involved in tumour proliferation and metastasis and hypothesise how detecting and identifying these chains may lead to vital information to discovering new chemotherapeutics.

Heparan sulfate mimetics is a new branch of oncological research ongoing to investigate how GAGs and GAG mimics can alter the role GAGs play, especially heparin sulfate binding proteins, in cancer growth and progression (Lanzi and Cassinelli, 2018).

### Method Theories:

The next few sub-sections of the introduction outline the theories behind the techniques and help to elaborate as to why they were employed for this study.

### SDS-PAGE:

Sodium Dodecyl Sulfate Polyacrylamide Gel Electrophoresis (SDS-PAGE) is a molecular biology technique/assay that is used to separate proteins between 1-100kDa and is the most widely used method for separating proteins 30kDa in size or below (Schagger, 2006). Polyacrylamide gel electrophoresis is usually used to

separate molecules by charge and size (Brunelle and Green, 2014). SDS-PAGE separates protein molecules by size and does this via the presence of SDS which is a denaturing detergent which affects secondary and nondisulfide-linked tertiary structures by coating them with a negative charge in correlation with the length of the protein molecule (Bruelle and Green, 2014). 2-mercaptoethanol is present in the loading buffer with the samples as a reducing agent which reduces the disulfide bonds present (MBL Life Science, 2017). The combination of both of these chemicals present in the loading buffer linearize the protein molecule into a negatively charged rod roughly proportionate to the molecular weight of the protein (Smith, 1984).

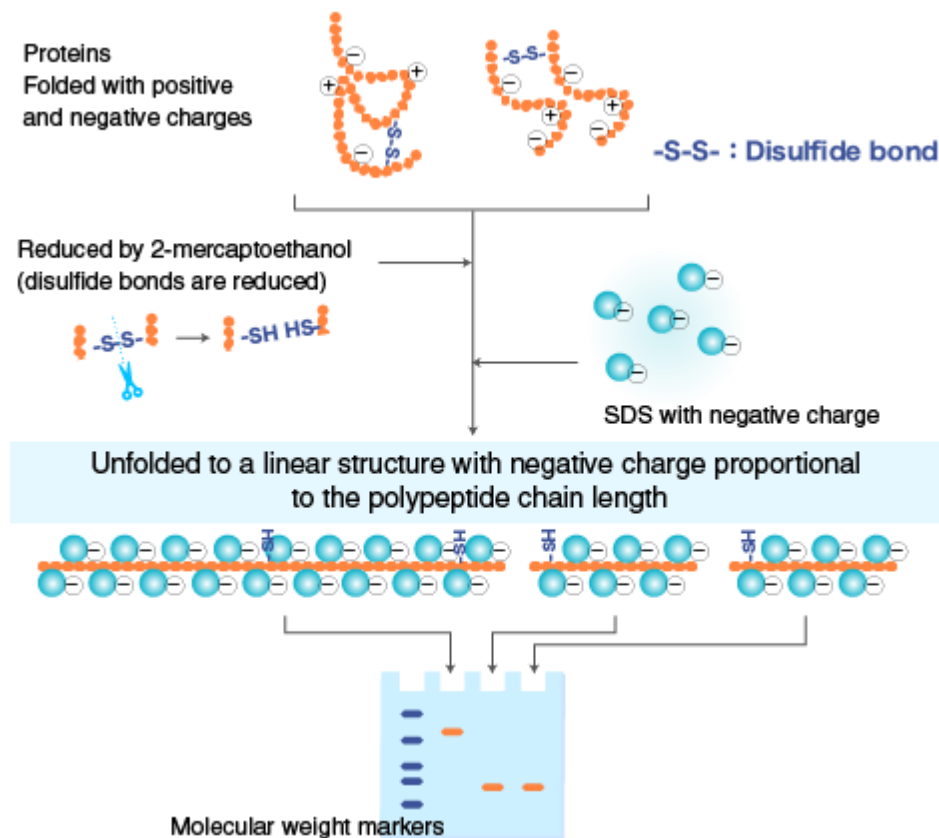


Figure 9: A graphic showing how 2-mercaptoethanol and sodium dodecyl sulphate reduce and linearize the protein molecules to be used on an SDS polyacrylamide gel (MBL Life Science, 2017).

The variation of SDS-PAGE used in the protocol later detailed used both a stacking gel and a resolving gel. The stacking gel has a lower concentration of polyacrylamide (4% for this study) and a different pH which allows the proteins to migrate through the gel faster and for a thin, concise band (Brunelle and Green, 2014). The resolving gel contains a higher concentration of polyacrylamide and like its' namesake, resolves the proteins by separating them according to size. Smaller proteins migrate faster through the gel and larger proteins migrate slower, resulting in separation of protein molecules according to their molecular weight (Brunelle and Green, 2014).

### Affinity Chromatography:

Affinity chromatography is a biochemical technique in which the reversible bio specific interactions between a ligand and the corresponding molecular species are used to separate said species from the biological milieu being studied (Mayers and Carel, 1998). The principle behind affinity chromatography is similar to most chromatography techniques. Affinity chromatography is usually performed in small columns (Goding, 1996). In the instance of this research investigation, the stationary phase the columns were packed with was affi-gel 10 beads that had been linked with the prawn derived GAGs.

The stationary phase is the component in chromatography which enables the separation of the components in the sample added. The stationary phase will always be a solid phase or a solid support with an absorbed liquid layer (Coskun, 2016).

Affi-gel 10 requires a ligand with a free alkyl or aryl amino group to couple with it. Due to the extraction process of the prawn derived GAGs, the GAGs are attached to small protein units that had been 'chopped' up by the alcalase enzyme in the extraction procedure. This protein core provides the free amino group which then displaces the N-hydroxysuccinimide and forms a stable amide bond (Bio-Rad, 2019).

The coupling of the ligands to the affi-gel beads is dependent on various factors that increase or decrease coupling efficiency. Affi-gel 10 is optimised for coupling the ligands near or below their isoelectric point (Bio-Rad, 2019).

Temperature for ligand coupling should always be kept at 4 degrees Celsius as this will not denature the ligands and also slows down the reaction rate to ensure a controlled coupling procedure.

The other two major factors are coupling time and ligand concentration. Coupling should always be attempted in saturation to ensure a maximum coupling concentration has taken place. Coupling usually is fully completed within 4 hours for affi-gel 10 but can be left safely overnight due to the stability of the molecules.

Due to the way the ligands are bound to the affi-gel beads via amide bonds, the stationary phase now consists of a solid gel medium made up of the affi-gel beads that have the prawn derived GAGs branching out into the spaces between the beads meaning any mobile phase and samples that are passed through the solid stationary phase have to pass the prawn derived GAGs.

In affinity chromatography, once the now coupled stationary phase is put inside the column, the sample for purification/separation is then added. In this instance, total cell protein lysate is added to the column in an amount equivalent to what fractions are to be taken. The GAGs usually bind to the cellular proteins via electrostatic interactions between uronic acids and negatively charged sulphate groups and via the proteins, positively charged amino acids (Esko, Prestegard and Linhardt, 2017). The excess unbound 'free' proteins pass through the stationary phase and exit into a collection eppendorf.

The bound proteins can be eluted by altering the ionic strength of these bonds between the GAGs and the cellular proteins, which can be done via altering the pH or adding a salt solution (Coskun, 2016). The concentrations used in this study are discussed in both the affinity chromatography methods and discussion sections.

Sham columns are usually employed as a negative control using an unlinked stationary phase as a negative control to help confirm that the results are due to the altering of the mobile phases and not just happening anyway.

### MTT Assay:

The MTT (3-(4,5-dimethylthiazol-2-yl)-2,5-diphenyltetrazolium bromide) tetrazolium reduction assay is a very common cell viability assay used in laboratories and was the first homogenous cell viability assay that was suitable for a 96 well format and high-throughput screening (Riss et al, 2013). Cell viability is defined as the number of healthy cells in a sample, in the case of the MTT assay, this is a well on the 96 well plate (Adan, Kiraz and Baran, 2016). To summarise this assay, viable cells that have an active metabolism will convert the MTT reagent via the mitochondria into a purple crystal known as formazan which has a near maximum absorbance at 570nm (Riss et al, 2013). The non-viable/dead cells will not convert the MTT reagent into formazan. Using a spectrophotometer, an absorbance reading at the near max can be recorded after the formazan is solubilised. There are many ways to solubilise MTT reagent such as but not limited to; DMSO, SDS, acidified isopropanol and dimethylformamide (Riss et al, 2013). By using controls at 100% cell viability and 0% cell viability, absorbance readings can be converted into a percentage of cell viability based upon this and be used comparatively against a multitude of differing experimental conditions and variables such as concentration of chemical/pharmaceutical added to cells, type of cells tested and media the cells are grown in to name a few. All this depends on other experimental conditions remaining consistent, especially amount of cells per well and incubation time both before adding the MTT reagent and afterwards.

This assay is also used to determine the half-maximal inhibitory concentration (IC<sub>50</sub>) of chemotherapeutic agents and is essential for discovering the biological and pharmacological properties of said agent (Yifeng et al, 2016).

### Aims:

This thesis is focused on investigating the extraction of GAGs from marine sources and investigating how they bind to cancerous (K562 leukemia) cells and investigate their potential efficacy on other cells both cancerous and healthy.

To explore these concepts the following procedures were used;

Chemical extraction was performed and undertaken on the common cockle (*Cerastoderma edule*) via various chemical additions and centrifugations followed finally by dialysis and lyophilisation with a freeze dry machine to form a soluble powder.

Nuclear magnetic resonance was undertaken on the extracted sample to visualise the extracted compound(s).

K562 cells were cultured and lysed to expose and make all internal and external components of the cell accessible for the GAGs to bind to during affinity chromatography.

Affinity chromatography coupled with SDS PAGE was used to show and isolate which cellular proteins the GAGs were binding to and to prove specific binding was occurring.

MTT assays were used on various cell lines to determine an IC<sub>50</sub> (if applicable) of the extracted marine GAGs to investigate their cytotoxicity.

External monosaccharide and disaccharide analysis was undertaken to help understand the components and structure of the GAG extract.



The following chapters present how all of this occurred and discusses the findings.

### Methods:

#### GAG Extraction:

The common cockle (*Cerastoderma edule*) and prawn were the marine species used for the GAG extraction. The purchased cockles had already been deshelled so were ready for defatting. The defatting occurred by incubation in acetone for 72 hours and then subsequently left to dry for a further 24 hours. A blender was then used to grind the dried defatted cockles into a soluble powder. 4 grams of this powder was removed and dissolved in a solution of 40ml of 0.05M sodium carbonate (pH 9.2) and 2mL of Alcalase enzyme. This was submersed in an oil bath set at 60 degrees Celsius whilst being agitated at 200rpm for 48 hours. The resulting product was cooled to 4 degrees Celsius and 5% trichloroacetic acid (2.1g) was added. This was centrifuged at 8000 rpm at 4 degrees Celsius for 20 minutes and the supernatant was removed and retained with the precipitate being discarded. Triple the supernatant volume of ethanol was added and 5g of 5% potassium acetate was added per 100ml of added ethanol. This was left at 4 degrees Celsius overnight. This was then centrifuged at 8000rpm for 30 mins at 4 degrees Celsius and the resulting supernatant discarded. The precipitate was dissolved in 40mL of 0.2M NaCl and centrifuged again using the same settings as last time. Any insoluble material formed a precipitate and was removed. 0.5mL of a 5% Cetylpyridinium chloride solution (5g in 100mL distilled water) was mixed with the supernatant and subsequently centrifuged with the same settings again. Once more the precipitate was recovered and the supernatant discarded. This was then dissolved in 10mL of 2.5M NaCl solution and 5 times the volume of the sample of ethanol was added. This was

centrifuged at 10000rpm for 30mins at 4 degrees Celsius and then dialysed for 72 hours. Finally, this was frozen in a freezer then placed into a freeze-dry machine overnight to produce a powdered GAG extract. For large scale extraction the measurements were scaled up accordingly.

#### Nuclear Magnetic Resonance:

The now powdered GAG was dissolved in deuterium water inside a nuclear magnetic resonance (NMR) tube and heated with a hairdryer to aid dissolution. This was then placed into an NMR machine to obtain an NMR spectrum for the extracted compound(s). The samples were then recovered using a rotary evaporator to evaporate the solvent and recover the GAG.

#### Cell Culturing:

The cell lines initially used were K562 Chronic Mylogenous Leukemia cells. These were cultured in RPMI-1640 medium. Additionally added to this medium was 1g/L of glucose and inactivated FBS. Penicillin and Streptomycin was also added to the medium to prevent unwanted bacterial growth. Before passaging, cells were observed under a microscope to confirm confluence. Cells were passaged in sterile cabinet and incubated in T75 flasks in an environment of 95% oxygen and 5% carbon dioxide at 37 degrees Celsius. K562 are suspension cells so passaging began with the centrifugation of the contents of the T75 flask for 5 minutes at 1500rpm. After centrifugation the supernatant was discarded and the cell pellet was re-suspended in pre-warmed media in a 20ml sterile tube. The contents of this tube was then evenly split into T75 flasks and pre-warmed media was then added to the T75 flasks to make up a final volume of 25ml in each flask. These were then placed into the incubator until confluence was observed. The cells were also cryogenically

preserved at -80 degrees Celsius after being mixed with FBS once a large number of T75 flasks containing cells at confluence were obtained.

#### Cell Lysis:

Once the cells had achieved confluency they were lysed. The cells were centrifuged at 2000rpm for 5 minutes and the supernatant discarded. The pellet was then washed in cold PBS. This was repeated 3-5 times. The supernatant was discarded and 2ml of cold RIPA buffer was added to the pellet. The pellet was suspended in the RIPA buffer and sonicated at regular intervals whilst being incubated in ice for a further 5-10 minutes. The solution was then centrifuged at 14000rpm for 15 minutes at 4 degrees Celsius. The insoluble cell debris was then discarded and the supernatant frozen at -80 degrees Celsius for future use.

#### Protein Quantification:

The cell lysate could be quantified for protein present. Protein standards were made up using BSA (bovine serum albumin). To these standards, a uniform amount of Bio-Rad reagent was added. The absorbance was then measured at 595nm wavelength in a spectrophotometer. These standards and their relative absorbance were used to make a standard curve. Bio-Rad reagent was then added to a set amount of cell lysate and its absorbance measured at 595nm wavelength. The standard curve was then used to quantify the amount of protein in the cell lysate.

#### SDS PAGE:

To begin with, the following was mixed together;

This was then poured into 2 casting stands and overlaid with deionised water to form a flat surface. This was left for 45 minutes to set and the water poured off the top.

The following was then mixed together;

Table 4: SDS-PAGE gel formula

<b>Reagent</b>	<b>Measurement</b>
dH <sub>2</sub> O	6.1ml
0.5M Tris HCl pH 6.8	2.5ml
30% Acrylamide Solution	1.3ml
10% SDS	100ul
10% Fresh APS	50ul
TEMED (Polymerising Agent)	10ul
TOTAL VOLUME	10ml

This was then poured over the separating gel and a comb inserted into the top to form wells. Once again, this was left to set for 45 minutes.

The gels were then placed into a holder inside the SDS-PAGE tank and locked into place to form a water-tight seal.

SDS running buffer was poured into the inner chamber of the set-up so the gels were submerged.

The protein samples were mixed with a standard SDS loading buffer in a 1:1 ratio and 10 microlitres of each sample was loaded into each corresponding well on the gel.

The outer chamber was then filled with SDS running buffer up to the fill line and the experiment was left to run at a constant voltage of 200 volts for approximately 30-45 minutes depending on the speed of travel of the samples through the gel.

The gels were then freed from the glass plating and submerged in Oriole Fluorescent Gel Stain in a darkened box and left to agitate for 90-120 minutes.

The gels were then washed in de-ionised water and imaged in a suitable imaging device that had an ethidium bromide filter.

### MTT Plating and Reading

For consistent scientific results, the MTT plates were plated at a cell density of 5000 cells per well. 10 microliters of the cultured cells were taken and mixed in a 1:1 dilution with Trypan Blue. 10 microliters of this mixture was then pipetted onto a C-chip/haemocytometer.

To begin with a total cell count was taken by counting all alive cells in the four corner quadrants of a C-chip. (Alternative haemocytometers will work if a corner quadrant corresponds to 0.1 microlitres). The average of the four was then taken. The dilution factor (1:1) was then accounted for to acquire a value of average alive cells per 0.1 microlitres. This was then multiplied by a factor of 10000 to acquire the number of cells per millilitre and then divided by 10 to acquire the number of cells per 100 microlitres (this is the usual standard for a 96 well plate).

$$C_1V_1 = C_2V_2$$

Figure 10: The mathematical equation used to calculate required amount of cell solution volume and media needed to acquire desired cell plating density.

Using Figure 10,  $C_1$  becomes the number of cells required per well and  $V_1$  becomes the volume per well.  $C_2$  becomes the number of cells per 100 microlitres recorded, and  $V_2$  is the variable needed to be calculated.

$$\frac{C_1 V_1}{C_2} = V_2$$

Figure 11: The re-arranged equation to achieve a calculation to work out  $V_2$ .

Using figure 11,  $V_2$  gives the required amount of cell solution needed to be added per well to achieve the required number of cells per well. Subtracting this value from 0.1 gives the amount of media needed to be added per well. A final multiplication of the number of wells needed was calculated to ascertain the total amount of cell solution mixed with fresh media to achieve desired cell plating density.

### Affinity Chromatography

To begin with, Affi-Gel 10 beads were defrosted from storage. A 50mM phosphate buffer was concocted to achieve a buffer close to a neutral pH. The prawn derived GAGs were added to the 50mM phosphate buffer and this was then added to the affi-gel 10 beads. This coupling reaction was kept at 4 degrees Celsius overnight with constant gentle agitation to allow maximum coupling of the ligands with the affi-gel 10 beads.

A second lot of affi-gel 10 beads were also mixed with 50mM phosphate buffer in the same conditions but without the addition of the GAGs. This was to form a sham column.

The test column was then packed with the coupled affi-gel 10 beads with the GAGs up to the maximum fill line and the excess liquid was drained off. The sham column was packed the same way but with the preparation lacking the GAGs.

The next stages were both repeated identically for the test column and the sham column.

1 ml of total cell lysate was applied to the columns and pushed through via positive pressure. The liquid that eluted from the column was collected in a 1ml eppendorf.

Five lots of 1 ml of 50mM phosphate buffer was then added and pushed through the stationary phase via positive pressure again and the elution collected in 1 ml eppendorf tubes once more.

Three different buffers were then created all in 50mM phosphate buffer. These were 0.2M, 0.5M and 2M NaCl respectively.

The 0.2M NaCl 50mM phosphate buffer was then added five times in 1ml increments and the elution collected in a 1ml eppendorf. This was repeated for the 0.5M and 2M buffers.

The collected fractions from affinity chromatography were analysed to see which fractions contained protein. Using Bio-Rad reagent (the same reagent used in 3.5), the absorbance of the fractions was measured at 595nm wavelength. To achieve consistent readings, 100 microlitres of fraction was mixed with 200 microlitres of Bio-Rad reagent and 700 microlitres of deionised water and incubated at room temperature for 5 minutes. The results were then plotted for each fraction to obtain a visible representation of protein present in each collected fraction.

#### Monosaccharide and Disaccharide Analysis:

For the monosaccharide and disaccharide analysis, the powdered extract was sent to the University of California for this procedure and the results sent back were interpreted and analysed.

## Results:

### MTT:

For cell viability tables and raw data of UV absorbance after background absorbance is subtracted, please refer to the appendix.

### Comparing Prawns against Cockles:

The corresponding results below are for the testing of prawn and cockle derived GAGs using an identical extraction procedure on K562 cells from the same culture with GAGs applied in concentrations ranging from 100 micrograms per millilitre down to 3.125 micrograms per millilitre.

#### **Prawn vs Cockle GAGs applied to K562 Cell Line.**

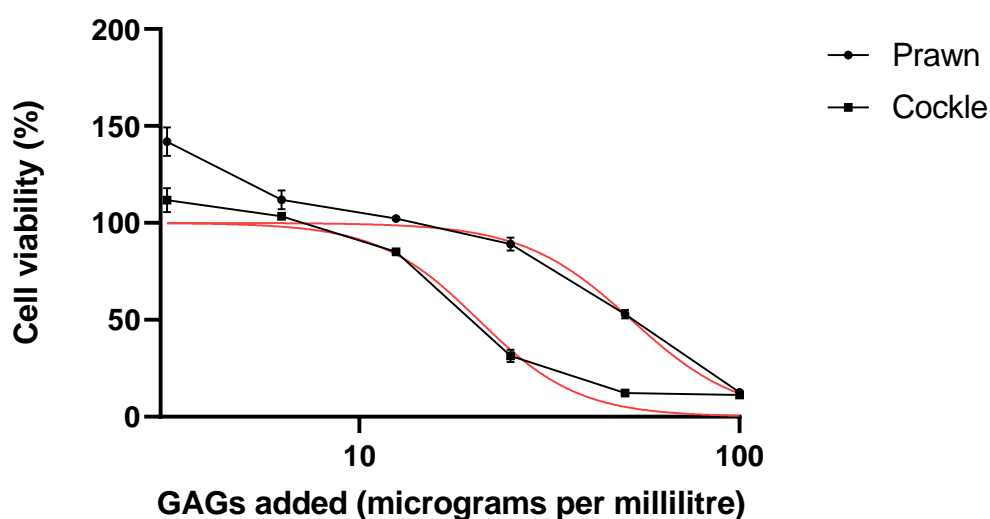


Figure 12: A comparative graph to show the dosage response of two marine derived GAGs on the K562 cell line using the MTT assay.

Analysis of the dataset showed that the Prawn GAGs had an IC<sub>50</sub> of 51.98 micrograms per ml (44.97- 60.30 with 95%CI) in comparison to the Cockle GAGs which had an IC<sub>50</sub> of 20.59 micrograms per ml (19.34-21.93 with 95% CI).



All data points showed a significant difference from one another with the exception of 6.25 micrograms per ml with the IC<sub>50</sub>'s being of significant difference from one another.

This data shows Cockle GAGs to be 2.52 (to 2 decimal places) times more cytotoxic than the Prawn GAGs.

#### Alternative Cell Lines:

The following results show the cell viabilities of the various cell lines when Prawn GAGs were added in concentrations ranging from 200 micrograms per ml to 0.098 micrograms per ml (to two significant figures).

#### U2OS:

##### **Cell viability of U2OS with prawn GAGs added.**

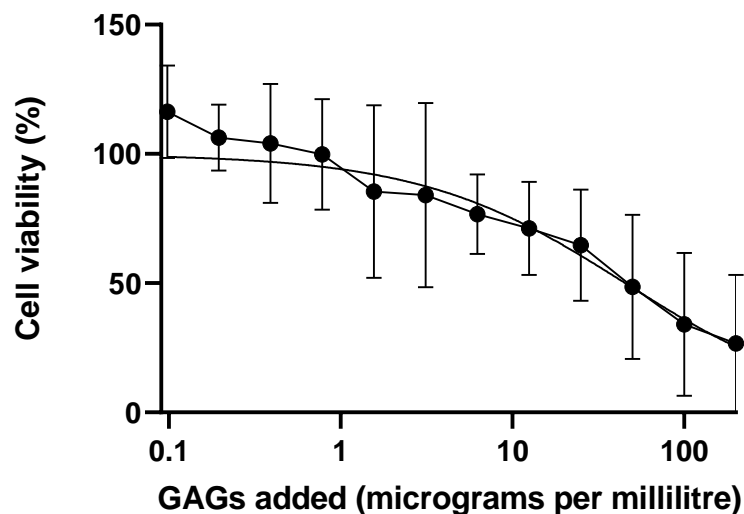


Figure 13: A graph of U2OS cell line viability when Prawn GAGs were added and results recorded via the MTT assay.

The U2OS cell line showed an IC<sub>50</sub> of 45.40 micrograms per ml (30.42-70.84 with 95% CI). These results show a correlation of decreased cell viability when concentration of GAGs was increased.

#### MDBK:

##### **Cell viability of MDBK with Prawn GAGs added**

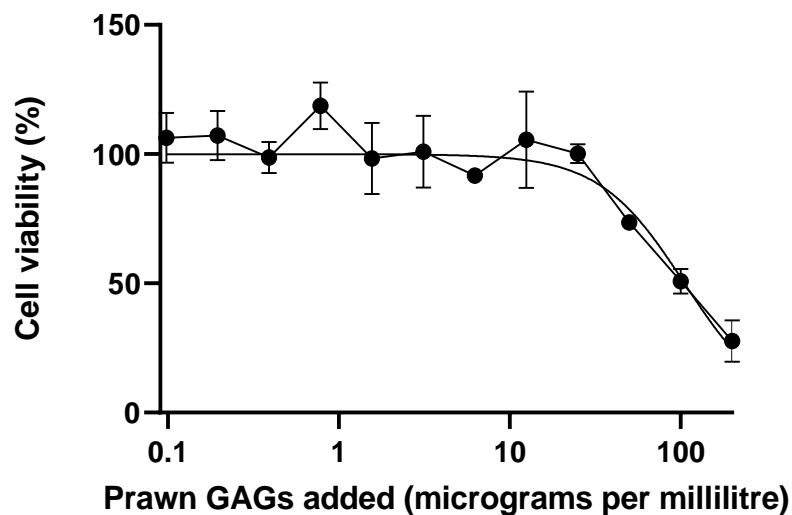
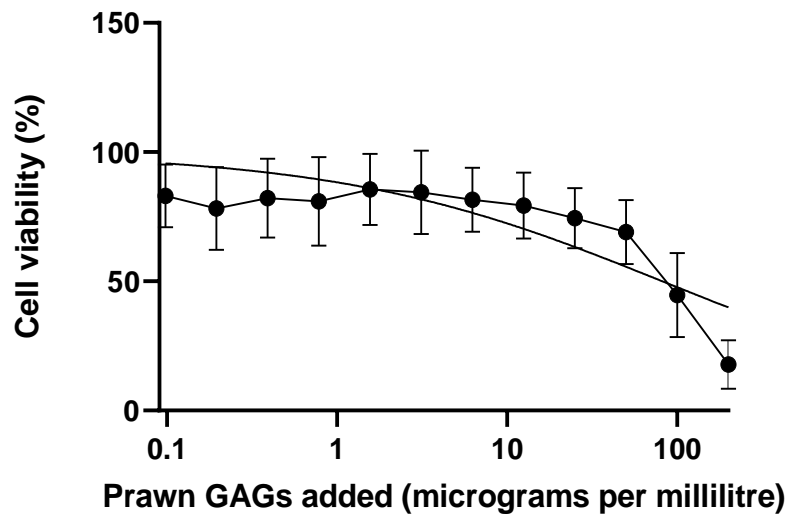


Figure 14: Cell viability of MDBK cells with various concentrations of Prawn GAGs added and results recorded via the MTT assay.

For the MDBK cell line, an IC<sub>50</sub> of 105.4 micrograms per ml (92.87 – 120.5 with a 95% CI) was obtained. There was a lack of correlation between 0 and 10 micrograms per ml with a negative correlation afterwards as cell viability decreased as prawn GAG concentration increased.

## BEAS-2B:

### **BEAS-2B Cells treated with Prawn GAGs**



The BEAS-2B cell line had an IC<sub>50</sub> of 82.01 micrograms per ml (49.44-181.5 with a 95% CI). The graph shows a slight negative correlation with cell viability decreasing as Prawn GAGs concentration increases.

An obvious outlier was identified and removed, as discussed further on in the BEAS-2B sub-section of the discussion chapter.

### **BEAS-2B Cells treated with Prawn GAGs**

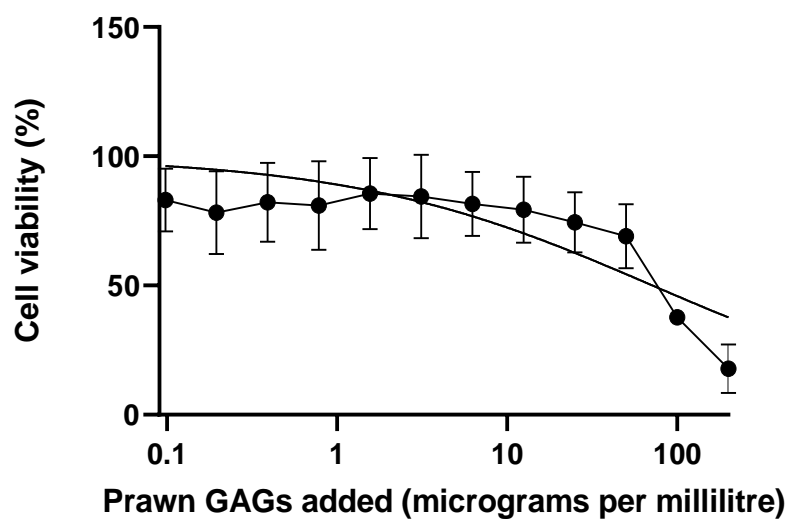


Figure 15: Outlier corrected BEAS-2B MTT cell viability graph.

This lead to a new IC<sub>50</sub> of 71.64 micrograms per ml (45.25- 142 with 95% CI) being discovered.

#### MOLT-4:

#### **Cell viability of MOLT-4 with Prawn GAGs added**

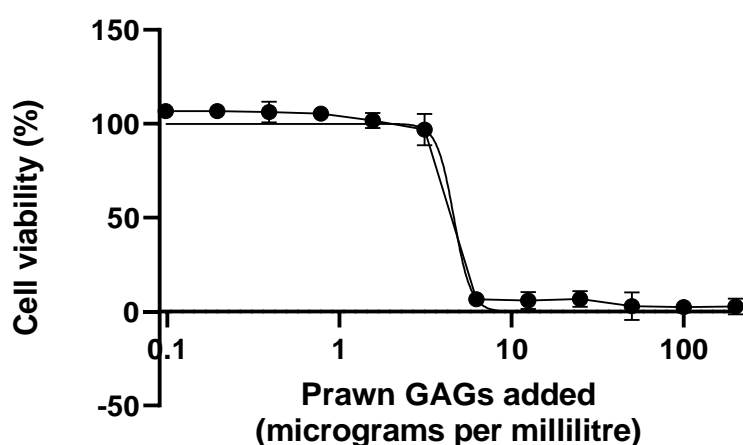


Figure 16: Cell viability graph of MOLT-4 cells with prawn GAGs added and recorded via the MTT assay.

MOLT-4 showed an IC<sub>50</sub> value of 4.627 micrograms per ml (4.274 – no upper limit due to the software being unable to calculate it) with no correlation before 1 microgram per ml with a very strong correlation dropping to basal level between 1 and 10 micrograms per ml.

Quantifying cell lysate protein:

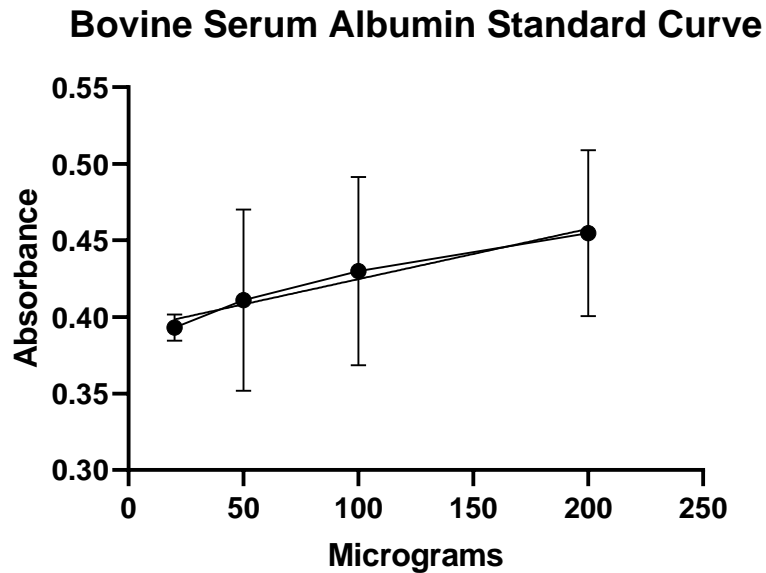


Figure 17: Bovine Serum Albumin Standard Curve.

Table 5: Absorbance readings in triplicate for the K562 lysates.

SAMPLE	REPEAT 1	REPEAT 2	REPEAT 3
Parental	0.424	0.428	0.420
Resistant	0.468	0.478	0.458

Using the standard curve for the BSA the K562 parental cell line lysate had a protein concentration of 6.81 mg per ml and the cisplatin resistant cell line lysate had a protein concentration of 14.16 mg per ml

## Affinity Chromatography:

### **Absorbance of Affinity Column Fractions K562 Cell Lysate**

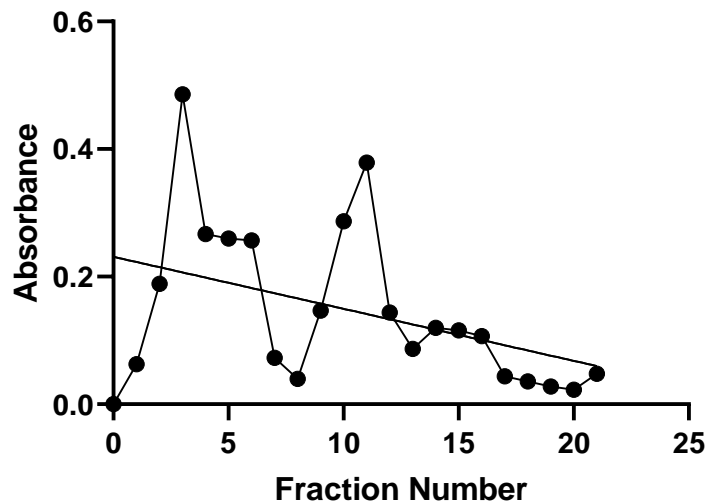


Figure 18: K562 cell lysate affinity chromatography absorbance readings.

The figure above shows a negative correlation that as the fraction number increased the amount of eluted protein decreased. There was a large spike in eluted proteins at fraction 3 which descends until fraction 8 with another elution spike occurring at fraction 11 with an overall decrease thereafter. The final five fractions which are the fractions of interest still show elution of proteins.

### Absorbance of Affinity Column Fractions K562 Cell Lysate Sham Column

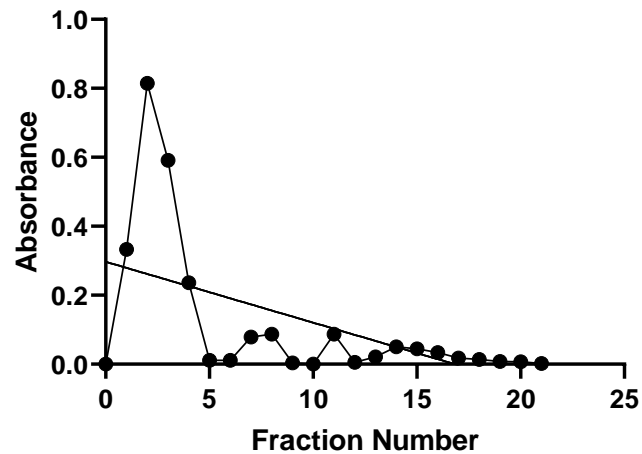


Figure 19: K562 cell lysate affinity chromatography absorbance readings of the sham column.

The figure above shows a negative correlation that as the fraction number increases the amount of eluted protein decreases. There was a solitary large elution spike at fraction 2 decreasing to a baseline reading at fraction 5. There was 3 minor spikes afterwards but from fraction 17 onwards there was a negligible reading representing little to no elution of proteins.

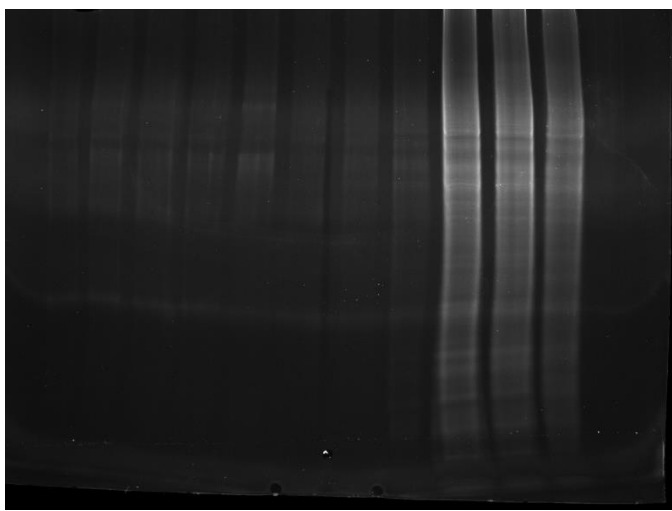


Figure 20: SDS-Gel of affinity fractions, stained with Oriole Fluorescent gel stain, 1-11 with the first column on the left being fraction 11 descending to the right down to fraction 1.

Fractions 1, 2 and 3 show a substantial amount of eluted proteins in comparison to fractions 4-11. Fractions 4-11 shows some banding and confirms the presence of eluted proteins.

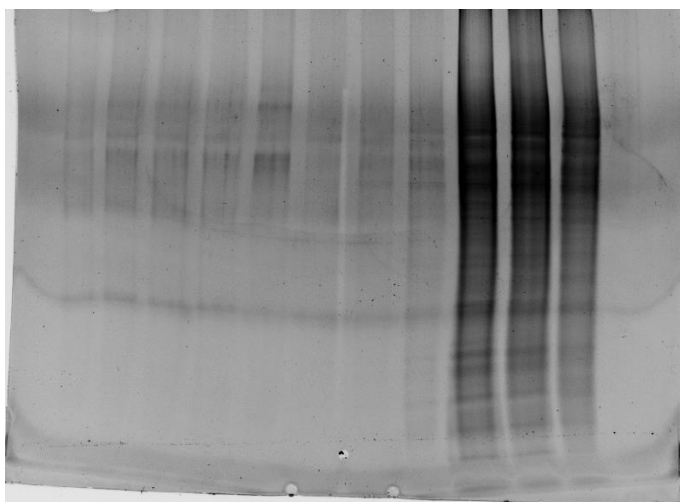


Figure 21: An inversed image of the SDS-PAGE gel for fractions 1-11.

The inversed figure above illustrates clearly which bands of proteins have been eluted. Fractions 1, 2 and 3 show significantly more elution of the lower molecular



weight proteins in comparison to fractions 4-11 which show little to no elution of the lower molecular weight proteins.

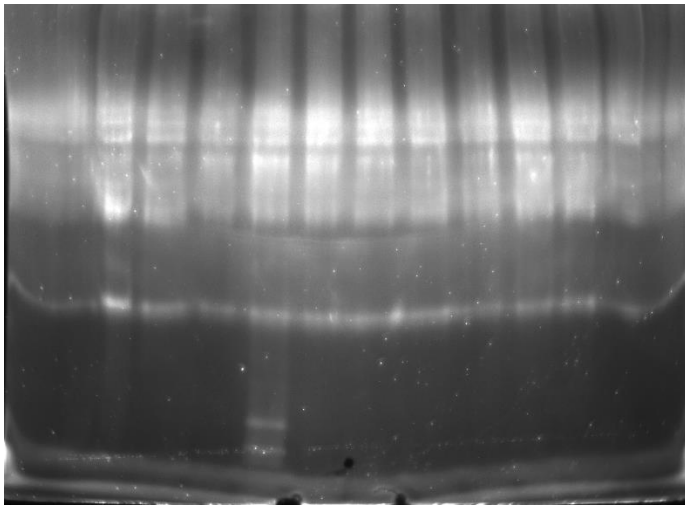


Figure 22: Fractions 12-21 (left hand side 21 descending down to fraction 12 on the right) of the affinity chromatography on SDS-Gel stained with Oriole Fluorescent stain.

The above figure shows elution of high molecular weight proteins across all the fractions which seem to be identical. Fraction 18 shows elution and separation of two protein bands of low molecular weight that have not been eluted in any of the other fractions due to their position on the gel.

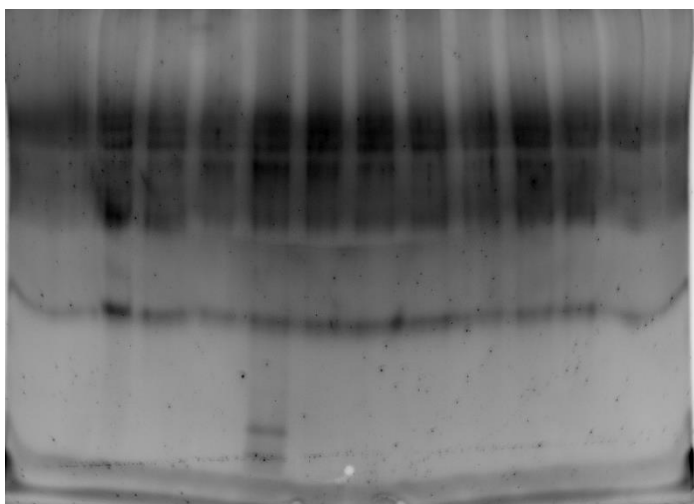


Figure 23: Inversed image of the SDS-PAGE gel for fractions 12-21.

The above inversed figure illustrates fraction 18 is the only fraction to elute/separate the two visible protein bands. The figure also confirms the common high molecular weight protein elution/separation.

## NMR results:

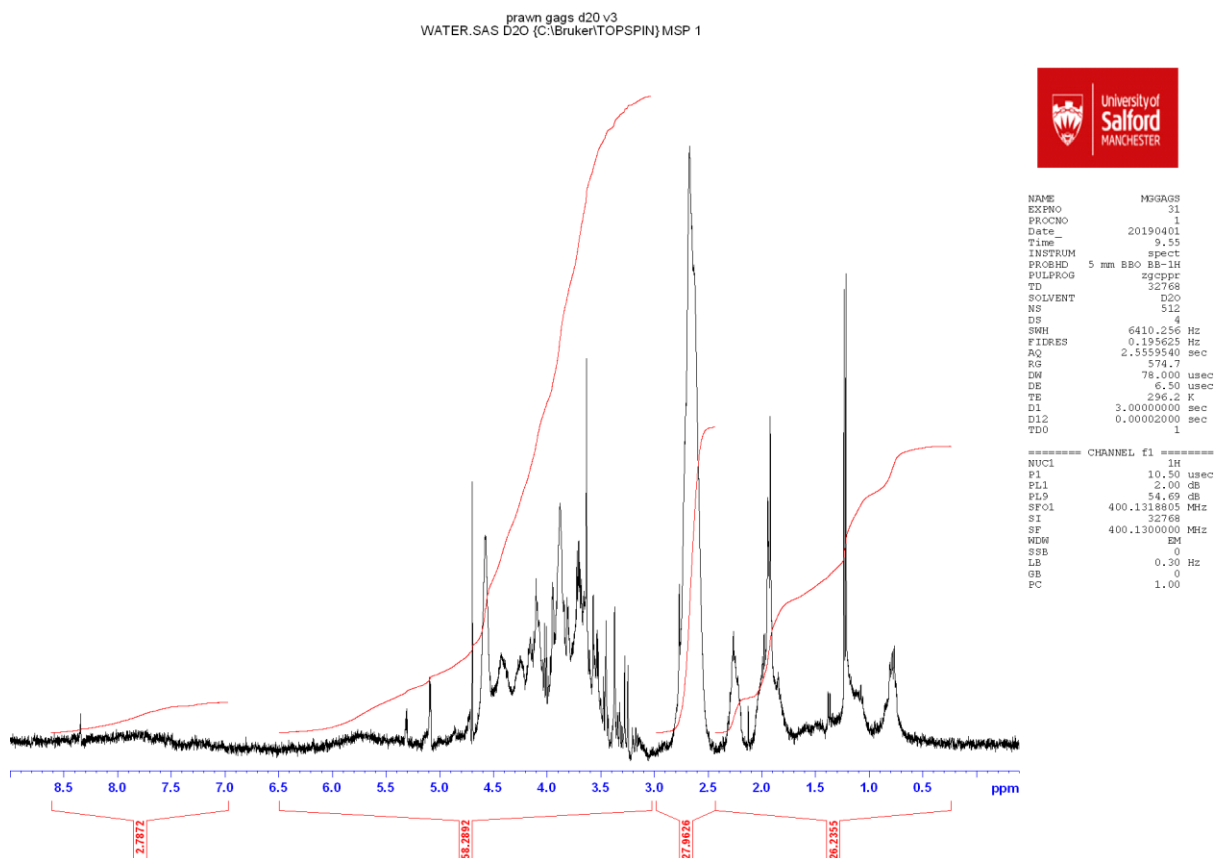


Figure 24: Proton NMR (solvent suppressed) of prawn derived GAGs.

The NMR spectra above cannot resolve individual peaks and is therefore a low resolution NMR spectra. The above spectra indicates six different hydrogen environments with analysis by sight, the integration trace however separates the spectra into four groups. Full analysis is provided in the discussion section.

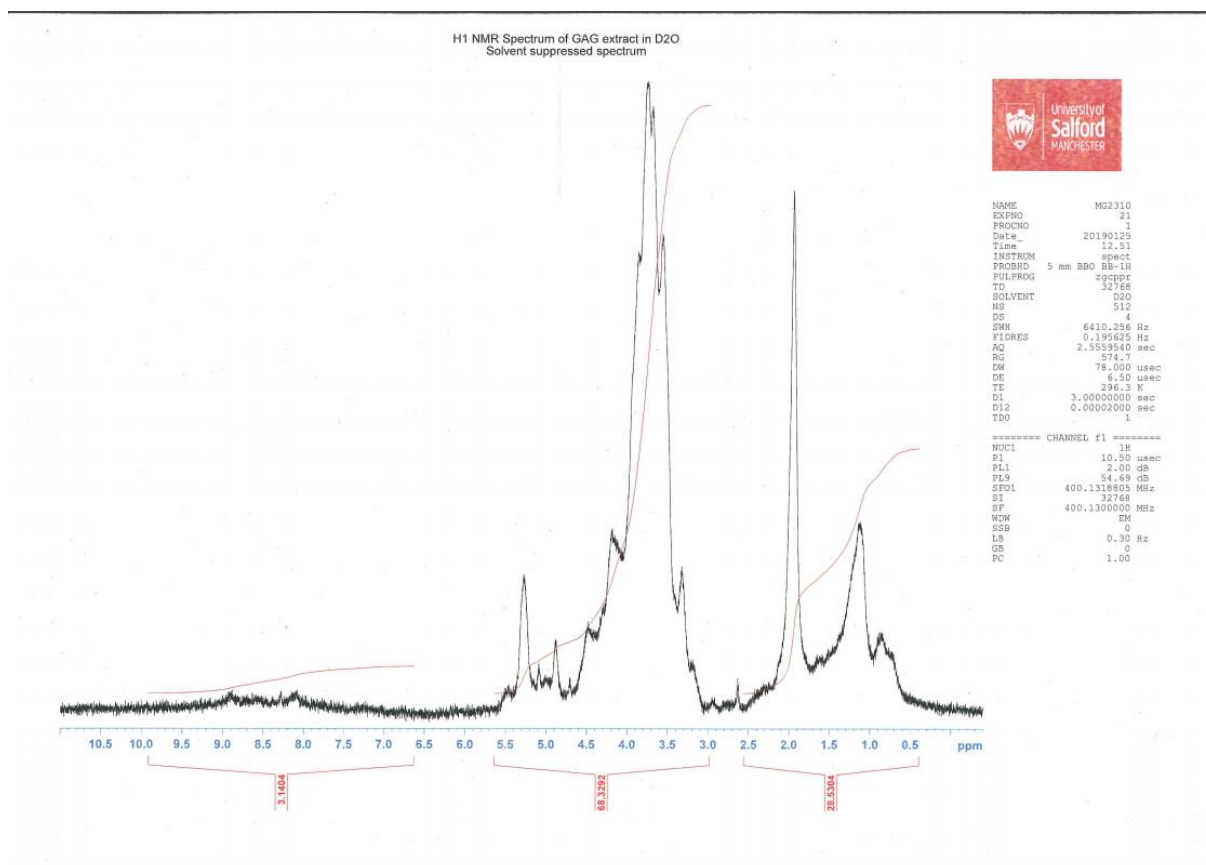


Figure 25: Proton NMR (solvent suppressed) of Cockle derived GAGs.

This NMR spectra cannot distinguish the individual peaks and is therefore a low resolution NMR spectra. The above spectra indicates three to four different hydrogen environments, this is confirmed by the integration trace which separates the spectra into three groups. Full analysis is provided in the discussion section.

### Disaccharide Analysis:

For the disaccharide analysis the following abbreviations and their respective disaccharide were used:

Table 6: Heparin Sulfate abbreviations and relative disaccharides.

<b>Abbreviation</b>	<b>Disaccharide</b>
<b>D0A0</b>	$\Delta$ HexA-GlcNAc
<b>D2A0</b>	$\Delta$ HexA(2S)-GlcNAc
<b>D2H0</b>	$\Delta$ HexA(2S)-GlcNH <sub>2</sub>
<b>D0A6</b>	$\Delta$ HexA-GlcNAc(6S)
<b>D2A6</b>	$\Delta$ HexA(2S)-GlcNAc(6S)
<b>D0S0</b>	$\Delta$ HexA- GlcNS
<b>D2S0</b>	$\Delta$ HexA(2S)-GlcNS
<b>D0S6</b>	$\Delta$ HexA-GlcNS(6S)
<b>D0H6</b>	$\Delta$ HexA-GlcNH <sub>2</sub> (6S)
<b>D2S6</b>	$\Delta$ HexA2S-GlcNS(6S)
<b>D2H6</b>	$\Delta$ HexA2S-GlcNH <sub>2</sub> (6S)

Table 7: Chondroitin Sulfate abbreviations and their relative disaccharide.

<b>Abbreviation</b>	<b>Disaccharide</b>
<b>D0ao</b>	$\Delta$ HexA-GalNAc
<b>D0a4</b>	$\Delta$ HexA-GalNAc(4S)
<b>D0a6</b>	$\Delta$ HexA-GalNAc(6S)
<b>D2a4</b>	$\Delta$ HexA(2S)-GalNAc(4S)
<b>D2a6</b>	$\Delta$ HexA(2S)-GalNAc(6S)
<b>D0a10</b>	$\Delta$ HexA-GalNAc(4S)(6S)
<b>D2a10</b>	$\Delta$ HexA(2S)-GalNAc(4S)(6S)

The disaccharide analysis showed the presence of the above disaccharides in the following percentages.

Table 8: Heparin Sulfate disaccharide analysis of prawn GAGs.

<b>Disaccharide</b>	<b>% of sample</b>
<b>D0H0</b>	0.00
<b>D0A0</b>	3.51
<b>D0H6</b>	11.44
<b>D2H0</b>	6.01
<b>D0S0</b>	3.52
<b>D0A6</b>	1.76
<b>D2A0</b>	0.02
<b>D2H6</b>	10.11
<b>D0S6</b>	27.11
<b>D2S0</b>	11.48
<b>D2A6</b>	0.04
<b>D2S6</b>	25.00

Table 9: Chondroitin Sulfate disaccharide analysis of prawn GAGs.

<b>Disaccharide</b>	<b>% of sample</b>
<b>D0a0</b>	0.39
<b>D0a4/D2a0</b>	84.16
<b>D0a6</b>	4.80
<b>D2a4</b>	0.06
<b>D2a6</b>	0.00
<b>D0a10</b>	10.59
<b>D2a10</b>	0.00

The heparin sulfate analysis shows a spread of heparin sulfate disaccharides present with only D0H0 not appearing. D0S6 and D2S6 are the most prominent disaccharides at 27.1% and 25% respectively.

The chondroitin sulfate is dominated by the D0a4/D2a0 at 84.16%. Both D2a6 and D2a10 were not present in this analysis.

For sulfation percentages, chondroitin sulfate showed 0.39% unsulfated, 0.06% with 2-SO<sub>3</sub> sulfation, 94.80% with 4-O-SO<sub>3</sub> sulfation and 15.39% with 6-O-SO<sub>3</sub> sulfation.

Heparin sulfate analysis showed 3.51% unsulfated, 67.1% with N-SO<sub>3</sub> sulfation, 52.66% with 2-O-SO<sub>3</sub> sulfation and 75.45% with 6-O-SO<sub>3</sub> sulfation.

Below are the graphical representations of this analysis.

DOH0 E:090219-Fly-Snail-GAGSnaill-GAG-HS

9/2/2019 7:04:18 PM

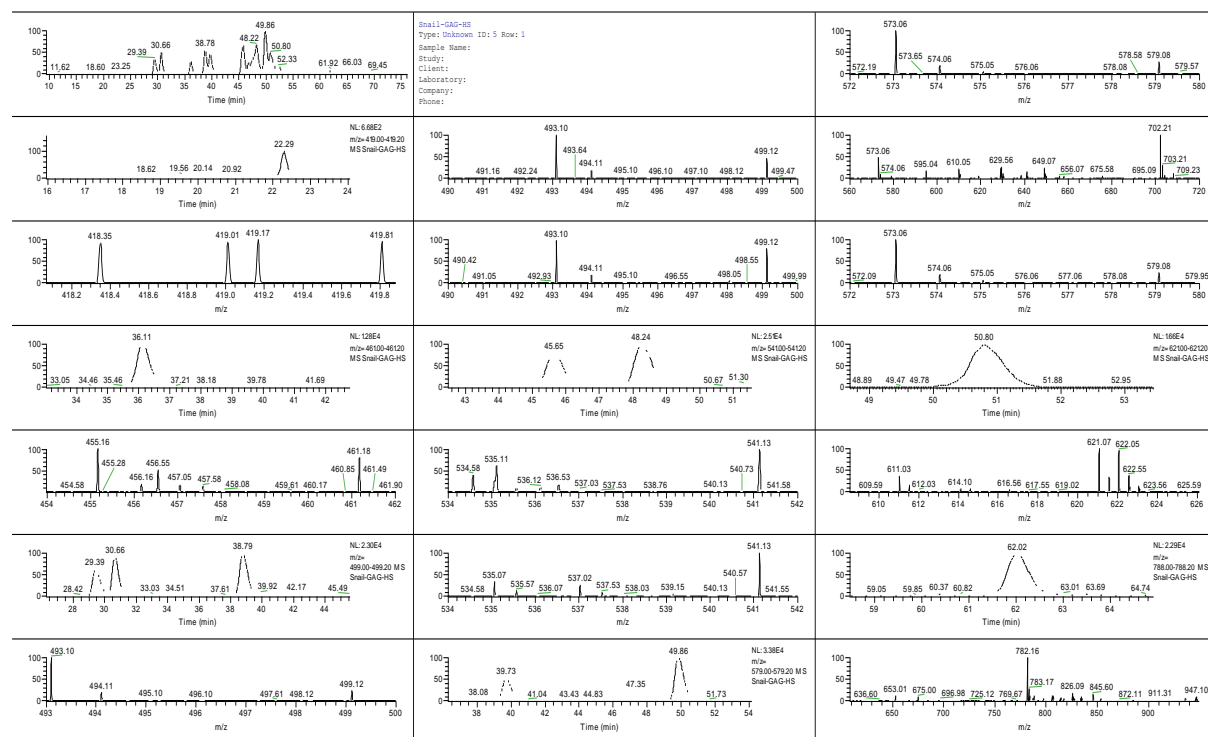


Figure 26: GRIL-LCMS of Heparin Sulfate.

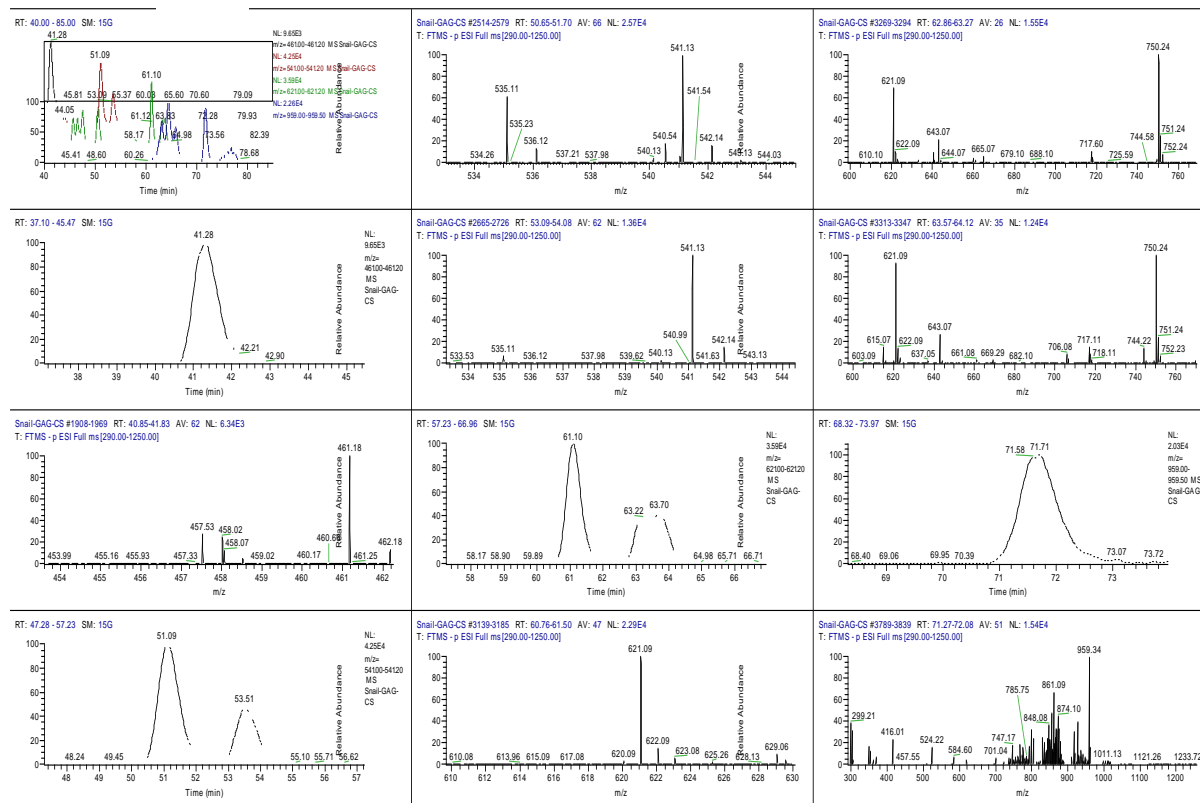


Figure 27: GRIL-LCMS of Chondroitin Sulfate.

Monosaccharide Analysis:

The results below are from 10 micrograms of prawn derived GAG extract.



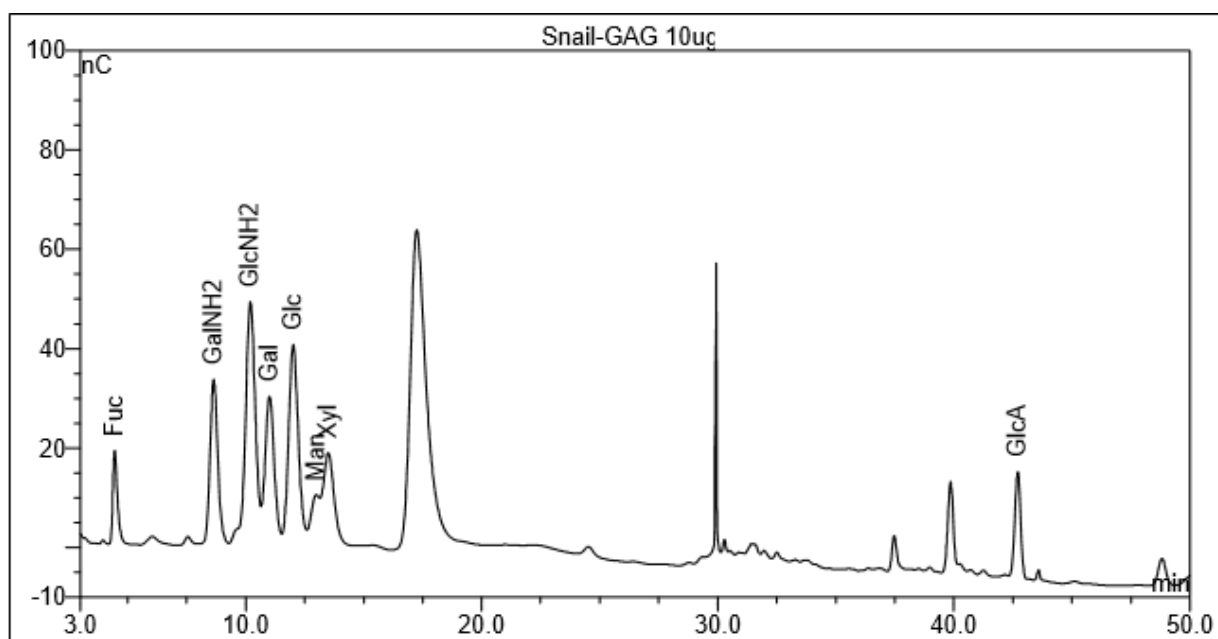


Figure 28: Chromatogram of monosaccharide analysis.

Table 10: Data represented by monosaccharide analysis chromatogram.

Peak no.	Name	Retention Time (min)	Area (n.a)	Relative Area (%)	Height (nC)	Amount (nmol)
1	Fuc	4.46	4.273	4.61	18.678	0.3779
2	GalNH2	8.65	12.448	13.44	32.960	0.4939
3	GlcNH2	10.20	22.704	24.51	48.541	1.0111
4	Gal	11.01	13.553	14.63	29.624	0.9879
5	Glc	12.02	19.347	20.88	40.099	1.1730
6	Man	12.99	4.036	4.36	10.011	0.3169
7	Xyl	13.51	10.144	10.95	18.527	n.a
8	GlcA	42.71	6.146	6.63	21.324	1.1162

From these results it is shown that GlcNH2 and Glc are the two largest components of the GAG extract with Man and Fuc being the least present. However based upon moles present Glc and GlcA have the highest result with Man and Fuc having the lowest.

## Discussion:

## NMR Analysis:

As an initial disclaimer, all NMR spectra were run with a H<sub>2</sub>O suppression to remove the H<sub>2</sub>O peak that would be present (unless otherwise stated).

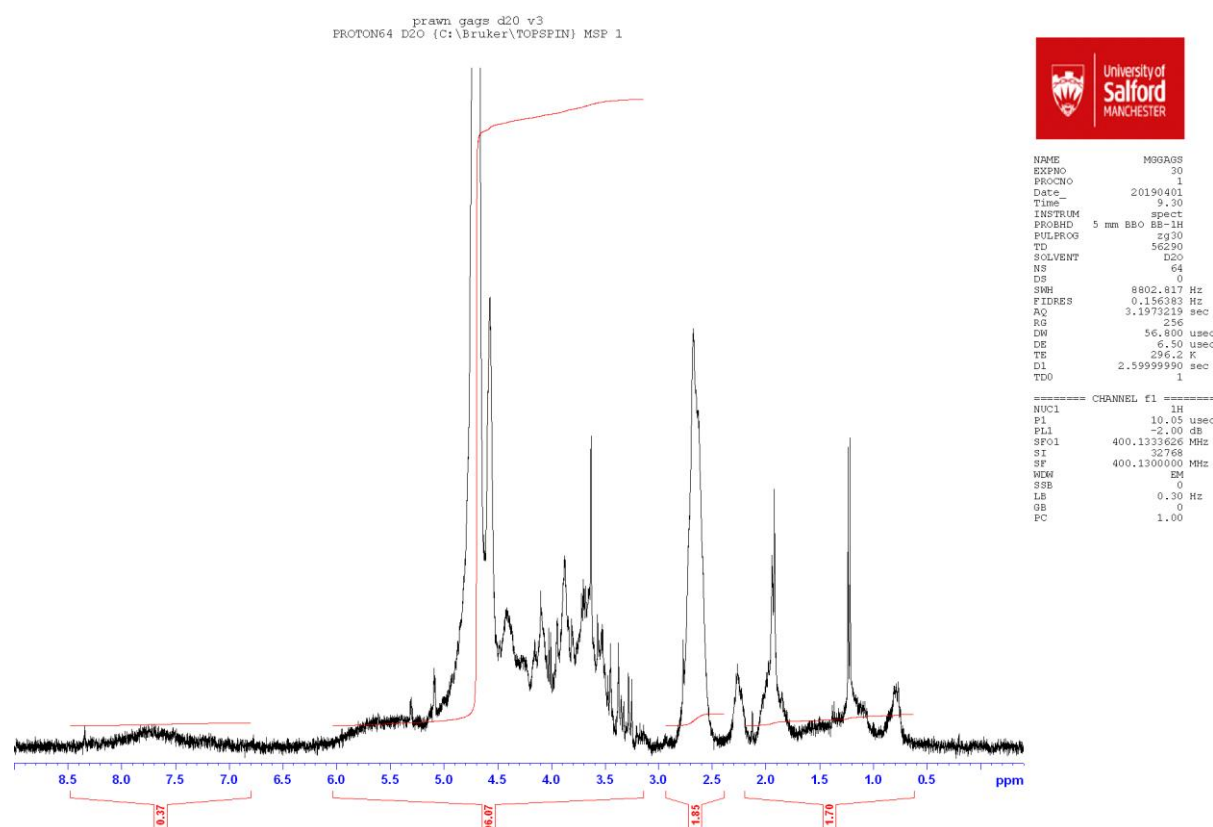


Figure 29: Unsuppressed spectra of proton NMR of prawn extract.

As you can see in the figure above, without H<sub>2</sub>O suppression, a large peak is observed at around 4.75 parts per million which severely impacts the overall spectra and its' ability to be analysed and interpreted.

Due to the complex mixtures of both the cockle and prawn GAG extracts, both of the NMR's ended up being low resolution as they could not distinguish/resolve the complex into individual peaks.

With proton NMR, a basic understanding is that the more electronegative components of the compound analysed cause corresponding hydrogens to shift to the left of the spectra with the less negatively charged components causing the corresponding hydrogens to not shift to the left as much. The closer to zero on the spectra, the less negatively charged the corresponding components to the hydrogens shifted.

First of all, by analysing the integration trace and its' corresponding values, we can analyse the ratio of hydrogens present that give rise to the signal. In the cockle derived GAGs, there is a ratio of hydrogens of 3.14 to 68.33 to 28.53 respectively with 3.14 being the most electro-negatively charged and the 28.53 being the least electro-negatively charged. These sections were split into the shifts of approximately; 10.0-6.5 parts per million, 5.5-3.0 ppm and 2.5-0.5 ppm.

For the prawn derived GAGs, the integration trace separated the shifts into four different hydrogen environments with respective ratios of 2.79 (shift of 8.5-7.0 parts per million) – 58.29 (6.5-3.0 ppm) – 27.96 (3.0-2.5 ppm) – 26.24 (2.5-0.3 ppm).

This can then be converted into percentages to make comparison between the samples easier.

For the cockles, the ratios and the percentages are equivalent. For the prawn derived GAGs, the ratio converts into percentages of; 2.42%, 50.69%, 24.31% and 22.82% respectively.

Upon this basic analysis of the separation of hydrogen environments, the major difference between the prawn and the cockle derived GAGs is the presence of a hydrogen environment at a shift of 3.0-2.5 parts per million that is present in the prawn GAGs which is not present in the cockle derived GAGs. This shift of 3.0-2.5

ppm is equivalent to 24.31% of the signal from the NMR caused by the hydrogens present in this environment. At the most electro-negatively charged aspect of the compound, both the cockles and the prawns are very similar with percentages of 3.14% and 2.42% so both compounds exhibit minimal hydrogen environments of high electro-negativity.

For the middle section of medium electro-negativity, despite the differences in the integration trace split (this is inconsequential as the lower limit of 3.0 is consistent for both compounds and the upper limit has minimal signal), the cockle derived GAGs has just under 18% more hydrogens present in this environment in comparison the prawn counterpart. Also at the lowest level of electro-negativity (where the integration trace has used almost identical limits with only a 0.2 difference on the lower limit), the cockle derived GAGS show just under a % increase on hydrogens present in this environment compared to the prawn counterparts. Overall, solely based upon the ratio of hydrogens observed by the integration trace of the proton NMR, it seems that the cockle GAGs contain more electro-negative environments than the prawn GAGs do.

Using chemical NMR tables, it can be theorised what is causing the 3.0-2.5 ppm shift signal in the prawn GAGs. The closest match on the chemical tables is an Alkynyl hydrogen which has a chemical shift of 2.5-3.0 ppm on a proton NMR spectroscopy.

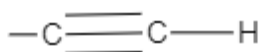


Figure 30: Alkynyl hydrogen diagram drawn via ChemDraw™.

Alkyl halides have a chemical shift pattern of 2.5-4.0 parts per million. However, this would have to be investigated for the presence of either fluorine, bromine, iodine or chlorine to see if it is possible for an alkyl halide to be formed. This is due to the fact that an Alkyl halide is a compound in which a hydrogen is replaced with a halide (Gal, Bucher and Burns, 2016). This potential result is of particular interest as halogenated marine products have been recently found to show unique bioactivity and to help illustrate the role of chiral alkyl halides in drug discovery (Gal, Bucher and Burns, 2016). Halogenation has been shown to affect bioactivity whether it be through ligand binding or lipophilicity through the halogenation of sp carbons (Gal, Bucher and Burns) and could explain the differences in chemotherapeutic effects between the cockles and prawn GAGs.

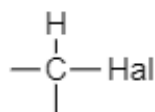


Figure 31: Alkyl Halide diagram drawn via ChemDraw™.

Alcohol has a proton NMR shift of 2.5-5.0 ppm. This would fall within the scope of the 2.5-3.0 ppm shift of the unidentified peak but would be expected to be a lot broader if it was alcohol so can be ruled out.

At the lower electro-negativity side of the spectra, even though the integration trace hasn't separated it itself, the prawn NMR looks to have resolved some individual peaks. At the lower end of a proton NMR spectra, you find the primary, secondary and tertiary alkyl groups.

Primary Alkyl groups can be found with a chemical shift pattern of 0.7-1.3 parts per million which looks to correspond with the far right peak of the prawn NMR.



Figure 32: Primary alkyl group drawn via ChemDraw™.

Secondary alkyl groups contain one less hydrogen and can be found with a chemical shift pattern of 1.2-1.6 parts per million. Again, this corresponds with the prawn NMR, with the second peak from the right at around 1.2 ppm.

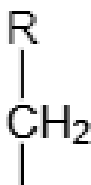


Figure 33: Secondary alkyl group drawn via ChemDraw™.

Finally, tertiary alkyl groups are found with a chemical shift pattern of 1.4-1.8 parts per million. This could correspond with the peak on the NMR prawn spectra of around 1.75-1.9 parts per million.

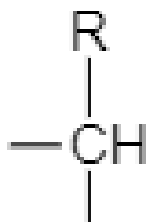


Figure 34: Tertiary alkyl structure drawn via ChemDraw™.

The cockle NMR was not able to provide such resolution, this may be down to the extract being a lot more complex compound(s) causing crossover between peaks and not allowing them to be separated.

Overall, the prawn NMR was a lot simpler extract due to the resolution of the peaks and how some can be clearly defined and identified. With the cockle extract, there was no clear identifiable peaks which makes analysis of the compound and structure a lot harder and complicates future analysis. The next logical stage would be to investigate the efficacy of the simpler prawn extract as if that is close to the effectiveness of the cockles as shown in the Aldairi et al, 2018 paper, future investigation and development will be easier and less consuming of resources as the extract can be more easily investigated and fully identified. This was investigated below in the MTT section.

To improve upon these results, proton NMR of a higher calibre could be employed to achieve a greater resolution which would lead to easier identification of peaks within the clusters that show little to no clearly resolved peaks.

#### Disaccharide Analysis:

The disaccharide analysis provides an insight into the composition of the GAG extract. Alone however, this information reveals very little. Using it comparatively with the cockle extract and mammalian extract in the Aldairi et al, 2018 paper, hypotheses and relationships can be theorised.

Table 11: Heparin Sulfate disaccharide analysis of prawn, cockle and mammalian GAGs.

Disaccharide	Prawn (%)	Cockles (%)	Mammalian (%)
D0H0	0.00	0	0
D0A0	3.51	26.6	48.4
D0H6	11.44	0	0
D2H0	6.01	0	0
D0S0	3.52	25.5	22.6
D0A6	1.76	4.1	8.6
D2A0	0.02	0	0
D2H6	10.11	0	0
D0S6	27.11	24.7	3.9
D2S0	11.48	9.5	10.4
D2A6	0.04	4	0
D2S6	25.00	5.6	5.4

Using these results, relationships can start to be hypothesised. With the exception of D0H0, prawn GAGs are the only GAG studied to show a signal for all of the other disaccharides. Both cockles and mammalian GAGs show no result for D0H6, D2H0, D2A0 and D2H6.

Mammalian GAGs have been shown to exhibit no anti-proliferative properties (Aldairi et al, 2018). Both prawn and cockle GAGS compose of D2A6 where mammalian GAGs do not. Interestingly, this study has shown cockles to have an IC50 2.2 times lower than the prawn GAGs on K562 leukemia cells and for this disaccharide prawns do compose of a lower amount. It could be hypothesised therefore that this disaccharide plays a major role in the anti-proliferative properties of a GAG extract. This would need further testing however by analysing other GAG extracts and using the percentage of D2A6 composing the GAG extract to be the variable tested. Additionally, if a digest could be designed to remove this disaccharide, the GAG extract after this digest from prawns and cockles could be once again tested upon K562 leukemia cells to see if there is a significant change in the IC50.



Another major difference is the presence of D0S6. Both prawn and cockle GAGs show this in high quantities (24-27%) whereas the mammalian GAGs show a much smaller composition. Again this could be hypothesised to play a major role in the anti-proliferative properties of GAG extracts and once again it would be recommended to test this as a variable or perform a digest to see if it does in fact affect the anti-proliferative properties.

The final major result of note is the substantially less presence of D0A0. In the mammalian GAG extract, this disaccharide is the major component making up 48.4% of the heparin sulfate disaccharides present. In cockles this is only 26.6% and only 3.51% in the prawn GAGs. Therefore, it could be theorised that this disaccharide is a potential inhibitor of the anti-proliferative properties GAG extracts can exhibit. Once again further study would need to be conducted as outlined with the previous two heparin sulfate disaccharides of interest.

The chondroitin sulfate results can also be comparatively analysed in the same regard.

Table 12: Chondroitin Sulfate disaccharide analysis of prawn, cockle and mammalian GAG extract.

<b>Disaccharide</b>	<b>Prawn (%)</b>	<b>Cockles (%)</b>	<b>Mammalian (%)</b>
<b>D0a0</b>	0.39	3.2	n/a
<b>D0a4/D2a0</b>	84.16	33.5	n/a
<b>D0a6</b>	4.80	17.2	n/a
<b>D2a4</b>	0.06	0.00	n/a
<b>D2a6</b>	0.00	0.7	n/a
<b>D0a10</b>	10.59	45.4	n/a
<b>D2a10</b>	0.00	0.00	n/a

Unfortunately, no results could be sourced for mammalian GAGs and the chondroitin sulfate disaccharide analysis.

With the chondroitin sulfate disaccharide analysis, the prawn GAGs appear to be more simple in nature as they show a very large result with 84.16% of the composition being D0a4/D2a0 and results of 0.39% or less for four of the seven disaccharides. This would help explain as to why the NMR spectra for prawns was a lot simpler than the overlapping complex NMR for the cockles.

Both cockles and prawns show no presence of D2a10 so it would be safe to hypothesise that this chondroitin sulfate disaccharide plays no positive role in the anti-proliferative nature of the GAG extract.

For both D2a4 and D2a6, only one of the extracts shows a minimal composition where the other extract shows none at all. Again, it could be hypothesised that these disaccharides do not play a major role in the anti-proliferative nature of the GAG extracts.

Based upon these findings, it would be recommended to test the hypothesis that D0a0, D0a4, D0a6 and D0a10 are the four major contributors to the anti-proliferative nature of the marine GAG extracts and should be further investigated.

Further analysis can also be conducted on the overall types of sulfation present.

Table 13: Chondroitin sulfate sulfation type analysis.

<b>Sulfation</b>	<b>Prawns (%)</b>	<b>Cockles (%)</b>
<b>Unulfated</b>	0.39	3.22
<b>2-SO3</b>	0.06	0.68
<b>4-O-SO3</b>	94.80	78.87
<b>6-O-SO3</b>	15.39	63.29

Clearly illustrated by the table above, cockles consist of a substantially greater proportion of 6-O-SO3 sulfation. The unsulfated and 2-SO3 results do not seem to have a significant difference from each other and it can be hypothesised these do

not play as much of a role in the anti-proliferative properties of the GAG extract that the other two types of sulfation do. As cockles have been shown to be a stronger anti-proliferative therapeutic on K562 cells, this could be caused by the increase in 6-O-SO<sub>3</sub> sulfation which may play a role in increasing the anti-proliferative properties or the reduction in 4-O-SO<sub>3</sub> sulfation which may be inhibitory to the anti-proliferative properties. This could be investigated further with similar analysis being performed on mammalian GAGs to identify differences and similarities.

Table 14: Heparin Sulfate sulfation type analysis.

<b>Sulfation</b>	<b>Prawns (%)</b>	<b>Cockles (%)</b>
<b>Unulfated</b>	3.51	26.61
<b>N-SO<sub>3</sub></b>	67.10	65.23
<b>2-O-SO<sub>3</sub></b>	52.66	19.06
<b>6-O-SO<sub>3</sub></b>	75.45	38.47

With the HS sulfation analysis, three of the four types of sulfation look to show significant difference from each other with only N-SO<sub>3</sub> sulfation being similar.

Cockles show an increase of unsulfated heparin disaccharides and a decrease in 2-O-SO<sub>3</sub> and 6-O-SO<sub>3</sub> disaccharides. With more differences than similarities it cannot be hypothesised which sulfation could potentially be affecting the differences in anti-proliferative activity. Theoretically it could be the combination of all three differences along with differences in the chondroitin sulfate disaccharides as well. With the similarities in the N-SO<sub>3</sub> sulfation however, it can be hypothesised that this type of sulfation does not account for the difference in anti-proliferative activity between prawns and cockles.

### Monosaccharide Analysis:

Aldairi et al, 2018, on which this study predominantly follows on from, used the same external source to perform the monosaccharide analysis on their cockle derived GAGs. By comparing the results between the prawns and the cockles we can begin to hypothesise the relationship between prawn and cockle GAGs and why there is a difference in anti-proliferative properties and hopefully begin to hypothesise why marine GAGs exhibit anti-proliferative properties where the mammalian GAGs do not.

Table 15: Cockle and prawn monosaccharide analysis comparison.

<b>Name</b>	<b>Cockles (%)</b>	<b>Prawns (%)</b>
<b>Fuc</b>	11.1	4.6
<b>GalNH<sub>2</sub></b>	16.7	13.4
<b>GlcNH<sub>2</sub></b>	9.9	24.5
<b>Gal</b>	19.1	14.6
<b>Glc</b>	35.2	20.9
<b>Man</b>	3.7	4.4
<b>Xyl</b>	n/a	11.0
<b>GlcA</b>	4.3	6.63

GlcA, GlcNH<sub>2</sub> and GalNH<sub>2</sub> are the main monosaccharides found when acid hydrolysis of marine and mammalian GAG chains occur. Their presence confirms that the extraction process for both cockles and prawns has produces GAG chains in the extract.

The major differences are the decrease of GlcNH<sub>2</sub> in cockles, the increase of Glc in cockles and the presence of Xyl in prawns but not cockles. (Gal and Fuc also show an increase in cockles but not at the magnitude of the larger differences).

Potentially, Xyl could be an inhibitor of anti-proliferative activity and explain the differences between the prawns and cockles. Subsequently, this could also be said

for GlcNH<sub>2</sub>. Furthermore, the difference in anti-proliferative activity could be affected by the presence of Glc as this may enhance the anti-proliferative nature of the GAGs. Without individual testing of these components it cannot accurately be determined which factor is contributing to the anti-proliferative activity of the marine derived GAGs and more than likely it is a combination of all the factors both monosaccharide and disaccharide differences alike.

Overall however, both the monosaccharide and disaccharide analysis has given an insight into the structure of these marine derived GAGs and has showed that there is a structural difference between the two sources which can be hypothesised to account for the differences in the anti-proliferative effectiveness on K562 cancer cells.

#### MTT Results:

For all the data analysis and graphical representation of the MTT results, the software GraphPad was used. GraphPad is highly regarded within the scientific community for its' ease of use and data representation.

#### Cockle vs Prawn K562 Comparison:

The cockle and prawn GAGs comparison was used to see if the Prawn GAGs which showed a much simpler structure via the NMR had the same cytotoxic effects as the cockle derived GAGS.

The IC<sub>50</sub> result for both of these as a result of the triplicate investigation showed that there was a significant difference between the results and at every single data point except from 6.25 micrograms per ml. These results suggest a difference in

cytotoxicity from the different sources of GAGs with cockles being 2.25 times more effective based upon this.

An IC<sub>50</sub> was reached however with the Prawn GAGs within the experiment parameters at 51.98 micrograms per ml which suggests a positive result for the Prawn GAGs and that they are cytotoxic towards K562 cells.

Aldairi et al in 2018 achieved an average cytotoxicity of 4 micrograms per ml for the cockles but did state that there was inter-batch variability with the results with the extracted cockles. The results from this experiment are higher than of Aldairi et al 2018, however, for each plate in the triplicate the same batch of derived GAGs was used as a bulk extraction was undertaken for this research topic. This may explain the higher results and could indicate a lower true IC<sub>50</sub> for the prawn GAGs as well.

Scrutiny of the data analysis can also be undertaken to judge the accuracy of the IC<sub>50</sub> calculated. The analytical software uses a non-linear fit line of regression to calculate the IC<sub>50</sub>. The accuracy of this line of regression can be determined using the R<sup>2</sup> value, which is the coefficient of determination. As standard, an R<sup>2</sup> value of over 0.95 (maximum 1 for perfect fit) is desired and deemed to be scientifically accurate. However, this needs to be coupled with physically looking at the graph to see the closeness of fit as a high R<sup>2</sup> value is not always a true indicator of closeness of fit.

For cockles, the coefficient of determination value was 0.9631. This indicates a close fit of the line of regression. Upon inspection, the line of regression shows slight underestimation at the higher and lower concentrations which would account for the coefficient of determination being below 1. This suggests the IC<sub>50</sub> from this experiment should therefore be accurate.

The prawn GAGs has a coefficient of determination of 0.8115. Upon inspection of the graph this seems to be due to a gross underestimation at the lowest concentration with the rest of the graph seeming to have a close fit. Based upon the coefficient of determination alone the IC50 could be suggested to not be accurate however coupled with visible inspection that may not be the case.

An interesting aspect of this data is that both the cockle and prawn GAGs show cell growth promotion at the lowest concentration of 3.125 micrograms per ml with Prawns showing 30-40% cell growth promotion. The mechanism of action behind this is unknown and could further be investigated to see if it was an anomaly or not. This potential property of the GAGs was therefore monitored in the other cell lines tested to see if it was a recurring property.

#### U2OS:

The U2OS cell line had an IC50 of 45.40 micrograms per ml. This suggests that prawn GAGs are cytotoxic on this cell line. This result indicated that this cell line is more responsive than the K562 cell line, however, the upper limit of the U2OS results were higher than the upper limit of the K562 results so this cannot be definitively determined.

The U2OS data points show a lot of variance so there is little significant difference between the data points at the various concentrations. In fact, the first indication of significant difference is between 200 micrograms per ml and 0.78125 micrograms per ml. This lower concentration also shows a significant difference when compared to 100 micrograms per ml.

The coefficient of determination also helps to show the variance between the results with a value of 0.5719. This indicates a very loose fit for the line of regression. Upon

visible inspection this could be due to the underestimation of the lowest four concentrations and overestimation of the middle four concentrations.

The reason for this inaccuracy could be due to the exclusion of the lower concentrations of plate two in the triplicate experiment due to contamination. The 6 triplicate wells on the 96 well plate of this experiment were somehow contaminated and had to be excluded altogether leading to only two sets of data being used for the lower six concentrations where the line of regression is most inaccurate.

To improve upon this given less time constraints, another plate could be performed to replace plate two in its entirety to see if better results are obtained.

Once again, at the lowest concentration (albeit significantly lower than the 3.125 micrograms per ml of the comparative experiment), cell growth looks to be promoted. However, due to the large variance the lower limit goes below 100% cell viability so this cannot be safely determined.

#### MDBK:

The MDBK cell line had an IC<sub>50</sub> of 105.4 micrograms per ml. This shows that the prawn GAGs have cytotoxic effects on the cell line.

The data points between 25 micrograms per ml and 200 micrograms per ml all showed significant difference from each other and individually showed very little variance between their own nine total readings/wells across the three triplicate plates. Once the cell line reached approximately 100% cell viability at 25 micrograms per ml the data points show no significant difference and the variance greatly increases. This may be caused due to the lower concentrations being prepared via



serial dilution leading to a greater level of inaccuracy and variation at the lower concentrations.

The coefficient of determination was 0.8071 for this experiment. Upon visible inspection, this is most likely due to the lack of correlation and erratic nature of the data points at the lower concentrations of GAGs added. Once the variance decreases post 25 micrograms per ml added, the line of regression seems to show an accurate fit. This can be shown by excluding the values that show erratic variance.

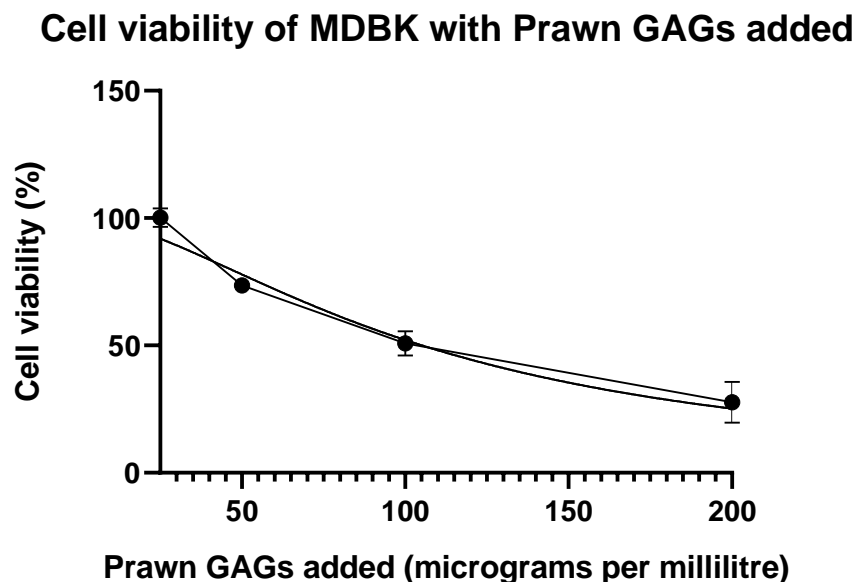


Figure 35: MDBK MTT graph as shown in the results section but with the lowest eight concentrations excluded.

These 4 data points show a coefficient of determination of 0.9378 showing that the line of regression is an accurate fit, especially in comparison for when it had to accommodate for the varied lower concentration values.

This only slightly changes the IC<sub>50</sub> value down to 105.2 micrograms per ml (97.29-113.9 with 95% CI) which has a very minimal effect on the actual result but narrows down the variance of the result substantially.

Once more at the lower concentrations the data points indicate slight promotion in growth but once more the variance does drop below 100% cell viability so cannot be accurately determined.

#### BEAS-2B:

The BEAS-2B cell line had an IC<sub>50</sub> of 82.01 (71.64 after outlier correction) micrograms per ml. This shows that the prawn GAGs are cytotoxic to this cell line. At the higher concentrations, some of the data points do show a significant difference from each other. 200 micrograms per ml shows significant difference with 50 micrograms per ml and below indicating the concentration does have an effect on the cell viability of this cell line.

Some of the data points in this data set do show a large variance (100 micrograms per ml) and could be further investigated for the removal of any potential outliers. When analysing the cell viabilities for this concentration, all the values fall between 34.40% and 43.56% with the exception of a 100.57%. Therefore, this can be removed as an outlier. This lead to a new IC<sub>50</sub> of 71.64 micrograms per ml being generated. This also vastly decreased the variance of the 100 microgram per ml data point making it significantly different from all the other data points compared to before when it shared no significant difference with the majority of data points.

The coefficient of variation for the new outlier corrected graph was 0.4079. With visible inspection this will be due to overestimation of the lowest four concentrations and the underestimation of the four concentrations after that and the large variance

of all eight data points. The steep negative decline after 25 micrograms per ml can then not be accounted for due to the horizontal nature of the points before that. Once again, we can do further analysis to exclude these initial points.

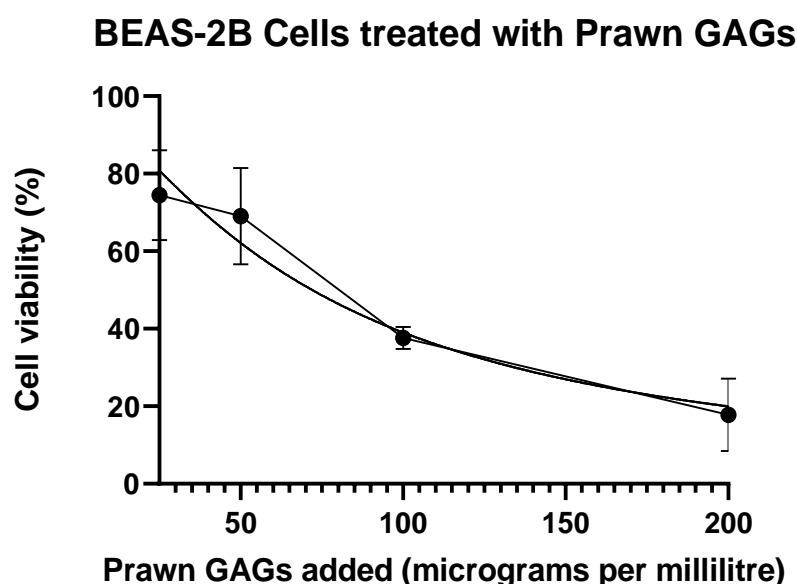


Figure 36: BEAS-2B MTT cell viability graph of highest four concentrations.

This graph gives an IC<sub>50</sub> value of 72.00 micrograms per ml (60.51 – 85.50 with 95% CI). This has only minimally changed the IC<sub>50</sub> value but has greatly narrowed down the variance range of the IC<sub>50</sub> value to give a better determination of the true IC<sub>50</sub> value. The coefficient of determination of this new graph was 0.7524. This is due to the overestimation of the starting points and still does not indicate a good, close fit but is substantial improvement than the fit on the graph as a whole.

Interestingly, unlike the other cell lines discussed and analysed so far, this is the first cell line to not reach 100% cell viability at any concentration even with the upper limits of variance of the data points. This contradicts the findings on K562 of promoted cell growth at the lower concentrations and suggests even at minimal concentrations the prawn GAGs may exhibit cytotoxic effects.

#### MOLT-4:

MOLT-4 showed an IC<sub>50</sub> of 4.627 micrograms per ml, this shows that the prawn derived GAGs are cytotoxic to the MOLT-4 cell line. The lowest six concentrations and highest six concentrations of GAGs showed a significant difference from each other. The two groups of six showed no significant differences within the group and within the groups they showed no correlation as well.

Aldairi et al, 2018, when experimenting on MOLT-4 cell lines derived a result of approximately 1 microgram per ml when using cockle derived GAGs as opposed to prawn GAGs. The K562 findings previously discussed showed that on the K562 cell line prawn GAGs were 2.25 times less cytotoxic than the cockle equivalent. Using this cytotoxicity factor based upon the assumption it would be approximately similar across cell lines it would result in the IC<sub>50</sub> being equivalent to roughly 2 micrograms per ml. This is in line with what Aldairi et al, 2018 discovered.

Between 3.125 and 6.25 micrograms per ml of GAGs added, there is a massive increase in the cytotoxic effects of the GAGs. This descends from an average of 96.9% cell viability down to 6.63% cell viability. This is a strong confirmation of the cytotoxicity of the prawn GAGs at the IC<sub>50</sub> of 4.627 micrograms per ml.

The coefficient of variation for this dataset was 0.9832. This implies a very close and accurate fit for the line of regression and when coupled up with visual observation and the very low variance of all the data points this is confirmed.

Like K562, at the lower GAGs concentrations, cell viability is promoted above 100%. Even with the lower limits of the variance these results are still above the 100% cell viability threshold and therefore in very small concentrations the prawn GAGs may in fact promote cell growth and proliferation.

### Inconclusive/Inaccurate Cell Lines:

Both the Wehi-3 and SAOS-2 cell line were also tested under the same experimental conditions as the other cell lines but had some unexpected problems with the results so were not included in the results section but will be presented and further discussed in this subsection.

The Wehi-3 cell line had a wide variance of results between the lowest concentration and 100 micrograms per ml in a similar fashion to the other cell lines when small concentrations were tested upon them. Between 100 micrograms per ml and 200 micrograms per ml the 50% cell viability threshold was crossed and gave an IC<sub>50</sub> of 196 micrograms per ml. Due to the wide variance of all the data points however, the software used could not calculate a range using a 95% confidence interval.

### **Cell viability of Wehi-3 with concentrations of Prawn GAGs added**

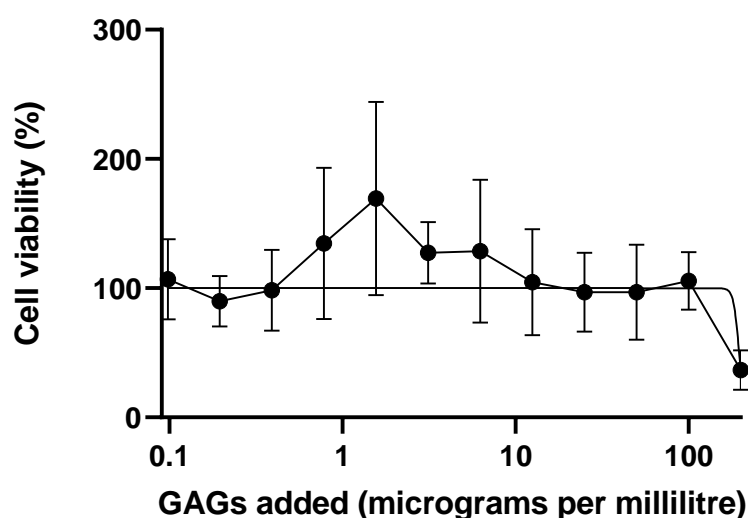


Figure 37: Cell viability graph of Wehi-3 cells when various concentrations of prawn GAGs were added and recorded via the MTT assay.

All the results below 100 micrograms per ml showed no significant difference, however the 200 micrograms per ml results did show a significant difference

compared to all the other data points. This could suggest that the IC50 may have been reached and may not just be an anomalous result.

If this cell line was to be incorporated into the actual results, it shows the strongest inclination for lower concentrations of GAGs to promote cell proliferation as a substantial amount of data points find their mean above the 100% cell viability threshold. However all apart from one (3.125 micrograms per ml) have their lower variance points below 100% cell viability so this cannot again be accurately concluded.

The only way to accurately confirm this would be to test higher concentrations to see if they followed suit with the results post 100 micrograms per ml. The reason this was not done however is because in a clinical setting, the concentrations higher than those tested in these experiments would be extremely difficult to actually use and administer effectively so the information gained from this would not be of much practical use. Furthermore, Wehi-3 is a mouse derived cell and the main target of this therapeutic would be human malignancies resulting in the further and prolonged testing of this cell line may not be a suitable use of resources and time.

The SAOS-2 cell line was only able to be completed in duplicate due to contamination of the incubator in the research establishment contaminating the stock of SAOS-2 cells currently in culture at the time and the in progress MTT plates. The duplicate plates also had a very large variance for each data point meaning that there was no significant difference (apart from the lowest and highest concentrations of GAGs added) between any of the results and an accurate conclusion could not have been generated from this.

### Cell viability of SAOS-2 cells with Prawn GAGs added

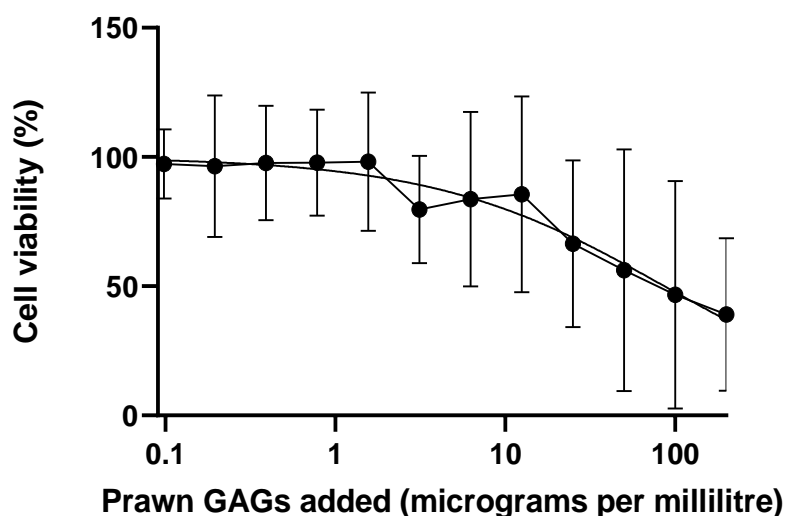


Figure 38: Cell viability of SAOS-2 cell line when various concentrations of prawn GAGs are added and results recorded via the MTT assay.

An IC<sub>50</sub> of 86.58 micrograms per ml was generated however with a 95% confidence interval the range was 44.69 – 255.1 micrograms per ml which branches between confirmation the GAGs are cytotoxic at the lower limit up to cytotoxicity at only an unusable concentration at the upper limit.

To improve upon this and have this cell line in a useable format, a new batch of SAOS-2 cells would have to be cultured and repeated again in triplicate using the MTT assay.

#### MTT Comparison:

Individually, it has now been established if the prawn GAGs are cytotoxic to each respective cell line. By comparing the results between the cell lines and investigating similarities and differences, there may be a potential to identify some relationships between these cell lines regarding the cell viabilities and increasing our understanding of how the prawn GAGs work.

Table 16: A master table of all cell lines tested on and their corresponding cell viability alongside various cell line characteristics.

CELL LINE	IC50 (MICROGRAMS PER ML)	HYPOTHESED COCKLE GAGS IC50 (MICROGRAMS PER ML)**	GROWTH MEDIUM	ADHERENT OR SUSPENSION	HUMAN OR ANIMAL
K562	51.98	23.10	RPMI	Suspension	Human
MOLT-4	4.627	2.06	RPMI	Suspension	Human
MDBK	105.4	46.84	DMEM	Adherent	Bovine
U2OS	45.4	20.18	DMEM	Adherent	Human
BEAS-2B	71.64	31.84	DMEM	Adherent	Human
SAOS-2*	86.58	38.48	DMEM	Adherent	Human
Wehi-3*	196	87.11	DMEM	Suspension	Mouse

(\*) indicates these cell lines were not used in results due to factors discussed in a previous subsection

(\*\*) A 2.25 cytotoxicity difference was shown between cockle and prawn GAGs on the K562 cell line. The hypothesis for this column is based upon the assumption the two differently sourced GAGs have a proportionate effect across the cell lines.

The first factor to be investigated is a factor that only effects the cells in an in-vitro setting which is the growth medium. The two growth mediums used in this investigation were RPMI and DMEM.

When excluding the two cell lines that were not included in the results, both the growth medium and the adherent/suspension characteristic contain the exact same cell lines so cannot be individually investigated and were therefore grouped together in the following graph.



## Graph of cell characteristics potentially affecting the IC50

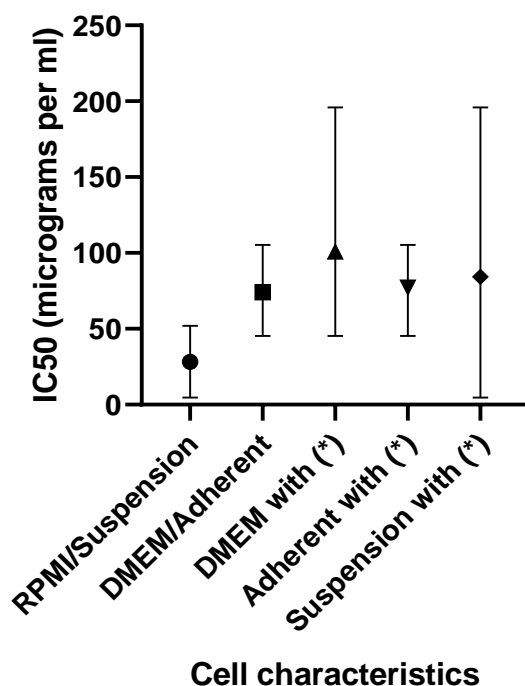


Figure 39: A graph of IC50 versus the cell characteristics.

The RPMI/Suspension cell lines (henceforth group 1) and the DMEM/Adherent cell lines (henceforth group 2) have an average IC50 of 28.3 micrograms per ml and 74.1 micrograms per ml respectively. Using an unpaired t-test to investigate whether there is a significant difference or not gives a p value of 0.2065. As this value is greater than 0.05 (which is the standard threshold for t-tests) it can be concluded that the null hypothesis of no significant difference between the two groups is true.

If the questionable results of the (\*) cell lines are used, we can separate the results into adherent and suspension independently due to the Wehi-3 cell line being suspension and cultured in DMEM media. A t-test of these two groups generates a p value of 0.8959 which strongly agrees with the null hypothesis that there is no significant difference between the groups.

A one way ANOVA was conducted of all five groups generated on the graph which gave a p value of 0.6627. Again, this indicates that the null hypothesis of no significant difference is true between all the groups.

This is a very basic statistical analysis that is limited by a few factors. To begin with, the groups are unbalanced. There is a larger amount of adherent cell lines and cell lines cultured in DMEM media. Secondly, this is an extremely small data set. In group 1 there is only two data points and in group 2 there is only three. The smallness of the sample size will not accommodate for any outliers or anomalous cell lines that may not fit the overall trend and therefore may be a limiting factor of this analysis. The other factors not accounted for are not evenly weighted between the two groups either. Group 1 only contains human leukemia and group 5 only contains leukemia in general. Group 2 contains both animal cell lines and healthy cell lines which may affect the results. These factors were further investigated below, however due to the uneven spread of these factors between the groups they may limit this statistical analysis.

To investigate the difference between animal and human sourced cell lines the (\*) will need to be incorporated otherwise there will only be a solitary animal sourced cell line to represent that group.

### Human versus Animal sourced IC50 of cell lines when Prawn GAGs are added

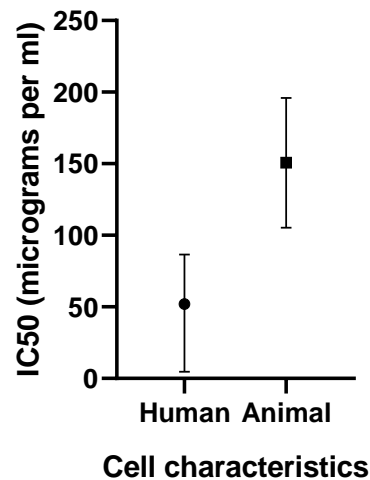


Figure 40: IC50 mean and range of cell lines when grouped based upon the sourcing of the cells.

When grouped via this way, the human sourced cell lines have a mean IC50 of 52.05 micrograms per ml and the animal sourced cell lines have an IC50 of 150.7 micrograms per ml. A two-tailed t-test generates a p value of 0.0318 which rejects the null hypothesis of no significant difference and suggests there is a significant difference between the two groups. This is further illustrated by the graph as the upper range of the human sourced cell lines does not overlap with the lower limit of the animal sourced cell lines.

Once more, this statistical analysis is limited by the sample size. The animal group only had two data points for reference in comparison to the five data points of the human sourced cell lines. Also, this data analysis had to incorporate the two (\*) cell lines which cannot be confirmed as accurate results. This may impact the accuracy of this analysis as a consequence however both groups contained one of these questionable results each which may balance it out.

The final and arguably most important analysis/comparison is comparing the healthy cell lines to the cancerous ones.

### Healthy versus Cancerous cell lines

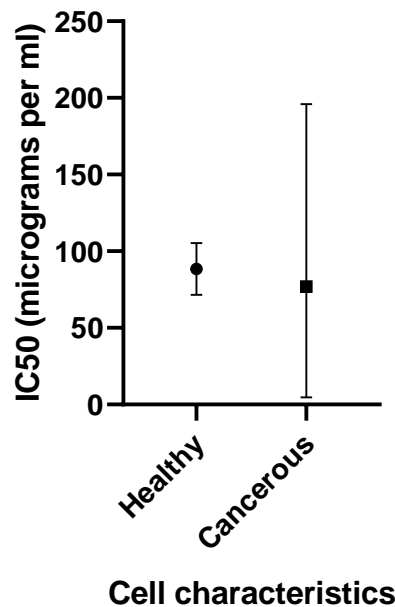


Figure 41: Comparing the mean and range IC50's of the investigated cell lines when grouped as healthy and cancerous.

The mean of the healthy cell lines was 88.52 micrograms per ml in comparison to the mean IC50 of the cancerous cell lines being 76.92. This suggests that cancerous cells are more responsive to the cytotoxic properties of the prawn GAGs. However, a two tailed t-test gives a p value of 0.8415 which accepts the null hypothesis of there being no significant difference between the two groups.

However, if we exclude the animal cells and the rejected SAOS-2 cells for being inaccurate and stick to the confirmed accurate results only, a different outcome is determined.

## Healthy versus Cancerous cell lines (human cells)

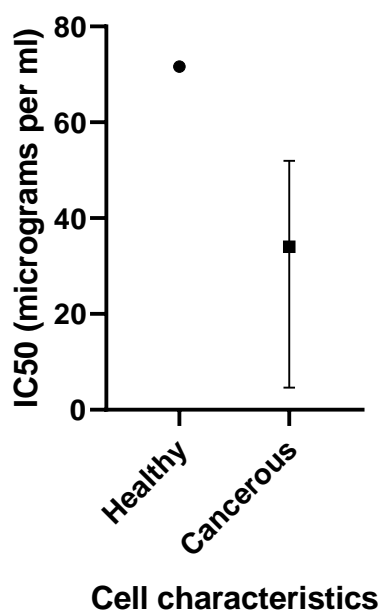


Figure 42: IC50 mean and range of human healthy and cancerous cells when prawn GAGS are added.

As shown above, the IC50 of the healthy human cell line (BEAS-2B) does not fall within the range of the cancerous cell lines and is over double (71.64 compared to 34.00 micrograms per ml) the mean IC50 of the cancerous cell lines. The t-test does however generate a p value of 0.3316 which accepts the null hypothesis of no significant difference however with the healthy cell line group only having one data point it cannot be decisively concluded either way.

This analysis is very limited due to only one human healthy cell line being investigated. It does however suggest that cancerous cells are more responsive to the cytotoxic properties of the prawn GAGs than healthy human cells are. This would need to be confirmed with a larger sample size.

Ideally, a final comparison would be made of cancerous cell lines against their direct healthy counterpart to determine on an individual basis based upon the *in vitro*

results if the prawn GAGs could be a potential effective treatment. As the main hypothesised use of the marine GAGS would be to treat leukemia, the K562 and MOLT-4 results should be investigated against healthy bone marrow cells such as human bone marrow mononuclear cells (BMNC's) or HEL 92.1.7 and AR230-s.

#### Cell Lines:

During this study a plethora of cell lines were used. This subsection will outline what the cell lines were and delve into a little bit of detail about them.

The primary focus of this study was on the cell line K562. K562 is a human erythroleukemic cell line as it expresses glycophorin on the surface, glycophorin is found exclusively in human bone marrow on erythroid cells (Andersson, Nilsson and Gahmberg, 1979). As shown by the age of the protocol cited, this cell line was discovered long ago and has been heavily researched since. K562 is a suspension cell line which was grown in RPMI-1640 media with penicillin and streptomycin added to prevent infection and bovine fetal serum and l-glutamine also added. These cells were cultured at 37 degrees Celsius in a cell culture incubator with carbon dioxide injection, as was all the cells to be further discussed. From investigation, the optimum incubation time was found to be 2-3 days before needing to be split when cultured in a T25 flask. These cell lines were both cultured as a parental cell line and a Cisplatin resistant cell line. These cells were found to be the most robust and easy to culture during this investigation.

MOLT-4 is a human acute lymphoblastic leukemia cell line which like K562, was also again cultured in suspension (Ma et al, 2014). These were also cultured in the same media as the K562 cells and once again had an optimum passage time of 3-4 days.

The only noticeable difference is that this cell line was a little less robust and was more prone to death if mishandled or over-cultured.

BEAS-2B are human bronchial epithelial cells (Kinnula et al, 1994) that are adherent cells cultured in DMEM (Dulbecco's Modified Eagle's Medium) again added with 10% fetal bovine serum and streptomycin and penicillin. This time l-glutamine was not needed to be added as the medium came with it present. The BEAS-2B cells required on average 4-5 days to reach confluence in a T25 flask. These were the only healthy human cell lines readily available at the research establishment within the timeframe this research was undertaken.

Another strain of healthy cells was also used, albeit from an animal source. MDBK (adult bovine kidney) are a cell line that is capable of continuous cultivation as discovered and published in 1958 by Madin and Darby. Once again they were cultured in DMEM and had an optimum time of confluence of approximately 4-5 days. Although healthy animal cells are not directly relevant to a therapeutic potentially designed to treat human derived leukemia, by investigating its' properties on healthy and malignant animal cells we may be able to help further understand the capabilities and mechanisms of action of the marine derived GAGs.

Wehi-3 is a mouse derived cancer cell line from the peripheral blood so was investigated to see if the efficacy of the therapeutic varied when used on an animal derived leukemia. Wehi-3 is also an interesting cell line as it secretes interleukin 1 and colony-stimulating factors (Booth, Prestidge and Watson, 1983). As it is a leukemia cell line, it is cultured in suspension but this time unlike the human equivalent, it is cultured in DMEM. Like K562 however, it was ready for passage approximately every 3 days.

U2OS cells are a human osteosarcoma cell line and was one of the first generated cell lines and is widely used in biomedical research (Niforou et al, 2008). Once again this was an adherent cell line cultured in DMEM. As blood cells develop from stem cells in the bone marrow, this cancer was of interest to investigate to see if there were any similarities with the therapeutic response compared with K562 and MOLT-4 leukemia.

Finally, SAOS-2 were also used which once again is a human osteosarcoma cell line, with this one recorded in publications as showing osteoblastic features (Prideaux et al, 2014). This once more was an adherent cell line grown in DMEM. This cell line was of relevant interest for the same reasons as U2OS and also because now intra-malignancy comparisons could be made between SAOS-2 with U2OS and K562 with MOLT-4 to see if there was therapeutic variation between the two cell lines when they are both from the same malignancy.

#### MTT Limiting Factors:

The MTT assay as previously discussed in this paper is persistently used across research laboratories around the world. However, it does not come without its' limitations.

As this study was conducted over a year, the stability of the MTT reagent could have been a limiting factor that may have potentially affected the results. The MTT reagent is light-sensitive and the batch used in this study was frequently opened and used throughout the year by many researchers in the establishment. This means that the time it was left in the light cannot be quantified or controlled as it was used by a wide range of differently skilled researchers ranging from undergraduate students to post-doctoral researchers.



To improve upon this, if financially viable, the experiments could be repeated and each time a small one use batch of MTT reagent could be prepared in a dark room, negating the destabilising factor of time and light exposure.

Solubilisation of the formazan crystals was not always uniform and consistent which may have led to false absorbance readings. One way to improve upon this would be to perform the MTS assay instead which produces water-soluble formazan and removes the need for solubilising the final product (Tonder, Joubert and Cromarty, 2015).

At the lower end of chemotherapeutic pharmaceutical concentration added to the wells, the results became very inconsistent and had great variation. This may be due to the sensitivity of the MTT assay itself. In a study conducted by Tonder, Joubert and Cromarty in 2005, they found that the SRB (sulforhodamine B) assay showed greater sensitivity and a smaller variation than the MTT assay. Potentially to improve upon the results this assay could be used in future studies.

#### Protein Lysis:

The BSA (Bovine serum albumin) standard curve as a standard is effectively used to determine the total amount of protein produced from the cell lysis procedure. This is of particular importance as the cell lysate is used in both the SDS-PAGE analysis and for the affinity chromatography, so a sufficient amount of protein is required for detection in both of these methods, especially as there is no prior knowledge as to how much protein is separated into each fraction via affinity chromatography. The amount of protein present in a sample also determines which stain to use on the SDS-PAGE gels as different staining methods have different sensitivities.

Coomassie blue for instance can detect microgram amounts of protein whereas

silver stain and Oriole fluorescent stain can detect nanogram amount of proteins on an SDS-PAGE gel.

There is an issue with one step in the cell lysis protocol used which could be improved upon. If incorrect cooling is applied during the sonication stage, localised heating could occur which could potentially lead to protein denaturation and aggregation. This would be detrimental to the affinity chromatography as if the protein that binds to the GAGs is sufficiently denatured it will not bind to the stationary phase in the column and will then elute with the first buffer wash causing a lower elution on the subsequent salt washes. This may give overall lower absorbance readings when analysed for protein concentration in the later fractions which would suggest less cellular proteins undergo strong binding with the GAGs.

Freeze-thaw cell lysis (Tansey, 2006) with careful temperature control when thawing could be a safer method for this procedure. Another alternative could be liquid homogenization (Myers, Rwxhadevi and Ramesh, 2011) if financial situation allows.

#### SDS-PAGE Results:

The SDS-PAGE results when stained with the Oriole fluorescent stain showed that there was multiple proteins that had high-specific binding to the immobilised GAGs in the stationary phase. Using a protein ladder as a rough size estimate (limitations discussed in the next sub-section) these proteins are shown to be between 2-10kDA. This is extremely small for a cellular membrane protein which was what was hypothesised to be the mechanism of action of the GAGs.

The SDS-PAGE gels show that in the first lane (total cell lysate) that there was a lot of excess run off of the cellular proteins which in theory should indicate that the

immobilised GAGs were saturated with binding complexes successfully and virtually all the available GAGs should have been bound to cellular proteins.

Wells 2-6 show that via the phosphate buffer wash that there was still excess proteins unbound and subsequently washed out. The volume of protein bands present in these wells suggest that there was not a lot of cellular proteins bound to the immobilised GAGs.

Wells 7-11 show that there was some non-specific binding between the cellular proteins and the GAGs as the low salt concentration interfered with this and negated it causing the proteins to detach and wash off

Wells 12-16 with the medium salt concentration shows that nearly all non-specific binding was removed with the low salt concentration, proteins may still have been removed by this wash just in minimal concentration.

Wells 17-21 shows a few remaining bands which represent the proteins that had high-specific binding which was negated by the high concentration salt wash. In theory these are the proteins that interact with the GAGs and cause them to have their cytotoxic action.

#### Highly specific binding proteins:

The low molecular weight of the highly specific bound proteins, according to the initial hypothesis, is a peculiar result as cellular membrane proteins are very rarely this low in molecular weight.

To investigate whether or not it is a cellular membrane protein, a cellular membrane preparation could be performed.

An efficient way to undertake this would be to use the ThermoFisher Mem-PER plus kit. This method works first by washing cultured cells in 3 millilitres of the cell wash supplied and and centrifuging, followed by a 1.5 millilitre cell wash and centrifugation, followed by a 0.75 millilitre suspension in permeabilisation buffer and centrifugation after a 10-minute incubation at 4 degrees Celsius. This is finally centrifuged at 4 degrees Celsius at 16000 xg and the supernatant collected (Cirbaite, Meier and Siurkus, 2013). This is then resuspended in 0.5 millilitres of the solubilisation buffer and incubated at 4 degrees Celsius for 30 minutes with constant agitation. Finally, this is centrifuged for 15 minutes at 4 degrees Celsius at 16000 xg and the supernatant extracted which should contain isolated cellular membrane proteins. These can then be added to the affinity column as done in this overarching study in place of the total cell lysate.

This should show less protein present between wells 1-16 as the intracellular proteins are no longer present. If the results for wells 17-21 are the same then this indicates the result is a very small membrane protein, if not, a different mechanism of action may be in place that was not hypothesised about.

One such mechanism may be endocytosis. This is where the cell engulfs the external agent (GAG in this case) and internalizes it. This would mean that the protein bands then represent an intracellular protein that binds to the GAGs and stars a cascade of chemical signalling that induces cell death.

Another interesting factor of the SDS-Gel PAGE results is that there is more than one protein band which means there is definitely more than one protein that the GAGs are binding to. To investigate if there is more than two you would have to

further separate the two present bands in wells 17-21 via another method such as 2D electrophoresis.

This could indicate the GAGs work in a multi-faceted approach and need a combination of proteins to be present to initiate cytotoxic action. On the other hand, just because the GAG binds to the proteins does not necessarily mean it is indicative of being the mechanism of action. *In vivo*, the GAG may not even be able to bind to that protein due to lack of access to it and may only be binding to it due to the experimental conditions of having the mammalian cell lysed and all intracellular and membrane proteins accessible.

#### SDS-PAGE Calibration:

SDS-PAGE is a complex protocol that has many different variables as part of it. Each variable can be changed and fine-tuned to have a plethora of effects on the experiment. A major variable is the type of stain used to visualise the separated proteins in the SDS-PAGE gel. Coomassie Blue is the common standard for staining SDS-PAGE gels. Briefly, this protocol uses a fixing solution followed by incubation in Coomassie blue stain to stain the entire gel blue finally followed by incubation in a destaining solution which destains the background faster than the protein bands leaving the protein bands a visible blue as the background destains to a lighter blue/transparent colour.

Silver stain is another commonly used staining method for SDS-PAGE gels. This method is more expensive per use but also more sensitive to proteins present. It uses a sensitising solution before staining and a developer solution after staining to further visualise present proteins. This protocol doesn't require background destaining as the developer solution 'darkens' the protein bands faster than the

background of the gel. Once the protein bands are visible a stopping solution is used to stop any further development.

Oriole fluorescent gel stain by BioRad is a simple yet expensive alternative way to stain the gels and more sensitive than the previous two stains discussed. This stain only requires incubation in a dark box then excitation underneath a UV lamp containing an ethidium bromide filter. This causes the bands to fluoresce and be easily imaged, it also requires no background destaining and once stained, the gels can be stored in their entirety for up to 6 months.

<b>Stain</b>	<b>Protein detection range</b>	<b>Background destaining</b>
<b>Coomassie Blue</b>		Yes
<b>Silver Stain</b>		No
<b>Oriole</b>		No

Over the course of this investigation, all three of these staining protocols were used to varying degrees of success. From a chronological perspective in relation to this investigation. Coomassie blue was the first staining procedure to be investigated.

When the gels with the applied affinity fractions were stained, it appeared that there was a negative result. The two most common probabilities from this were either a faulty stain or the protein bands being under the limit of detection for coomassie blue. To investigate this, bacterium lysed with BugBuster™ was used in place of the affinity columns and ran under the same experimental conditions.

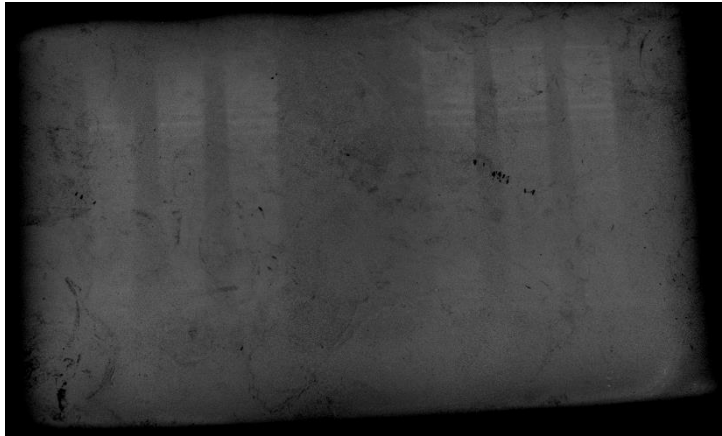


Figure 43: Lysed bacterium stained with Coomassie Blue.

As illustrated by the above figure, the lysed bacterium were visualised fine with the Coomassie blue stain, suggesting it was a limit of detection issue. This lead to the next step of using silver stain to visualise the protein bands.

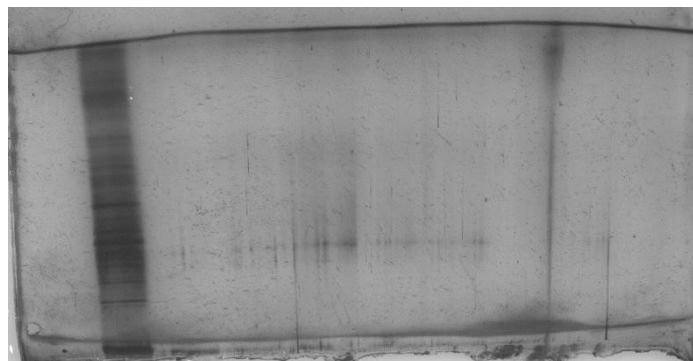


Figure 44: SDS-PAGE gel loaded with affinity fractions 1-11 stained with silver lysate.

As shown by the figure above, fraction 1 which is where the total cell lysate was added to the column shows a very strong positive result which was to be expected. However, every fraction after that (5 times phosphate buffer wash and 5 times low salt concentration wash) shows negligible results which goes against the theory of this experiment. To investigate if it was a limit of detection issue again, the gel was put back into the developer solution and allowed to over-develop.

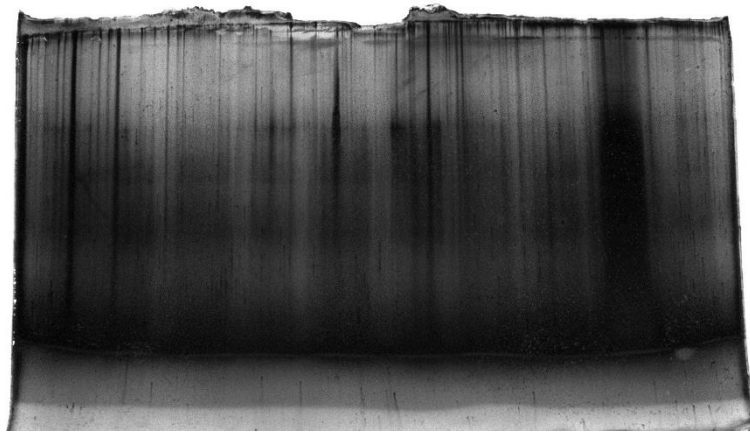


Figure 45: Over-developed SDS-Page gel with silver stain.

Overdeveloping the gel potentially shows present proteins in fractions 2-11 which is to be as of expected, however the lack of clarity of the gel once over-developed results in an unusable gel/result for scientific purposes. As once again the most suitable hypothesis is the limit of detection of the proteins is limiting this experiment, the next stage was to use Oriole fluorescent stain.

Using the Oriole fluorescent stain lead to the clear results as seen in the results section prior to this. However, there was still an issue with the fluorescent stain that wasn't rectified. The only molecular weight marker available in the research establishment only worked with visible protein stains such as Coomassie Blue and silver stain. If used with Oriole fluorescent stain it lead to gel images as follows.



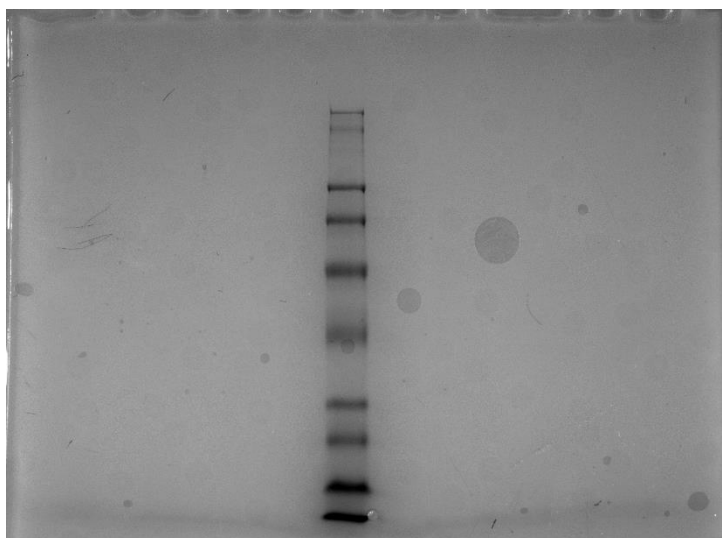


Figure 46: Molecular weight ladder with Oriole stain under the visible protein setting of the gel imager.

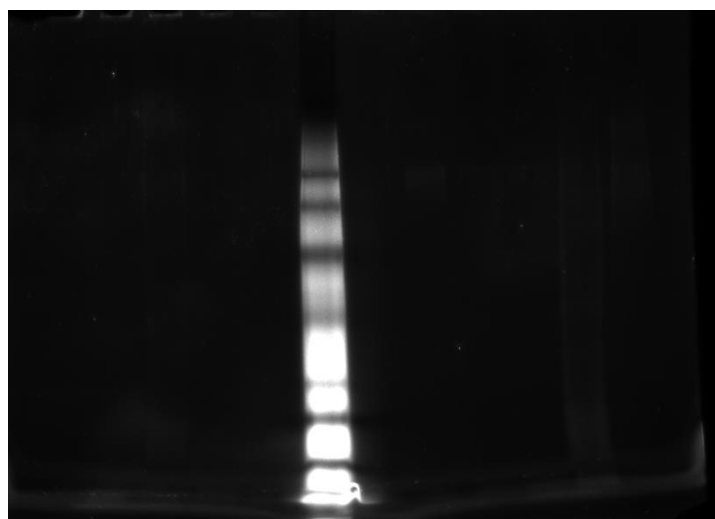


Figure 47: Molecular weight ladder with Oriole stain under the fluorescent protein setting of the gel imager.

As shown above, the protein ladder is only visible and usable when used on the visible protein setting of the gel imager which results in the fluorescent proteins not being visible on the gel. Due to financial limitations, a UV molecular weight ladder was unable to be obtained and a not ideal workaround was used to obtain a rough estimate of protein sizes. Using pre-cast gels from the exact same batch and under

the exact same experimental conditions even down to small details such as using the exact same gel tank. The experiment was repeated for the affinity fractions and a molecular weight marker and the molecular weight marker was super-imposed onto the gel to give a rough estimate of the size of the proteins isolated.

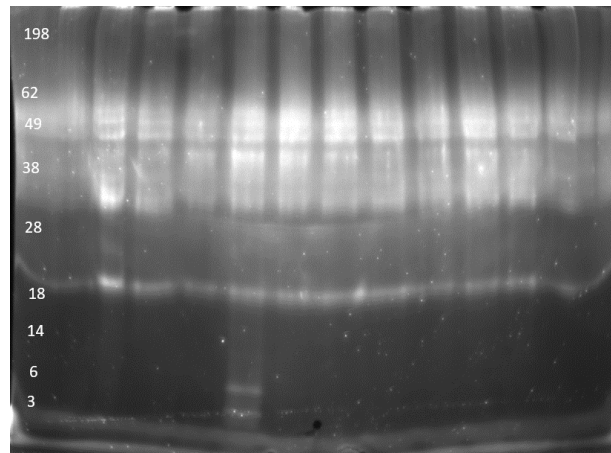


Figure 48: SDS-PAGE gel stained with Oriole fluorescent stain and superimposed molecular weight marker to roughly estimate the separated proteins in the affinity fractions after the high salt concentration wash (2M NaCl in phosphate buffer).

#### Affinity Chromatography:

For successful separation/purification of the total cell lysate and to isolate the highly specific binding proteins that had bound to the GAGs from the less specific binding proteins, differing salt concentrations were used (theory discussed in the affinity chromatography sub-section of the introduction).

Table 17: A brief overview of the contents of each affinity fraction and the reasoning behind the contents of the mobile phase.

<b>FRACTION NUMBER</b>	<b>1</b>	<b>2-6</b>	<b>7-11</b>	<b>12-16</b>	<b>17-21</b>
Mobile Phase Contents	Cell Lysate	50mM Phosphate buffer	0.2M NaCl in phosphate buffer	0.5M NaCl in phosphate buffer	2M NaCl in phosphate buffer
Reason	To allow proteins in cell lysate to bind to immobilised GAGs	To wash away any excess cell lysate left in the column	Slightly alters ionic binding of proteins to GAGs to remove non-specific binding	Larger alteration of ionic binding of proteins to GAGs to remove stronger non-specific binding of proteins	Largest alteration of ionic binding of proteins to remove specifically bound proteins from GAGs

As evidenced by the protein absorbance spectra, these various salt concentrations did in fact result in separation of the bound proteins to the GAGs. Having five fractions for each addition of buffer allowed the peak elution for each section to be captured within the five repeats and allowed for minimal overlap between the different additions of the buffers.

The buffer wash for fractions 2-6 was essential as evidenced by the SDS-Gel images as these gave a positive result and showed up proteins which would have been incorporated and interpreted as low specific binding proteins if not washed off first.

A stronger NaCl concentration potentially could have been applied afterwards to completely remove and specifically bound proteins and to check for their presence, however based upon the results it seems like the 2M NaCl concentration did a sufficient job and any stronger salt concentration would have been overkill.

The sham column was employed as a negative control with no GAGs linked to the stationary phase. This gives a negative control as it accounts and illustrates any

direct binding between the total cell lysate and the affi-gel 10 beads. There is no GAGs present for electrostatic bonds to be formed with by the total cellular proteins so in theory there should be a close to basal level of binding as the only binding will be non-specific binding directly to the affi-gel 10 beads which should be removed by the low salt concentration wash.

By analysing both absorbance spectra for the parental and cisplatin resistant K562 cell lines it is evident that the affinity chromatography was successful in the separation of the total cell lysate. The initial peak and subsequent wash with phosphate buffer alone shows that a substantial amount of the total cell lysate does not bind to the GAGs present in the stationary phase as the collected fractions show a high level of protein present that has run through. The introduction of a weak salt concentration shows an elution of proteins once more. This indicates that there was weak/non-specific binding between some of the total cell lysate and the GAGs that was disrupted by this salt concentration. Another increase in the salt concentration of the mobile phase shows a small elution of proteins in the parental cell line column and minimal elution in the cisplatin resistant cell line column. This indicates there may be a few proteins present in the cell lysate that incur slightly stronger bonding with the GAGs. When a high salt concentration is put through both columns a small protein elution is once more recorded. This indicates that between the GAGs and the total cell lysate there was some strong, specific binding with the GAGs linked to the stationary phase.

However, these absorbance spectra do not account for anything without comparison to a 'sham' column that has no GAGs linked to the stationary phase. Referring to the sham column spectra, it is shown that a much higher emission is recorded for the initial peak when a phosphate buffer is put through the column. This indicates that a

lot more of the total cell lysate has eluted from the column and not bound to the stationary phase. There are still very slight absorbance recordings for all three different salt concentrations, especially with the strongest salt concentration which borders on a baseline reading. This shows that when no GAGs are present, there is little to none strong binding of total cell lysate to the stationary phase and a lot less weak binding between the cell lysate and the stationary phase. This is due to no GAGs being present for electrostatic bonds to be formed with the cellular proteins and to be affected by ionic change due to the differing NaCl concentrations.

The overall outcome of this result is that potentially in the fractions after the final strong salt wash, there is the cellular protein that binds to the GAGs which the discovery of could lead to more in depth investigation into the mechanisms of GAG action in cancer cell lines and help to shine some light on why marine derived GAGs have anti-cancer activity but mammalian ones do not.

To further analyse this, these fractions could be analysed with a multitude of further analytical and purification techniques. These include gel chromatography to further purify the fractions which has a more precise separation. Another further analytical technique could be running the fractions on an SDS-PAGE gel to visualise which cell lysate proteins are in each fraction in comparison to the total cell lysate. The bands visualised after staining in the fractions after the strong salt wash could then be cut out and mass spectrometry performed on them to find out which cellular protein(s) is in the end fractions which would be indicative of the cellular protein(s) the GAGs bind to.

### Future Study:

Due to the nature of this study and the novel results produced, a plethora of future research paths have potentially opened to take this research further.

The discovery of prawn GAGs being a much simpler mixture when extracted, an investigation in to other marine sources could develop from there. One such approach could involve investigating the phylogeny of prawns and seeing any other marine species sharing a close evolutionary history also share a simpler GAG extract. This could be of particular interest when investigating the reasoning behind marine GAGs containing anti-cancer activity with mammalian GAGs not as a simpler complex would be easier and more efficient to analyse and notice differences in. Prawns belong to the class Malacostraca which contains approximately 30,000 individual species (Thorp and Rogers, 2016). With regard to taxonomic classification, this could be too broad and will more than likely be far too impractical to investigate, so another approach may be to look further down the taxonomic classifications and investigate species in the same genus and potentially family. The relevant taxonomic family for this would be Penaeidae.

Another approach to further study could be to test the anti-cancer activity of the various sourced GAGs on other cancer cell lines. This could be facilitated before or after identifying the binding protein in the cancer cell for the GAGs that gives the GAG anticancer activity. If it is after, a more efficient approach of testing GAGs on other cancer cells could be undertaken to see if it still shows anticancer activity on these. This would once again be done via the MTT assay and should be compared to a known cell line that has been shown to be responsive to GAGs (MOLT4 or K562

as used in the Aldairi et al (2018) paper would be the most efficient at the time of writing).

If time and resources were not a limiting factor to this study, affinity chromatography could be performed on both the cancer cell lines and the healthy cell lines to see if there is a difference in the proteins present in the final fractions of the affinity column. If there is a different protein present in the cancer cell line compared to the healthy cell line then this could suggest that that protein is specific to when the cell line is cancerous and could be specifically targeted therapeutically.

The study conducted in this research was mainly aimed at investigating the cytotoxicity of the chemotherapeutic derived from marine sources. Another property of the chemotherapeutic that could be further investigated is the anti-proliferative properties of the GAGs. The HGF-MET axis, which contributes to tumour progression in various cancers and accelerates cellular invasion linked with tumour metastasis (Cecchi, Rabe and Bottaro, 2010), is currently being investigated by using synthetic GAGs to inhibit this axis at the University of Salford. Although they are showing no cytotoxic effects, positive anti-proliferative results have been obtained via the scratch assay on the 'sonic hedgehog' (SHH) line of medulloblastoma cells. The scratch assay consists of plating adherent cells in a well and using a sharp point (usually a pipette tip), scratching a line through the plated cells. The cells are regularly imaged using a microscope linked up to imaging software at regular intervals and the average width of the scratch is measured (Liang, Park and Guan, 2007). This can then be converted into a percentage of distance closed and be illustrated as a variable over time and used comparatively with other differing experimental conditions such as concentration of chemotherapeutic agent added.

However, there are two main issues with this for this investigation, the most sensitive cancer cells and the main focus of this study (K562 and MOLT-4) are both suspension cells. Additionally, this study has found that in these cells lines and many others, an IC50 can be reasonably achieved and therefore the marine derived GAGs are cytotoxic.

The first and second issue can both be simultaneously be addressed by using different cancer cell lines. An initial and scientifically interesting step to take would be to first test the marine derived GAGs on the SHH DAOY medulloblastoma cells the synthetic GAGs were tested on using the MTT assay to see if there is any cytotoxicity. If not, then the scratch assay can be performed using the marine derived GAGs and can be compared to the synthetic GAGs. Alternatively, the adherent cancer cell lines that an IC50 was not reached at could be tested on via the scratch assay as even though the marine GAGs will not be cytotoxic, a chemotherapeutic that negates metastasis would still be very beneficial.

For the cancer cell lines that do achieve an IC50 with the marine derived GAGs, it may be possible to conduct the scratch assay at a lower concentration such as the IC10 to limit the death of the cancer cells and investigate and anti-proliferative properties.

### Conclusion:

To conclude, this study has shown that cockles are not the only marine source of glycosaminoglycans that have anti-proliferative properties *in vitro*. It has identified a range of cancerous cell lines that a reasonable IC50 can be achieved on and has begun to establish a relationship that the marine derived GAGs are less cytotoxic on healthy cells than they are on cancerous cells.



This study has also successfully isolated and illustrated the potential cellular proteins involved in the binding/activity of the GAGs via affinity chromatography and SDS-PAGE.

Furthermore, this study has also performed structural and compositional analysis on the prawn derived GAGs and used this with already established literature to identify differences between prawn, cockle and mammalian derived GAGs which may begin to explain the differences, and in the case of mammalian GAGs, lack of anti-proliferative activity.

This study could provide a solid foundation for multiple future studies into the use of marine derived GAGs in cancer therapeutics.

## References:

- Adan, A., Kiraz, Y., Baran, Y. (2016). Cell Proliferation and Cytotoxicity Assays. *Current pharmaceutical biotechnology*, 17(14), 1213-1221.
- Adhikari, H., Yadav, P. (2018). Anticancer activity of chitosan, chitosan derivatives, and their mechanism of action. *International Journal of Biomaterials*.
- Aldairi, A., Ogundipe, O., Pye, D. (2018). Antiproliferative Activity of Glycosaminoglycan-Like Polysaccharides Derived from Marine Molluscs. *Marine drugs*.
- Andersson, L., Nilsson, K., Gahmberg, C. (1979). K562- A human erythroleukemic cell line. *International Journal of Cancer*, 23(2).
- Andre, P. (2004). Hyaluronic acid and its use as a “rejuvenation” agent in cosmetic dermatology. *Seminars in cutaneous medicine and surgery*, 23(4), 218-222.
- Babu, A., Ramesh, R. (2017). Multifaceted Applications of Chitosan in Cancer Drug Delivery and Therapy. *Marine drugs*, 15(4), 96.
- Baskar, R., Lee, K., Yeo, R., Yeoh, K-W. (2012). Cancer and Radiation Therapy: Current Advances and Future Directions. *International Journal of Medical Sciences*, 9(3), 193-199.
- Berkey, F. (2010). Managing the adverse effects of radiation therapy. *American family physician*, 82(4), 381-388.
- Bio-Rad. (2019). Activated Immunoaffinity Supports. <http://www.bio-rad.com/webroot/web/pdf/lsr/literature/LIT156.pdf> [Accessed on 14th August 2019].

- Booth, R.J., Prestidge, R.L., Watson, J.D. (1983). Constitutive production by the WEHI-3 cell line of B cell growth and differentiation factor that co-purifies with interleukin 1. *Journal of immunology*, 13(3), 1289-1293.
- Bowman, S., Awad, M., Hamrick, M., Hunter, M., Fulzele, S. (2018). Recent advances in hyaluronic acid based therapy for osteoarthritis. *Clinical and Translational Medicine*, 7, 6.
- Brunelle, J., Green, R. (2014). Chapter Twelve- One-dimensional SDS-Polyacrylamide Gel Electrophoresis (1D SDS-PAGE). *Methods in Enzymology*, 541. 151-159.
- Butterfield, L. (2015). Cancer vaccines. *BMJ*.
- Byrd, J., Stilgenbauer, S., FLinn, I. (2004). Chronic lymphocytic leukemia. *American society of hematology*, 163-183.
- Cecchi, F., Rabe, D., Bottaro, D. (2010). Targeting the HGF/Met Signalling Pathway in Cancer. *European journal of cancer*, 46(7), 1260-1270.
- Cirbaite, E., Meier, S., Siurkus, J. (2013). Fast and simple enrichment of integral membrane proteins and membrane-associated proteins.
- Cornell University College of Veterinary Medicine. (2013). <http://eclinpath.com/hematology/leukemia/transforming-algorithm/> [Accessed on 20<sup>th</sup> August 2019]
- Coskun, O. (2016). Separation techniques: Chromatography. *Northern Clinics of Istanbul*, 3(2), 156-160.

Darvin, P., Toor, S., Sasidharan, V., Elkord, E. (2018). Immune checkpoint inhibitors: recent progress and potential biomarkers. *Experimental & Molecular Medicine*, 50(12), 165.

Deleris, P., Nazih, H., Bard, J. (2016). Chapter 10 – Seaweeds in Human Health. *Seaweed in Health and Disease Prevention*, 319-367.

Ding, L., Ley, T., Larson, D., Miller, C., Koboldt, D., Welch, J., Ritchey, J., Young, M., Lamprecht, T., McLellan, M., McMichael, J., Wallis, J., Lu, C., Shen, D., Harris, C., Dooling, D., Fulton, R., Fulton, L., Chen, K., Schmidt, H., Veizer, J., Magrini, V., Cook, L., McGrath, S., Vickery, T., Wendl, M., Heath, S., Watson, M., Link, D., Tomasson, M., Shannon, W., Payton, J., Kulkarni, S., Westervelt, P., Walter, M., Graubert, T., Mardis, E., Wilson, R., DiPersio, J. (2012). Clonal evolution in relapsed acute myeloid leukemia revealed by whole-genome sequencing. *Nature*, 481, 506-510.

Eden, R., Coviello, J. (2019). Cancer, chronic myelogenous leukemia (CML, Chronic Granulocytic Leukemia). *StatPearls*.

English, R., Ettedgui, J. (2010). Cardiological aspects of systemic disease. *Paediatric Cardiology*, 3.

Esko, J., Prestegard, J., Linhardt, R. (2017). Proteins That Bind Sulfated Glycosaminoglycans. *Essentials of Glycobiology*. (3).

Estey, E., Dohner, H. (2006). Acute myeloid leukemia. *The Lancet*, 368(9550), 1894-1907.

Fitton, J., Stringer, D., Karpiniec, S. (2015). Therapies from Fucoidan: An update. *Marine drugs*, 13(9), 5920-5946

- Gal, B., Bucher, C., Burns, N. (2016). Chiral Alkyl Halides: Underexplored Motifs in Medicine. *Marine Drugs*, 14(11), 206.
- Gandhi, N., Mancera, R. (2008). The structure of Glycosaminoglycans and their Interactions with Proteins. *Chemical Biology and Drug Design*, 72,455-482.
- Goding, J. (1996) Monoclonal Antibodies (Third Edition).
- Gooden, M., de Bock, G., Leffers, N., Daemen, T., Nijman, H. (2011). The prognostic influence of tumour-infiltrating lymphocytes in cancer: a systematic review with meta-analysis. *British Journal of Cancer*, 105(1), 93-103.
- Granatowicz, A., Piatek, C., Moschiano, E., El-Hemaidi, I., Armitage, J., AKhtari, M. (2015). An overview and update of chronic myeloid leukemia for primary care physicians. *Korean journal of family medicine*, 36(5), 197-202.
- Gyurkocza, B., Rezvani, A., Storb, R. (2010). Allogenic hematopoietic cell transplantation: the state of the art. *Expert Rev Hematology*, 3(3), 285-299.
- Hallek, M. (2017). Chronic lymphocytic leukemia: 2017 update on diagnosis, risk stratification and treatment. *American journal of hematology*, 92(9), 946-965.
- Hartmann, J., Haap, M., Kopp, H., Lipp, H. (2009). Tyrosine kinase inhibitors – a review on pharmacology, metabolism and side effects. *Current drug metabolism*, 10(5), 470-481.
- Henrotin, Y., Mathy, M., Sanchez, C., Lambert, C. (2010). Chondroitin sulphate in the treatment of Osteoarthritis: From *in vitro* studies to clinical recommendations. *Therapeutic advances in Musculoskeletal Disease*, 2(6), 335-348.

Huang, C., Ju, D., Chang, C., Muralidhar, R., Velmurugan, B. (2017). A review on the effects of current chemotherapy drugs and natural agents in treating non-small cell lung cancer. *BioMedicine*, 7(4), 23.

Hus, I., Rolinski, J. (2015). Current concepts in diagnosis and treatment of chronic lymphocytic leukemia. *Contemporary Oncology*, 19(5), 361-367.

Institute for Quality and Efficiency in Health Care (IQWiG), (2016). InformedHealth.

Jabbour, E., Kantarian, H. (2018). Chronic myeloid leukemia: 2018 update on diagnosis, therapy and monitoring. *American journal of hematology*, 93(3), 442-459.

Jamwal, S., Kumar, P. (2017). Chapter 19 – Animal Models of Inflammatory Bowel Disease. *Animal Models for the Study of Human Disease (Second Edition)*, 467-477.

Kariduraganavar, M., Kittur, A., Kamble, R. (2014). Chapter 1 – Polymer Synthesis and Processing. *Natural and Synthetic Biomedical Polymers*. 1-31.

Khan, A., Saba, A., Nawazish, S., Akhtar, F., Rashid, R., Mir, S., Nasir, B., Iqbal, F., Afzal, S., Pervaiz, F., Murtaza, G. (2017). Carrageenan based bionanocomposites as drug delivery tool with special emphasis on the influence of ferromagnetic nanoparticles. *Oxidative medicine and cellular longevity*.

Kidgell, J., Magnusson, M., de Nys, R., Glasson, C. (2019). Ulvan: A systematic review of extraction, composition and function. *Algal Research*, 39, 101422.

Kinnula, VL., Yankaskas, JR., Chang, L., Virtanen, I., Linnala, A., Kang, BH., Crapo, JD. (1994). Primary and immortalized (BEAS “B) human bronchial epithelial cells have significant antioxidative capacity *in vitro*. *American journal of respiratory cell and molecular biology*, 11(5), 568-576.

Kitic, N., Gschwandtner, M., Derler, R., Gerlza, T., Kungl, A. (2016). Preparation and Characterization of Glycosaminoglycan Chemokine Coreceptors. *Methods in Enzymology*, 570, 517-538.

Kouchkovsky, D., Abdul-Hay, M. (2016). Acute myeloid leukemia: a comprehensive review and 2016 update. *Blood cancer journal*, 6(7), 441.

Kumari, A. (2018). Mucopolysaccharidoses. *Sweet Biochemistry*.

Kusche-Gullberg, M., Kjellen, L. (2003). Sulfotransferases in glycosaminoglycan biosynthesis. *Current opinion in structural biology*, 13(5), 605-611.

Lacetera, A., Galante, S., Jimenez-Barbero, J., Martin-Santamaria, S. (2016). *Reference module in Chemistry, Molecular Sciences and Chemical Engineering*.  
<https://doi.org/10.1016/B978-0-12-409547-2.11712-3>

Lanzi, C., Cassinelli, G. (2018). Heparan Sulfate Mimetics in Cancer Therapy: The Challenge to Define Structural Determinants and the Relevance of Targets for Optimal Activity. *Molecules*, 23(11), 2915.

Lee, K., Mooney, D. (2012). Alginate: properties and biomedical applications. *Progress in Polymer Science*, 37(1), 106-126

Liang, C., Park, J., Guan, J-L. (2007). *In vitro* scratch assay: a convenient and inexpensive method for analysis of cell migration *in vitro*. *Nature Protocols*, 2, 329-333.

Liu, M., Guo, F. (2018). Recent updates on cancer immunotherapy. *Precision Clinical Medicine*, 1(2), 65-74.

Lodhi, G., Kim, Y., Hwang, J., Kim, S., Jeon, Y., Ahn, C., Moon, S., Jeon, B., Park, P. (2014). Chitooligosaccharide and its derivatives: preparation and biological applications. *BioMed research international*.

Lorente-Gea, L., Garcia, B., Martin, C., Quiros, L., Fernandez-Vega, I. (2017). Heparan sulfate proteoglycans and heparanases in Alzheimer's disease: current outlook and potential therapeutic targets. *Neural Regeneration Research*, 12(6). 914-915.

Ma, XC., Liu, CY., Sun, XJ., Wan, SG., Sun, WL. (2014). Genetic characteristics of human acute lymphoblastic leukemia cell line Molt-4. *Zhongguo Shi Yan Xue Ye Xue Za Zhi*, 22(2), 280-284.

Madin, S., Darby, N. (1958). Established Kidney Cell Lines of Normal Adult Bovine and Ovine Origin.

Mayers, G., Carel, J. (1998). Encyclopedia of Immunology (Second Edition).

Medical & Biological Laboratories Life Science, (2017). The principle and method of polyacrylamide gel electrophoresis (SDS-PAGE).

<http://ruo.mbl.co.jp/bio/e/support/method/sds-page.html> [Accessed on 1st August 2019].

Mehta, S., Suhag, V., Semwal, M., Sharma, N. (2011). Radiotherapy: Basic concepts and Recent Advances. *Medical Journal, Armed Forces India*, 66(2), 158-162.

Mohan, K., Ravichandran, S., Muralisankar, T., Uthayakumar, V., Chandirasekar, R., Seedeivi, P., Abirami, R., Rajan, D. (2019). Application of marine-derived polysaccharides as immunostimulants in aquaculture: A review of current knowledge and further perspectives. *Fish and Shellfish Immunology*, 86, 1177-1193.



Myers, J., Rekhadevi, P., Ramesh, A. (2011). Comparative Evaluation of Different Cell Lysis and Extraction Methods for Studying Benzo(a)pyrene Metabolism in HT-29 Colon Cancer Cell Cultures. *Cell Physiol Biochem*, 28(2), 209-218.

Naini, S., Soussi-Yannicostas, N. (2018). Heparan Sulfate as a Therapeutic Target in Taupathies: Insights From Zebrafish. *Frontiers in cell and developmental biology*, 6, 163.

Naveed, M., Phil, L., Sohali, M., Hasnat, M., Baig, M., Ihsan, A., Shumzaid, M., Kakar, M., Mehmood-Khan, T., Akabar, M., Hussain, M., Zhou, Q. (2019). Chitosan oligosaccharide (COS): An overview. *International journal of biological macromolecules*, 129, 827-843.

Nesic, A., Seslija, S. (2017). The influence of nanofillers on physical-chemical properties of polysaccharide-based film intended for food packaging, *Food Packaging*, 637-697.

Niforou, KM., Anagnostopoulos, AK., VOugas, K., Kittas, C., GOrgoulis, VG., Tsangaris, GT. (2008). The proteome profile of the human osteosarcoma U2OS cell line. *Cancer Genomics Proteomics*, 5(1), 63-78.

Ojima, T. (2013). Polysaccharide-degrading enzymes from herbivorous marine invertebrates. *Marine Enzymes for Biocatalysis*.

Olgierd, B., Sklarek, A., Siwek, P., Waluga, E. (2019). Methods of Biomaterial-Aided Cell or Drug Delivery: Extracellular Matrix proteins as Biomaterials. *Stem Cells and Biomaterials for Regenerative Medicine*, 163-189.

Paliwal, R., Paliwal, S., Agrawal, G., Vyas, S. (2012). Recent advances in search of oral heparin therapeutics. *Medicimnal Research Reviews*, 32(2), 388-409.

- Pandolfi, A., Stanley, R., Yu, Y., Bartholdy, B., Pendurti, G., Gritsman, K., Boultonwood, J., Chernoff, J., Verma, A., Steidl, U. (2015). PAK1 is a therapeutic target in acute myeloid leukemia and myelodysplastic syndrome. *Blood*, 126(9), 1118-1127.
- Papakonstantinou, E., Roth, M., Karakiulakis, G. (2012). Hyaluronic acid: A key molecule in skin aging. *Dermatoendocrinol*, 4(3), 253-258.
- Park, KM., Kim, MM. (2010). Applications of chitin and its derivatives in biological medicine. *International journal of molecular science*, 11(12), 5152-5164.
- Patel, S. (2012). Therapeutic importance of sulphated polysaccharides from seaweeds: updating the recent findings. *3 biotech*, 2(3), 171-185.
- Patil, N., Le, V., Sligar, A., Mei, L., Chavarria, D., Yang, E., Baker, A. (2018). Algal polysaccharides as therapeutic agents for atherosclerosis. *Frontiers in Cardiovascular Medicine*, 26.
- Pearce, A., Haas, M., Viney, R., Pearson, S., Haywood, P., Brown, C., Ward, R. (2017). Incidence and severity of self-reported chemotherapy side effects in routine care: A prospective cohort study. *PLoS One*, 12(10).
- Penalver, F., Sancho, J., Fuente, A., Olave, M., Martin, A., Panizo, C., Perez, E., Salar, A., Orfao, A. (2017). Guidelines for diagnosis, prevention and management of central nervous system involvement in diffuse large B-cell lymphoma patients by the Spanish Lymphoma Group (GELTAMO). *Haematologica*, 102(2), 235-245.
- Ping, Y., Liu, C., Zhang, Y. (2018). T-cell receptor-engineered T cells for cancer treatment: current status and future directions. *Protein & Cell*, 9(3), 254-266.

- Pomin, V. (2015). Keratan sulphate: An up-to-date review. *International journal of Biological Macromolecules*, 72, 282-289.
- Pomin, V., Mulloy, B. (2018). Glycosaminoglycans and Proteoglycans. *Pharmaceuticals (Basel)*, 11(1), 27.
- Prideaux, M., Wijenayaka, AR., Kumarasinghe, DD., Ormsby, RT., Evdokiou, A., Findlay, DM., Atkins, GJ. (2014). SaOS2 Osteosarcoma cells as an *in vitro* model for studying the transition of human osteoblasts to osteocytes. *Calcified tissue international*, 95(2), 183-193.
- Pucktt, Y., Chan, O. (2019). Cancer, Acute Lymphocytic Leukemia (ALL). *StatPearls*.
- Riss, T., Moravec, R., Niles, A., Duellman, S., Benink, H., Worzella, T., Minor, L. (2013). Assay Guidance Manual [Internet].
- Sarrazin, S., Lamanna, W., Esko, J. (2011). Heparan Sulfate Proteoglycans. *Cold Spring Harbor Perspectives in Biology*, 3(7).
- Sasarman, F., Maftai, C., Campeau, P., Brunel-Guitton, C., Mitchell, G., Allard, P. (2016). Biosynthesis of glycosaminoglycans: associated disorders and biochemical tests. *Journal of inherited metablc disease*. 39(2), 173-188.
- Saultz, J., GARzon, R. (2016). Acute myeloid leukemia: A concise review. *Journal of clinical medicine*, 5(3), 33.
- Schagger, H. (2006). Tricine-SDS-PAGE. *Nature*, 1. 16-22.
- Slack, J. (2014). *Principles of Tissue Engineering (Fourth Edition)*. Stem Cell Institute, University of Minnesota, Minneapolis, Minnesota.
- <https://doi.org/10.1016/B978-0-12-398358-9.00007-0>

Smith, B.J. (1984). SDS Polyacrylamide Gel Electrophoresis of Proteins. *Methods in molecular biology*, 1, 41-55.

Song, K., Xu, L., Zhang, W., Cai, Y., Jang, B., Oh, J., Jin, J-O. (2017). Laminarin promotes anti-cancer immunity by the maturation of dendritic cells. *Oncotarget*, 8(24), 38554-38567.

Spicer, S., Adams, J., Thomas, D., Gallagher, J., Winters, A. (2017). Novel rapid method for the characterisation of polymeric sugars from macroalgae. *Journal of Applied Phycology*, 29(3), 1507-1513.

Talati, C., Sweet, K. (2018). Recently approved therapies in acute myeloid leukemia: A complex treatment landscape. *Leukemia research*.

Taneja, A., Master, S. Cancer, Chronic Lymphocytic Leukemia (CLL). *StatPearls*.

Tansey, W. (2006). Freeze-Thaw Lysis for Extraction of Proteins from Mammalian Cells. *Cold Spring Harbor Protocols*. <https://doi:10.1101/pdb.prot4614>.

Thomas, S., Prendergast, G. (2016). Cancer vaccines: A brief overview. *Methods in molecular biology*, 1403, 755-761.

Thorp, J., Rogers, D. (2016). Thorp and Covich's Freshwater Invertebrates (Fourth Edition). *Keys to Nearctic Fauna*, 291-711.

Tonder, A., Joubert, A., Cromarty, A. (2015). Limitations of the 3-(4,5-dimethylthiazol-2-yl)-2,5-diphenyl-2H-tetrazolium bromide (MTT) assay when compared to three commonly used cell enumeration assays, *BioMed Central*, 8.

Torre, L., Siegel, R., Ward, E., Jemal, A. (2016). Global cancer incidence and mortality rates and trends – an update. *Cancer epidemiology, biomarkers and prevention*.

- Van Weelden, G., Bobinski, M., Okla, K., van Weelden, W., Romano, A., Pijnenborg, J. (2019). Fucoidan structure and activity in relation to anti-cancer mechanisms. *Marine drugs*, 17(1). 32.
- Varki, A., Cummings, R., Esko, J. (1999). Essentials of Glycobiology. Cold Spring Harbor Laboratory Press, New York.
- Vasconcellos, A., Pomin, V. (2017). The sea as a rich source of structurally unique glycosaminoglycans and mimetics. *Mdpi microorganisms*, 5(3), 51.
- Victor, X., Nguyen, T., Ethirajan, M., Tran, V., Nguyen, K., Kuberan, B. (2009). Investigating the elusive mechanism of glycosaminoglycan biosynthesis. *Journal of biological chemistry*.
- Volpi, N. (2006). Therapeutic applications of glycosaminoglycans. *Current medicinal chemistry*, 13(15), 1799-1810.
- Walseng, E., Koksai, H., Sektioglu, I., Fane, A., SKorstad, G., Kvalheim, G., Gaudernack, G., Inderberg, E., Walchli, S. (2017). A TCR-based Chimeric Antigen Receptor. *Scientific reports*, 7(1), 10713.
- Wang, H., Song, G., Chuang, H., Chiu, C., Abdelmaksoud, A., Ye, Y., Zhao, L. (2018). Portrait of glial scar in neurological diseases. *International journal of immunopathology and pharmacology*.
- Willerth, S. (2017). Design considerations when engineering neural tissue from stem cells. *Engineering neural tissue from stem cells*.
- Williams, P., Phillips, G. (2003). GUMS Properties of Individual Gums. *Encyclopedia of Food Sciences and Nutrition (Second Edition)*, 2992-3001.

Yamada, S., Sugahara, K. (2008). Potential therapeutic application of chondroitin sulphate/dermatan sulphate. *Current drug discovery techniques*, 5(4), 289-301.

Yamada, S., Sugahara, K., Ozbek, S. (2011). Evolution of glycosaminoglycans. *Communicative & Integrative Biology*, 4(2), 150-158.

Yifeng, H., Qiujeng, Z., Mo, C., Qihong, H., Wenjing, W., Qing, L., Yuting, H., Wen, D. (2016). The changing 50% inhibitory concentration (IC50) of cisplatin: a pilot study on the artifacts of the MTT assay and the precise measurement of density-dependent chemoresistance in ovarian cancer. *Oncotarget*. 7(43), 70803-70821.

Zhu, J., Lei., Hu. (2015). Intraarticular hyaluronate injection for knee osteoarthritis – reconsider the rationale. *Annals of Translational Medicine*, 3(15), 214.